

Studies on Mongolian Environmental Issues Using Remote Sensing and Geographical Information System



RenchinTsolmon and Ryutaro Tateishi

**STUDIES ON MONGOLIAN ENVIRONMENTAL ISSUES
USING REMOTE SENSING AND
GEOGRAPHICAL INFORMATION SYSTEM**

Renchin Tsolmon and Ryutaro Tateishi

Chiba University 2005

STUDIES ON MONGOLIAN ENVIRONMENTAL ISSUES
USING REMOTE SENSING AND
GEOGRAPHICAL INFORMATION SYSTEM

CONTENTS

INTRODUCTION	3
TRENDS AND CHALLENGES OF GLOBAL LAND COVER MAPPING AND MONITORING <i>Ryutaro Tateishi</i>	4
CORRELATIONS OF SATELLITE-DERIVED PRECIPITATION AND NDVI WITH TREE RING DATA IN CENTRAL MONGOLIA <i>G. C. Jacoby, R. D. D'Arrigo, N. Baatarbileg, N. Davi, P. Arkin, H. Cullen</i>	10
THE VEGETATION DYNAMICS IN ECOTONE ZONE OF MONGOLIA USING NDVI DATA IN THE PERIOD OF 1982 – 2001 <i>P.D. Gunin, A.N. Zolotokrylin, S.N. Bazha</i>	23
THE NEED OF GIS FOR NATURAL RESOURCES MANAGEMENT AND POLICY DEVELOPMENT IN MONGOLIA <i>Tsutomu Suzuki</i>	33
LAND COVER CLASSIFICATION IN THE YELLOW RIVER BASIN USING MODIS DATA <i>Masayuki Matsuoka, Tadahiro Hayasaka, Yoshihiro Fukushima, Yoshiaki Honda</i>	39
AERIAL PHOTOGRAPHY INTERPRETATION OF VEGETATION IN THE FLOODPLAIN ZONE OF SHISHKHED RIVER VALLEY, MONGOLIA <i>E. Munguntulga, G. Punsalpaamuu, H. Nishida, Ts. Jamsran</i>	45
MULTI-TEMPORAL ANALYSIS OF VEGETATION INDICES FOR CHARACTERIZING VEGETATION DYNAMICS IN MONGOLIAN GRASSLAND <i>Ts. Javzandulam, R. Tateishi, R. Tsolmon</i>	49
MAPPING SNOW COVERAGE USING LINEAR MIXING MODEL ON MODIS/TERRA SATELLITE DATA <i>L. Ochirkhuyag, R. Tsolmon</i>	57
TEXTURE BASED SEGMENTATION OF REMOTELY SENSED IMAGERY FOR IDENTIFICATION OF GEOLOGICAL UNITS <i>Tsolmongerel Orkhonselenge, Arko Lucieer, Alfred Stein</i>	61
LAND TENURE, ROADS AND BIODIVERSITY; AN INTERCONTINENTAL COMPARISON <i>Hein van Gils</i>	71

USE OF REMOTE SENSING (RS) AND GEOGRAPHIC INFORMATION SYSTEM (GIS) TECHNOLOGY FOR IMPROVING SPECIAL PROTECTED AREAS MANAGEMENT: CASE STUDY; UVS LAKE BASIN, WESTERN MONGOLIA <i>Byamba Tsend-Ayush</i>	75
ANALYSIS OF DYNAMIC CHANGE ON LAND USE IN EAST TWO ALLIANCES AND TWO CITIES IN INNER MONGOLIA <i>Bao-yu-hai, A-la-ten-tu-ya, Sa-re-na, A-mu-gu-leng</i>	81
STUDY OF ELECTRIC POWER CONSUMPTION AND CARBON DIOXIDE EMISSION BY USING DMSP/OLS DATA <i>Husiletu, Masanao Hara, Fumihiko Nisio</i>	87
COMPARISON OF VEGETATION PHENOLOGY BETWEEN MONGOLIA AND KAZAKH STEPPESBY USING REMOTELY SENSED DATA VEGETATION INDEX <i>Rikie Suzuki, Tomoyuki Nomaki</i>	93
DROUGHT MONITORING <i>M. Bayasgalan</i>	99
ESTIMATION OF ATMOSPHERIC OPTICAL THICKNESSES IN ULAANBAATAR CITY <i>G.Batsukh, Ts.Baatarchuluun, D.Ochirvaani, S.Lantuu, D.Ganbaatar, N.Tugjsuren, B.Ganbat, J.Osorjamaa</i>	103
LAND COVER CHANGE MONITORING IN MONGOLIA <i>M. Erdenetuya, Sh. Munkhtuya</i>	109
SNOW RETREAT AS A KEY INDICATOR OF GLOBAL WARMING <i>Tarzad Ulaanbaatar, Lkhamjav Ochirkhuyag</i>	119
FOREST MAPPING WITH THE AID OF ERS SAR AND OPTICAL LANDSAT DATA IN THE UVS LAKE BASIN, WESTERN MONGOLIA <i>Davaasuren Narangerel, Gankhuyag Bulgan, Damdinsuren Dejiidmaa</i>	127
REFLECTOMETERS <i>D. Enkhbat, S. Damdinsuren</i>	131
APPLICATION OF REMOTE SENSING FOR ECONOMIC GROWTH ANALYSIS IN PARTICULAR AREAS OF MONGOLIA <i>B. Erdene, R. Tsolmon</i>	139

Studies on Mongolian Environmental Issues Using Remote Sensing and Geographical Information System

Introduction

In this book we cover a small subset of recent and important topics in Remote Sensing and Geographical Information Systems with emphasis on recent theoretical developments and applications. The book aims to bring the literature up to date as well as provide new perspectives on developments in RS and GIS in developing countries.

The First International Workshop on Land Cover Study of Mongolia Using RS & GIS was held on 8th-10th, June 2004, in Ulaanbaatar, Mongolia. The workshop was endorsed by the Mongolian Geoscience and Remote Sensing Society and the National University of Mongolia. This book contains a selection of carefully refereed papers based on talks presented at the workshop and papers submitted after the workshop by distinguished scientists working on Mongolian environmental issues.

RS is rapidly becoming accepted as an excellent tool for mapping, monitoring and modeling of environmental variables and processes in developing countries. There are several efforts already being made by different international organizations and institutions related to the Mongolian and Central Asian environment.

For developing countries that have enormous territories like Mongolia, RS offers a unique access to primary data about the research of land surfaces. The workshop provided a forum for researchers working on different aspects of RS and GIS to present their recent discoveries, initiate scientific collaborations, and discuss their experiences.

The target audience for this book includes graduate students in geosciences and environmental research and academic researchers who use RS and GIS or their specific applications.

We would like to take this opportunity to thank the sponsors of this work, the authors of the papers, and Center for Environmental Remote Sensing (CEReS) Publishers for making the publication of this book possible.

Renchin Tsolmon
Ryutaro Tateishi
November 2004

Acknowledgement

The authors thank Dr. Peter K.Marsh from American Center for Mongolian Studies in Ulaanbaatar, Mongolia for editing.

TRENDS AND CHALLENGES OF GLOBAL LAND COVER MAPPING AND MONITORING

Ryutaro Tateishi

Center for Environmental Remote Sensing (CEReS), Chiba University

E-mail: tateishi@faculty.chiba-u.jp

Abstract

This paper describes existing global land cover data, trend of global land cover mapping, and going global land cover mapping projects including Global Mapping project. Furthermore, a study to extract/analyze land cover changed/unchanged areas using global AVHRR NDVI data from 1982 to 2000 is described.

1. Introduction

Land cover is the observed physical cover on the Earth's surface (FAO 2000). On the other hand, land use is characterized by the arrangements, activities and inputs people undertake in a certain land cover type to produce, change or maintain it (FAO 2000). Another definition of land use is that it is a series of operations on land, carried out by humans, with the intention to obtain products and/or benefits through the use of land resources (de Bie 2000). Land cover is a part of information about real land surface from the view point of mainly vegetation.

Why is land cover information necessary? Because land cover provides some of the basic data needed for the purpose of; global change research (e.g. carbon circulation, water circulation, energy circulation, ecosystem), global environmental policy (e.g. policies for desertification, food security, poverty), national policy (e.g. land use planning/management), and environmental education.

Land cover information can be derived more easily than land use information by remote sensing techniques because the existence of vegetation and phenological information can be obtained by the techniques. The obtained land cover information at a certain time (year) is portrayed in the form of a map. Another form of land cover information is land cover change detection for a certain period (years).

Concerning geographical scale, land cover information is necessary for local, national, regional, continental and global areas. This paper is focused on global land cover.

2. Existing global land cover data

The following four global land cover data sets derived from satellite data are available.

(1) IGBP-DISCover

The first 1-km global land cover data were developed by the U.S. Geological Survey (USGS) and other organizations. Working under the auspices of the IGBP, Loveland et al. (1999, 2000) developed and applied a global land cover characterization methodology using 1992-1993 1-km AVHRR NDVI data. The methodology is based on unsupervised classification with extensive post-classification refinement. The IGBP DISCover classification provides a general picture of global land cover based on a 17-class land cover legend. The accuracy of the IGBP DISCover land cover data set was established through an independent IGBP accuracy assessment. Scean (1999)

determined that the DISCover overall accuracy was 59-71 percent depending on the specific validation procedures used.

(2) University of Maryland

A group of John Townshend of Department of Geography, University of Maryland used the same satellite data as IGBP-DISCover to make a global land cover map with the different land cover legend from IGBP-DISCover land cover data. This group focuses now not on categorical classification but on the estimate of area percentage representation of basic land cover types in a pixel.

(3) Boston University

A group of Mark Friedl of Boston University uses MODIS data for the global 1-km land cover classification with the same legend of 17 classes as the IGBP-DISCover. This group tries to make a global map periodically to detect land cover changes.

(4) GLC2000

The Joint Research Centre (JRC) of European Commission coordinated the GLOBAL LAND COVER 2000 Project (GLC 2000) in collaboration with a network of partners around the world. The general objective of GLC2000 is to provide for the year 2000 a harmonized land cover database over the whole globe. The year Two Thousand is considered as a reference year for environmental assessment in relation to various activities, in particular the United Nation's Ecosystem-related International Conventions. To achieve this objective GLC 2000 makes use of a dataset of 14 months of pre-processed daily global data acquired by the VEGETATION instrument on board the SPOT 4 satellite. The legend of GLC2000 is defined by FAO's Land Cover Classification System (LCCS).

3. Trend of global land cover mapping

The present global land cover mapping projects have the following features and trends.

(1) improvement of resolution

1 km resolution of AVHRR data was improved to 500 m of MODIS, 300 m of MERIS, and 250 m of GLI and MODIS.

(2) optical sensor + SAR + lidar

In addition to optical sensor data, global SAR data or lidar data may be used for global land cover mapping. SAR data have a potential to derive information of wetland and forest, and lidar data have a potential to derive vegetation height.

(3) harmonization of land cover legend

Different land cover legends are used in different projects and in different regions. In order to convert one legend to another, or to compare different legends, we need a tool to define land cover classes by a common system. The ideal tool for this purpose is Land Cover Classification System (LCCS) developed by FAO.

(4) development of global land cover ground truth data

Quality of land cover map is mainly dependent of training sample data (ground truth data) used for the classification. However ground truth data are not exchanged and accumulated. Development of global land cover ground truth data by the cooperation of different projects and for the common use will improve the quality of a land cover map.

(5) global mapping of individual land cover classes

Some key land cover classes important for environmental studies such as wetland, paddy, mangrove, and lake are planned to be mapped individually in different projects.

(6) categorical data + percent area cover of basic land cover types

In addition to the categorical classified land cover map, percent area cover of basic land cover types in a pixel is considered to give actual information of land surface. Tree, grass, cropland, urban, and bare ground are examples of basic land cover types.

4. On-going global land cover mapping projects

The following four global land cover mapping projects are going on.

(1) U.S. Geological Survey initiative

A new global land cover mapping project using MODIS 500 m data has encountered budget problem.

(2) EC/JRC initiative

A new global land cover mapping project called "GLOBECOVER" using ENVISAT/MERIS 300 m data has started. The mapping will be completed within a few years.

(3) Japan Aerospace Exploration Agency (JAXA) initiative

The initially planned global land cover mapping project using GLI 250 m data was replaced by Asia land cover mapping project using GLI 250 m data from April to October 2003 because of the failure of ADEOS II satellite in October 2003.

(4) Global Mapping project

A new global land cover map with the resolution of 1 km will be produced by the cooperation with national mapping organizations and other land cover mapping projects by 2007 as Global Map version 2.

5. Global Mapping project

The Global Mapping project organized by the International Steering Committee for Global Mapping (ISCGM) has a plan to produce global land cover data and global percent tree cover data as follows.

(1) global land cover data

- A land cover legend will be defined by Land Cover Classification System (LCCS) of FAO.

- Land cover ground truth data will be collected by the cooperation with National Mapping Organizations.

- Decision tree method will be used for classification.

(2) global percent tree cover data

- The percent tree cover is defined by area percentage of tree canopy cover per a unit ground area.

(3) for both data

- The ISCGM is seeking international cooperation with similar projects.

- MODIS 500m data will be used for data production. The final product will have 1 km resolution based on the policy of the ISCGM.

- Validation of the classified result will be done by the cooperation with National Mapping Organizations.

- The product will be completed by 2007.

6. Global land cover change monitoring

AVHRR data is the only satellite data which covers global land area daily for more than five years with a resolution of 1km. Though global 1km resolution AVHRR data are available only for 1992-3 and 1995-6, global 8 km resampled AVHRR data are available since 1981. Using time-series global 8 km AVHRR normalized difference vegetation index (NDVI) data, extraction of land cover changed areas was tried in global area.

6.1 Data used

10-day composite Normalized Difference Vegetation Index (NDVI) of NOAA NASA Pathfinder Land Data Set (PAL data) from 1982 to 2000 were used in this study. In order to remove cloud effects, Temporal Window Operation (TWO) method (Park and Tateishi 1999) was applied to NDVI data. The TWO method is an algorithm to make a seasonally smooth change pattern for temporal variables at least longer than one year. The TWO-processed data were resampled to 4' (approximately 8 km at the equator) grid raster data in the geographic (latitude/longitude) coordinate system.

6.2 Methodology

- (1) The averages of 10-day NDVI from 1982 to 1984 were calculated, and similarly from 1998 to 2000 too.
- (2) The difference from the averaged NDVI of 1982-84 to the averaged NDVI of 1998-2000 were calculated for the corresponding 10-day time period.
- (3) The sum of the above difference was calculated for thirty-six 10-day (or one year).
- (4) The positive value of the above sum is considered as areas of increasing vegetation activity, and negative value is considered as areas of decreasing vegetation activity.
- (5) In order to investigate the trend of time series NDVI values, time-series NDVI curves of unchanged areas of different land cover types such as desert, snow, and forest were analyzed.

6.3 Result

By using large positive and negative threshold values, potential of land cover changed areas were extracted. Figure 1 and Table 1 shows examples of extracted sites as potential land cover changed areas because of large NDVI change between 1982-4 and 1998-2000. However, the following noises and distortions cause wrong results as land cover changed areas.

- high or low NDVI noises remaining after preprocessing
- misregistration along seashore lines
- difference of NDVI levels in different NOAA satellites

7. Conclusions

- Four global land cover data are available.
- Several global land cover mapping projects are going on.
- Trends of global land cover mapping were identified. Especially, collection of land cover ground truth is important. The use of LCCS is recommended for harmonization of different legends.
- Global Mapping project has a plan to produce new global land cover data and percent tree cover data by 2007.
- Time series NDVI data are effective for global land cover change detection. Noises and trend of NDVI must be eliminated.

References

Boston University, land cover data

<http://geography.bu.edu/GEOG/research/remote.html> (accessed on 6 May 2004)

de Bie, C.A.J.M., 2000, Comparative performance analysis of agro-systems, ITC dissertation no.75, 232p.

FAO, 2000, Land Cover Classification System (LCCS): Classification Concepts and User Manual

http://www.fao.org/SD/2001/EN0101a_en.htm (accessed on 18 March 2004)

GLC2000

<http://www.gvm.sai.jrc.it/glc2000/defaultGLC2000.htm> (accessed on 18 March 2004)

Global Land Cover Ground Truth (GLCGT) Database Version 1.2
<http://www.cr.chiba-u.jp/database.html> (accessed on 18 March 2004)

Global Mapping project
<http://www1.gsi.go.jp/geowww/globalmap-gsi/iscgm-sec/index.html>
(accessed on 18 March 2004)

Loveland, T.R., Zhu, Zhiliang, Ohlen, D.O., Brown, J.F., Reed, B.C., and Yang, Limin, 1999, An analysis of the IGBP global land-cover characterization process: *Photogrammetric Engineering and Remote Sensing*, v. 65, no. 9, p. 1,021-1,032.

Loveland, T.R., Reed, B.C., Brown, J.F., Ohlen, D.O., Zhu, Z., Yang, L., Merchant, J.W., 2000. Development of a global land cover characteristics database and IGBP DISCover from 1 km AVHRR data. *International Journal of Remote Sensing* 21(6/7): 1303-1330.

Park, J.G. and Tateishi, R., 1999, A proposal of the Temporal Window Operation (TWO) method to remove high-frequency noises in AVHRR NDVI time series data, *Journal of the Japan Society of Photogrammetry and Remote Sensing*, 38(5) , 36-47.

Scepan, J., 1999. Thematic Validation of High-Resolution Global Land-Cover Data Sets. *Photogrammetric Engineering and Remote Sensing* 65(9): 1051-1060.

University of Maryland, land cover data
<http://glcf.umiacs.umd.edu/data/landcover/index.shtml> (accessed on 6 May 2004)

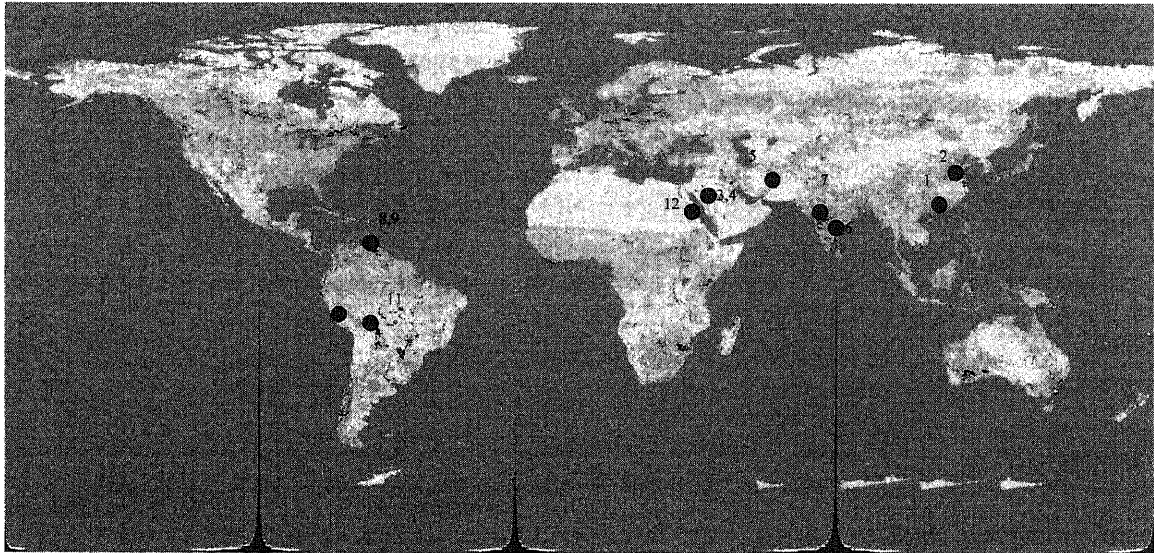


Figure 1 Examples of sites extracted as land cover changed area

Table 1 Examples of sites extracted as land cover changed area
increase/decrease: increase/decrease of NDVI

No.	Area	Name of Place	Lat/Long	increase/decrease
1	China	Guang zhou	23° 08' N, 113° 12' E	decrease
2		Shanghai	31° 16' N, 121° 20' E	decrease
3	Middle East	Saudi Arabia-1	19° 52' N, 44° 48' E	increase
4		Saudi Arabia-2	28° 36' N, 36° E	increase
5		Lake Hamoun	31° 16' N, 61° 12' E	decrease
6	Southeast Asia	Eastern India	15° 36' N, 79° 52' E	increase
7		Western India	18° 12' N, 74° 56' E	increase
8	South America	Northern Venezuela-1	8° 52' N, 63° 04' W	increase
9		Northern Venezuela-2	7° 04' N, 63° 04' W	decrease
10		Southern Peru	16° 20' S, 72° 20' W	increase
11		Bolivia	17° 04' S, 62° 36' W	decrease
12	Africa	Sudan	18° 32' N, 37° 48' E	increase

CORRELATIONS OF SATELLITE-DERIVED PRECIPITATION AND NDVI WITH TREE RING DATA IN CENTRAL MONGOLIA

G. C. Jacoby¹, R. D. D'Arrigo¹, N. Baatarbileg¹, N. Davi, P. Arkin², H. Cullen³

¹Lamont-Doherty Earth Observatory, Palisades, New York

²NOAA, Silver Spring, Maryland

³KPFA, Atlanta, Georgia

Abstract

Precipitation and vegetation indices based on satellite measurements can be of major importance in environmental monitoring over wide regions. Yet, these records are only about two decades in length and must be evaluated by comparisons to other ground-based data. Herein we compare both types of data to annual data based on the ring width variations of trees growing on semiarid sites in Mongolia. Previous studies showed a strong precipitation signal in the tree-ring data. The comparisons indicate that there are significant correlations between the tree-ring data and the satellite information.

The correlations are due to moisture being the limiting factor to growth for the trees and other vegetation in the region studied. These results support the accuracy of the satellite-based parameters for the semiarid, low-relief region studied and support similar results elsewhere.

1. Introduction

Water is a key limiting factor to livestock raising and agricultural productivity in Mongolia. These activities are a major part of the economy of the nation. The primary source of water is precipitation, most of which occurs during the warm-season months.

There are rain gages at numerous sites in Mongolia but few records go back farther than about 1950 and vast areas have no gages at all. This sparse coverage could be significantly augmented if new data sets that combine gage observations with estimates derived from satellite data (Xie and Arkin 1995 & 1997) are proven to be accurate measures of areal precipitation. The satellite record is short and needs to be tested by independent ground information. Both types of precipitation data can be examined by comparison to time series based on annual ring widths of trees at sites where moisture is the limiting factor to growth.

Vegetation growth information for rangeland production estimates and for carbon budget studies can also be estimated by satellite measurements developed into the normalized difference vegetation indices (NDVI) (Kumar and Monteith 1982, Goward et al. 1994, Sellers et al. 1996, Zhou et al. 2003). (See detailed definition below.) The NDVI also needs to be tested by ground truth information. In semiarid regions like much of Mongolia, the single parameter of precipitation can be a dominant factor for most vegetation growth including the annual ring widths of trees. Thus for the region studied, both satellite-derived precipitation and NDVI estimates may be related to annual ring-width data from trees and herein we test the correlations.

Annual rings of trees have been used to reconstruct and study hydrometeorological parameters for some time (e. g. Schulman 1945, Fritts 1974). Such reconstructions create longer records of climate variations which better represent the full range of variations, extremes and trends than the limited information in most recorded data. Tree rings have extended the records of temperature, precipitation, streamflow, and drought in parts of Mongolia by centuries to millennia (Jacoboy et al. 1996, D'Arrigo et al. 2000a, Pederson et al. 2001, Jacoboy et al. 2003).

In semi-arid regions of Mongolia, contents of precipitation gages and the widths of

annual tree rings can record common response to precipitation. Areal coverage of gage data is limited by the number of gages that are set out and monitored. Representative areal coverage is sometimes a problem in dry regions like central Mongolia where much summer rainfall is from localized convective storms. We sampled trees at two sites of extreme aridity in the study region where tree rings respond very much to changes in moisture availability; growing wider rings in wet years and more narrow, or even missing rings, in very dry years (Pederson et al. 2001). We have compared the dated annual ring-width data to variations in satellite-derived precipitation data, NDVI data, ground-recorded precipitation, and soil moisture in mutual testing analyses.

2. Hydrometeorological, satellite and tree-ring data precipitation gage data

We use a precipitation series that includes the eight gage stations that cover the east-central Mongolian region represented by the tree-ring sampling sites (Figure 1). Individual missing values were estimated using the closest station with data. Records are sparse in Mongolia and these are the only stations for this area with records going back to the early 1940s. The eight stations' data were averaged to produce a regional series that has less noise than single station data (Blasing et al. 1981). Mean annual precipitation for this eight-station average is 273.7 mm per year with the warm season (May-October) producing 92.4% of the mean annual total for the time period 1940-1995.

For the period of the satellite-derived precipitation data, 1979-1995, the mean and percentage summer are similar, mean of 279.9 mm and May-October percentage of summer 92.9%. Similar station data were used in a previous tree-ring study that reconstructed precipitation and streamflow for central and eastern Mongolia (Pederson et al. 2001).

Snow-in-winter precipitation generally plays a small quantitative role in the hydrologic regime at the relatively lower elevations of this study region. The mean winter precipitation during the 1940-95 period, November-April, was 20.8 mm.; 1979-1995, 19.5 mm. In times of the "zud" (severe winters) and at higher elevations, snow is a larger factor. There can be snow flurries any month of the year in the high mountains.

The measurement of snow by precipitation gages is very inaccurate. The effects of snow on soil moisture in this region is unknown because the soil moisture was not measured during the cold season at the sites in the study area. Both the satellitederived precipitation and NDVI data are of lesser quality during the colder seasons (See below). Since the correlations between the tree-ring data and rain gage precipitation are higher during the warmer season (this study and Pederson et al. 2000)and fortuitously this is the season of better quality satellite-derived data; this season is the focus of these analyses.

3. Satellite-Derived Precipitation Data

Rain gages provide accurate measurements of rainfall at specific points. However they are often too few in number for assessing variations in precipitation over large areas of the globe. The need for comprehensive and complete analyses of precipitation for climate monitoring and diagnosis, and the verification of climate models, has led to the development of data sets that make use of a variety of estimates derived from satellite observations to supplement gage measurements (Huffman et al., 1997; Xie and Arkin, 1996, 1997).

In this paper we use the observation-only analysis of Xie and Arkin (1997), which has a spatial resolution of 2.5° latitude/longitude and monthly temporal resolution (Figure 1). This analysis uses a number of satellite-based estimates, including two based

on infrared cloud-top temperature from polar orbiting and geostationary satellites, two derived from passive microwave observations from the Special Sensor Microwave/Imager (SSM/I) on the U.S. Air Force DMSP satellites, and one based on observations from the Microwave Sounding Unit on the NOAA polar orbiting satellites. These estimates, where available, are combined into a single global field using weights estimated by comparison with the available gage observations over land and from a priori validation studies and extrapolation over the oceans. Each of the satellite estimates has significant bias (Xie and Arkin, 1995).

Therefore, a final analysis used values from gage observations at approximately 6000 stations worldwide as fixed points but retained the spatial gradients of the satellite-based field. The final product is referred to as the CPC Merged Analysis of Precipitation (CMAP). CMAP has been used in a variety of diagnostic and model validation studies (Stephenson et al., 1998; Yang et al., 1999), and evaluated in comparison to similar products (Gruber et al., 2000) with positive results.

However, shortcomings are known to exist. The various satellite estimates have systematic errors that vary with season and latitude. Areas with few or no gages are poorly defined where/when the satellite estimates have large errors. In the study region here, mid-latitude central Asia, only the infrared estimates and one of the microwave estimates are usable, and may have large errors in winter. The warm season values are expected to be superior and are used here. Fortunately for the comparisons, most of the precipitation in Mongolia occurs during the warm season.

4. Normalized Difference Vegetation Index (NDVI)

NDVI data are the vegetation index or “greenness” based on differences between visible and near-infrared radiance (e.g. Kumar and Montieth 1982, Sellers et al. 1996, Zhou et al. 2003). The data used here are from the continental data set at 8 km resolution, available from July 1981 to December 1999, produced by the Global Inventory Monitoring and Modeling Systems (GIMMS) group from the Advanced Very High Resolution Radiometers (AVHRR) onboard afternoon-viewing satellites (NOAA 7, 9, 11 and 14). NDVI expressed on a scale from -1 to + 1. Various corrections to the data set are described in Zhou et al. (2001). Data correspond to the maximum NDVI value during a 15-day compositing period. In this study, we used one grid cell centered near the Zuun Mod tree site, and another centered near the Urgan Nars tree site.

We averaged the values to obtain monthly means and determined correlations for the individual months of May through September. Significant correlations were previously shown between NDVI and tree-ring data where tree and other vegetation growth was limited by temperature (D’Arrigo et al. 2000b) and where sufficient tree species were sampled to represent the major plant cover for an area (Malmstrom et al. 1997).

5. Soil Moisture

Soil moisture data for sites in Mongolia have been compiled by Robock et al.(1999). These data comprise measurements at 11 depths in the top meter of the soil. Three series of measurements were made each month from April through October. In Mongolia measurements were compiled from 42 stations for the years 1970 through 1993, with some exceptions (Robock et al. 1999).

We examined the data for the three soil moisture stations within the central area of our tree-ring sites; Zuunmod, Undurkhaan, and Binder (Figure 1). All had many missing values. To integrate shallow moisture content of the soil we summed the values for 10, 20, and 30 cm. depths and averaged at each location for each month to produce monthly

averages for April through October. (Missing values increase with depth.)

The three depths were chosen just to obtain more representative data for soil moisture and are unrelated to estimates of root depth which is unknown for these trees at these sites. Octobers had so many missing third values we only used the first two measurements for October as the monthly sum. It was noticed that the correlations of values in the vertical direction for the upper layers at Undurkhaan were very high, ranging from .90 to 1.0. We therefore estimated eleven missing values where there were enough other values in the upper .5 meter to establish a trend. There were no simple patterns in the temporal direction nor in either vertical or temporal directions at Zuunmod or Binder and no missing values were estimated. We could not average the three location records because they never all had a complete season of data for the same year, even just May-September.

6. Tree-Ring Data

Tree-ring data from two sites in north central Mongolia (Figure 1) were compared to the precipitation and NDVI data. The Zuun Mod (Mongolian for "100 trees") tree-ring sampling site is an isolated stand of old larch (*Larix sibirica*) trees in a semi-arid grassland at 47° 47.02' North, 107° 30.00' East, and 1415 m elevation in central Mongolia. The Urgun Nars ("wide pines") site near the northern margin of the semi-arid grasslands is a stand of large old-growth scots pine (*Pinus sylvestris*) at 48° 34.62' North, 110° 32.75' East, and 1,070 m elevation. These trees grow on fairly level ground with a gentle slope towards the south in east-central Mongolia. These two sites are central to the precipitation data sets' coverage and are the only appropriate moisture-stressed tree-ring sites we have in the area.

Standard dendrochronological procedures were followed in generating the time series or chronology of mean ring-width variations (Fritts 1976, Holmes 1983, and Cook & Kairiukstis 1990). Core samples (which are taken nondestructively) were obtained from almost all the old, undecayed trees at the Zuun Mod site and the final chronology comprises 30 cores from 13 trees.

We truncate the series at 1600 because the sample size is down to only 12 cores by that year. At Urgun Nars the ring-width chronology comprises 33 cores from 16 trees and extends to 1668 with 8 core series. We standardize to remove the age trend in the raw data series (Cook 1985) and to create a mean-value series of ring-width indices. The mean correlation coefficient between all series (RBAR, Briffa 1995) and expressed population signal (EPS, Wigley et al. 1984) are two parameters for evaluating the quality of tree-ring series. For Zuun Mod the RBAR is 0.69, for Urgun Nars RBAR is 0.65, and EPS is above 0.965 for every 30-year segment over the length of both series. The RBARs are high relative to many other tree-ring series and EPS is well above the 0.85 level which is considered a threshold for acceptability by some researchers (Wigley et al. 1984). Therefore these are two excellent chronologies with stable qualities throughout the length of the time series used.

7. Analyses

Correlations were calculated between the satellite-derived monthly precipitation data, gage precipitation data, and the annual tree-ring data. The data were tested for the same common time period 1979 to 1995 (n=17). There was no detrending of any data set.

The correlations were made using the precipitation data for the current year of growth and the prior year. Correlations were calculated using precipitation data for each of the 20 grid cells surrounding the tree-ring sites and each tree series (Figure 1) and for averaged data. Based on the strength and patterns of the correlations between

precipitation and the ring-width indices, a regression was made using principal component analysis (PCA).

Replication and/or regionalization of both tree-ring and climatic records serves to reduce the noise present in single series by combining series to produce the common variations for the selected series. (Fritts 1976, Blasing et al. 1981, Jacoby et al. 2000).

We combined both tree-ring series using PCA to produce two eigenvectors, the first of which contains 64.5% of the variance. We then used this first eigenvector from the two tree ring series to estimate warm-season precipitation (May-October) for the average of the six grid cells most closely encompassing the tree sites (Figure 1).

Correlations were calculated between individual monthly NDVI data series and individual tree-ring series; and between the mean monthly NDVI series and tree-ring first eigenvector. The NDVI data span is 1982-1995 (n=14). In addition, correlations were calculated between NDVI and the satellite-derived precipitation; and NDVI and soil moisture data.

Soil moisture correlations were only calculated for individual soil moisture records and the closest tree-ring series due to the many missing values as described above. The number of pairs ranged from 20 to as few as 2. Thus the significance is questionable in many cases. However the temporal pattern of correlation is of interest to compare to the other relationships. Soil moisture was compared with trees, satellite derived precipitation, and NDVI.

8. Results

Correlations were significant between the satellite-derived monthly precipitation data and tree-ring indices for July, August, September, (0.95 level) and October (0.90 level) of the year prior to the growth year and weak response during the growth year (Figure 2a).

Results are similar with the gage precipitation data for the same time period, except for October being lower and July of the growth year being significant (0.95 level) (Figure 2b).

The correlations for the cold-season months were low or inconsistent from month to month for both satellite and gage data. The correlations between monthly satellite-derived and gaged precipitation were all between 0.64 and 0.92. The pattern of strong response of trees to prior year moisture was also present in our previous hydrometeorological results comparing longer (55-year) periods (Pederson et al. 2001) but not as strongly biased towards the prior year as this shorter term data set. Because the common period is only 17 years, the standard calibration-verification procedures used in many dendroclimatological studies could not be followed (Cook and Kairiukstis 1990).

Varying terrain influences the results for both Zuun Mod and Urgun Nars (Figure 1). At Urgun Nars the tree rings correlated at .65 with May-October precipitation for its encompassing grid cell but at 0.75 with the grid cell immediately to the south (Figure 1). Urgun Nars lies at the northern extent of the semi-arid grasslands to the south. Correlations drop to the north of the sites across the Hentiyn Mts. of Mongolia and the Yablonovyi Mts. of Russia.

The correlation between the first eigenvector and satellite precipitation estimates for the previously-mentioned six encompassing blocks is 0.85 (0.999 level) and the regression explained 71% of the variance in the precipitation data (Figure 3a), confirming the regional signal in the trees and validity of the satellite estimates.

The variance explained is always adjusted here for loss of degrees of freedom due to the regression and labeled R² a. The NDVI results add to the establishment of tree-

rings as vegetation indices in situations where there is primarily a single limiting factor to growth (e. g. D'Arrigo et al. 2000b). Single series correlations between trees and NDVI for the averaged May-September months are 0.82 and 0.72 for Zuun Mod, and Urgun Nars respectively (0.99 level). The eigenvector from both sites and the averaged NDVI values correlate at 0.77 (Figure 3b) and the regression explains 59% of the variance in NDVI. Correlations between monthly values of the first eigenvector for the two NDVI sites and the ring width eigenvector are shown in Figure 4a.

The soil moisture results showed similar patterns to the precipitation correlations with a strong effect of prior year on tree growth but a more consistent positive pattern for the growth year (Figure 4b). Due to the many missing values, the soil moisture data could not be averaged into integrated time series to compare with the tree-ring data.

Again, it should be noted that the *n* values for the soil moisture comparisons are as low as 2 on occasion and although the patterns are interesting the actual values should be regarded with caution. The correlations between satellite-precipitation and soil moisture are relatively weak and inconsistent except for July. This result can be partly attributed to the high warm-season evapo-transpiration losses in semi-arid areas of Mongolia.

Correlations for colder months merely showed that during that season of poorer satellite-derived precipitation and NDVI data along with the less accurate precipitation data, there is not a meaningful pattern in the correlations.

9. Discussion

The trees in this study show very strong effect of prior year precipitation on ring-width during the growth year, results similar to Pederson et al. (2001). In many tree species the buds, formed in the prior year, contain all the primordial for the leaves, shoots, and internodes to be grown the next year; as well as growth hormones, called auxins, that move from the buds to the twigs, branches and trunk of the tree early the next growth year (Kozłowski et al. 1991). Also, late in the growing season carbohydrates are produced that are stored for the next year's growth as the current year's growth (including cambial-cell division for radial growth) slows at the end of the warm season (Kozłowski et al. 1991). Hence much of the following year's growth is significantly determined by growing conditions of prior year.

These effects appear to be stronger in the particular period used for regression because if the entire common period of precipitation and tree-ring data (1941-1995) is used, the response of the trees to growing-season precipitation is more evident. However, the prior season is still the stronger influence on ring-widths, in agreement with Pederson et al. (2001). The correlations with NDVI are more direct as it is the "greenness" of the growth year that is being measured.

10. Conclusions

The correlation results indicate the satellite-derived precipitation data are valid estimators of area precipitation in this region. Relative to other dendroclimatic regressions using these same tree-ring data (Pederson et al 2001), the variance explained of 71% is slightly higher even for the same time period (1979-1995).

This confirms the sensitivity of the tree rings and also helps confirm the validity of the satellite observations. The systematic decrease in correlations as one moves to grid cells further away from the tree-ring sites strongly suggests that the interrelationships are causal and not artifacts in spite of limited length of concurrent records.

The NDVI results add to the evidence of D'Arrigo et al. (2000b) that if a single limiting factor, in this case precipitation, influences tree and other vegetation growth,

the tree-ring data can serve as an excellent index to vegetation growth even if the trees are a minor percentage of the land cover. This case primarily involves landscape of relatively low relief.

Montane regions may differ. There is need for replication to test the correlations using other tree-ring sites from the same region and to test other types of regions.

Acknowledgements

This work was supported by NSF grant ATM96-31750. We thank B. Buckley, Ch. Dugarjav and D. Munkzorig for assistance in collecting samples and meteorological data. N. Peterson aided in processing and analyses. NDVI data was developed by C. J. Tucker at Goddard Space Flight Center and provided to us by Ranga Myneni and Liming Zhou of Boston University (now at Georgia Institute of Technology).

References Cited:

Blasing, T.J., D.N. Duvick, and D.C. West (1981) Dendroclimatic calibration and verification using regionally averaged and single station precipitation data. *Tree-Ring Bulletin*, 41, 37-43.

Briffa, K.R. (1995) Interpreting high-resolution proxy climate data-The example of dendroclimatology. *Analysis of Climate Data Variability, Applications of Statistical Techniques*, H. von Storch and A. Navarra, Eds., Springer, 77-94.

Cook, E.R. (1985) A Time Series Analysis Approach to Tree-Ring Standardization. Ph.D. Thesis. University of Arizona. Tucson. 171 p.

Cook, E. R., and Kairiukstis, L.A. (Eds.) (1990) *Methods of Dendrochronology, Applications in the Environmental Sciences*, Dordrecht: Kluwer Academic Press, Boston, 394 p.

D'Arrigo, R.D., G.C. Jacoby, N. Pederson, D. Frank, B.M. Buckley, B. Nachin, R. Mijiddorj, and Ch. Dugarjav (2000a) Mongolian tree rings, temperature sensitivity and reconstructions of Northern Hemisphere temperature, *Holocene*, 10, 669-672.

D'Arrigo, R.D., C.M. Malmstrom, G.C. Jacoby, S.O. Los, and D.E. Bunker (2000b) Correlation between Maximum Latewood Density of Annual Tree Rings and NDVI based Estimates of Forest Productivity, *Int. J. Remote Sensing*, 21 (11) 2329-2336.

Fritts, H.C. (1974) Relationships of ring widths in arid-site conifers to variations in monthly temperature and precipitation, *Ecological Monographs*, 44 (4) 411-440.

Fritts, H. C. (1976) *Tree Rings and Climate*, Academic Press, New York, 567 p.

Goward, S. N., Turner, S., Dye, D. G., and Liang, S. (1994) The University of Maryland improved Global Vegetation Index product, *Internat. J. Remote Sens.*, 15, 3365-3395.

Gruber, A., X. Su, M. Kanamitsu, and J. Schemm (2000) The comparison of two merged rain gauge-satellite precipitation datasets. *Bull. Amer. Meteor. Soc.*, 81, 2631-2644.

Holmes, R.L. 1983. Computer-assisted quality control in tree-ring dating and measurement. *Tree-Ring Bulletin*, 44, 69-75.

Huffman, G.J. and co-authors (1997: The Global Precipitation Climatology Project (GPCP) combined precipitation dataset. *Bull. Amer. Meteor. Soc.*, 78, 5-20.

Jacoby, G.C., R.D. D'Arrigo and Ts. Davaajamts (1996) Mongolian tree rings and 20th century warming, *Science*, 273, 771-773.

Jacoby, G.C., N. Pederson, and R.D. D'Arrigo (2003) Temperature and precipitation in Mongolia based on dendroclimatic investigations, *Chinese Science Bull.*, 48, (14) 1474-1479.

Jacoby, G.C., N.V. Lovelius, O.I. Shumilov, O.M. Raspopov, Y. Karbainov, D.C. Frank (2000). Long-term temperature trends and tree growth in the Taymir region of northern Siberia, *Quaternary Research*, 53, 312-318.

Kozlowski, T.T., P.J. Kramer, S.G. Pallardy (1991) *The Physiological Ecology of Woody Plants*, Academic Press, San Diego, 657 p.

Kumar, M., and Monteith, J.L. (1982) Remote sensing of plant growth. in *Plants and the Daylight Spectrum*, Academic Press, London.

Malmstrom, C. M., Thompson, M. V., Juday, G., Los, S. O., Randerson, J. T., Field, C. B. (1997) Interannual variation in global-scale net primary production: testing model estimates, *Global Biogeochemical Cycles*, 11, 367-392.

Pederson, N., G.C. Jacoby, R.D. D'Arrigo, E.R. Cook, B.M. Buckley, C. Dugarjav & R. Mijidorj (2001) Hydrometeorological reconstructions for Northeastern Mongolia derived from tree rings: 1651-1995, *Journal of Climate* 14, 872-881.

Robock, A., E. Entin, K. Vinnikov, A. Namkhai and Ts. Adyasuren (2001) Mongolian Soil Moisture Data: Plant available soil moisture gravimetric observations and maps (1970-1993).

Website: http://climate.envsci.rutgers.edu/soil_moisture/mongolia2.html

Schulman, E. (1945) Tree-ring hydrology of the Colorado River Basin, Univ. of Arizona Bulletin Series, v. XVI No. 4., *Lab. of Tree-Ring Res., Bull. No. 2*, 51 p.

Sellers, P.J., Los, S. O., Tucker, C. J., Justice, C. O., Dazlich, D. A., Collatz, G. J., and Randall, D. A. (1996) A revised land surface parameterisation (SiB-2) for atmospheric GCMs. Part 2: The generation of global fields of terrestrial biophysical parameters from satellite data, *J. of Climate* 9, 706-737.

Stephenson, D.B., F. Chauvin, and J.-F. Royer (1998) Simulation of the Asian Summer Monsoon and its dependence on model horizontal resolution. *J. Meteor. Soc. Jap.*, 76, 237-265.

Wigley, T.M.L., K.R. Briffa, and P.D. Jones (1984) On the average value of correlated time series, with applications in dendroclimatology and hydrometeorology, *J. Climate Appl. Meteor.*, 23, 201-213.

Xie, P. and P.A. Arkin (1995) An intercomparison of gauge observations and satellite estimates of monthly precipitation. *J. Appl. Meteor.*, 24, 1143-1160.

_____ and _____ (1996) Analyses of global monthly precipitation using gauge observations, satellite estimates, and numerical model predictions. *J. Climate*, 9, 840-858. _____ and _____ (1997) Global precipitation: A 17-year monthly analysis based on gauge observations, satellite estimates, and numerical model outputs. *Bull. Amer. Meteor. Soc.*, 78, 2539-2558.

Yang, S., K.-M. Lau, and P.S. Schopf (1999) Sensitivity of the tropical Pacific Ocean to precipitation-induced freshwater flux. *Climate Dyn.*, 15, 737-750.

Zhou, L., C. Tucker, R. Kaufmann, D. Slayback, N. Shabanovi and R. Myneni (2001) Variations in northern vegetation activity inferred from satellite data of vegetation index during 1981 to 1999, *J. Geophys. Res.*, 106, 20,069-20,083.

Zhou, L., R.K. Kaufmann, Y. Tian, R.B. Myneni, and C.J. Tucker (2003) Relation between interannual variations in satellite measures of greenness and climate between 1982 and 1999, *J. Geophys. Res.*, 108, (D1), 4004, doi:10.1029/2002JD002510.

Figure Captions:

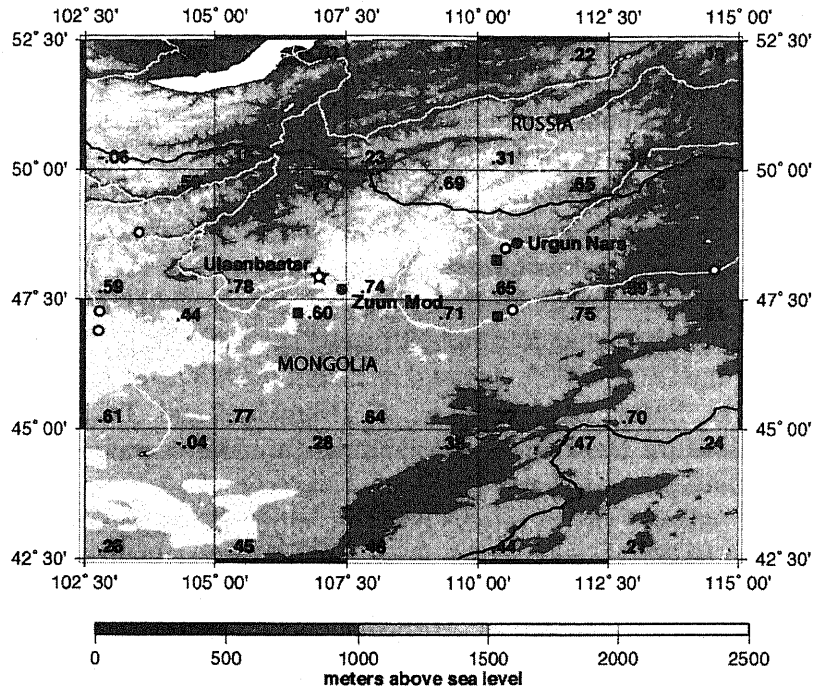


Figure 1: Map of Eastern Mongolia with 2.5 degree grid cells used for areal estimation of precipitation using satellite observations. The solid circles are the two tree-ring sites. The open circles are rain gage sites. One gage is just off the map to the east. The solid squares are soil moisture measurement sites. Ulaanbaatar is the capital city and a rain gage site. The numbers in each grid cell are correlations between the tree-ring series and the grid-cell precipitation. The upper right are for Urgun Nars and precipitation, and the lower left are for Zuun Mod and precipitation. Correlations decrease across the mountains and to the north. The grid squares are approximately 200 kilometers on each side

Satellite-Derived Precip. & Ring-Width First Eigenvector

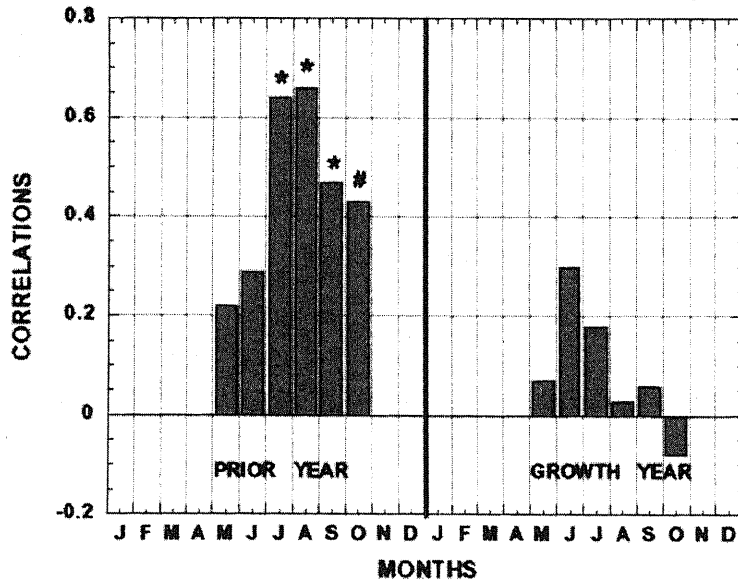


Figure 2a: Correlations between the tree-ring first eigenvector and monthly

precipitation estimates utilizing satellite information, 1979-1995. The * indicates significance at 0.95 level, # indicates significance at 0.90 level.

Rain Gage Precipitation & Ring-Width First Eigenvector

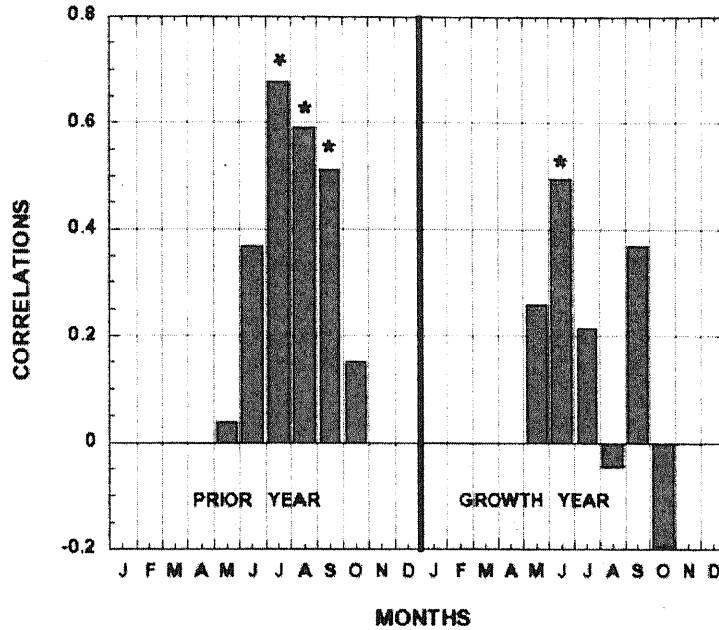


Figure 2b: Correlations between the tree-ring first eigenvector and monthly precipitation estimates utilizing only gage information averaged from 8 stations in east central Mongolia, 1979-1995. Symbols are as in 2a.

Satellite Precipitation Estimated by Ring-Width First Eigenvector

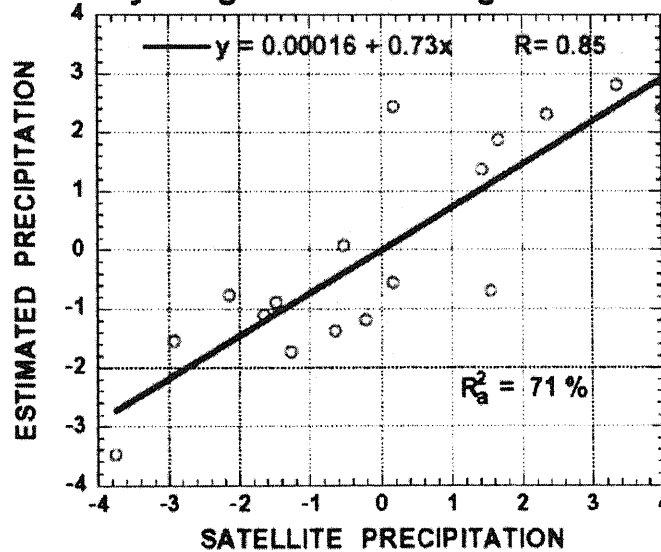


Figure 3a: Scatterplot showing regression using first eigenvector from the two tree-ring series and the normalized precipitation (using satellite information) averaged for the central 6 grid cells in Figure 1 encompassing the tree-ring sites, May through October, 1979-1995.

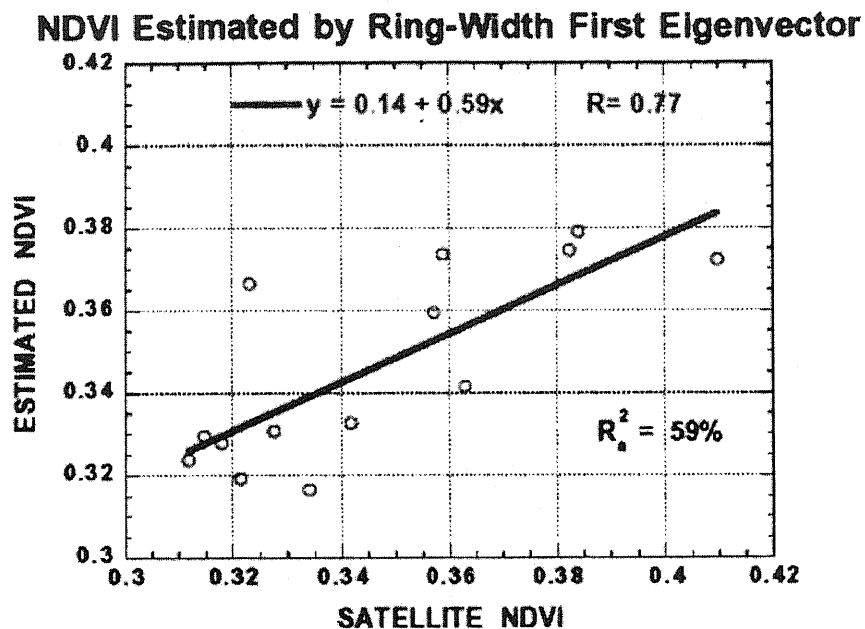


Figure 3b: Scatterplot showing regression using the first eigenvector from the two tree-ring series and the NDVI averaged for two locations centered on the two tree-ring sites, May through September, 1982-1995.

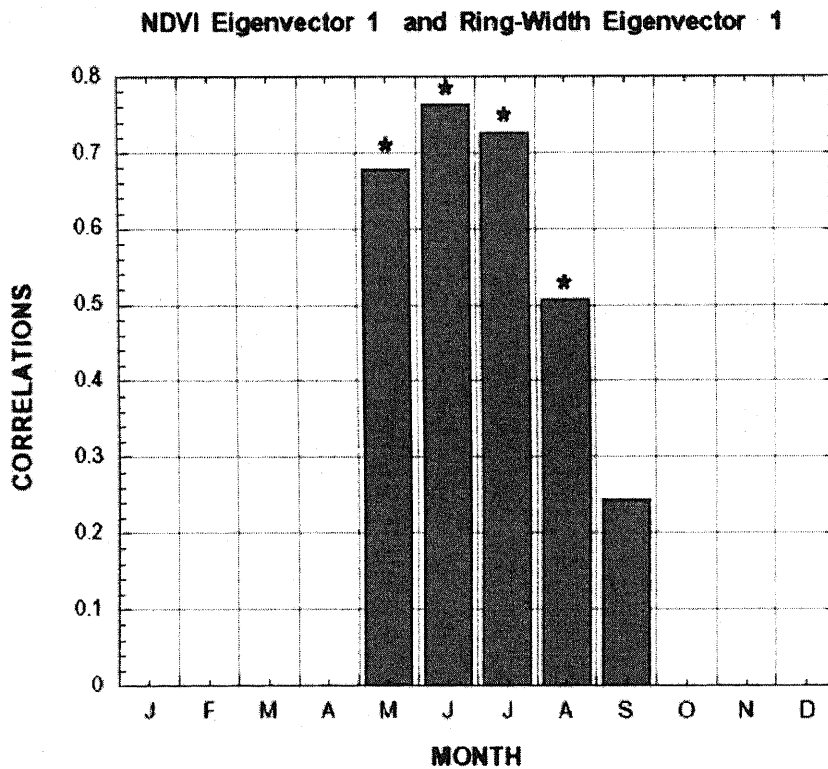


Figure 4a: Correlations between the tree-ring first eigenvector and the first eigenvector of the two NDVI records. The “greening” season starts in May and diminishes in value and correlation with the trees in October. The * indicates significance at 0.95 level.

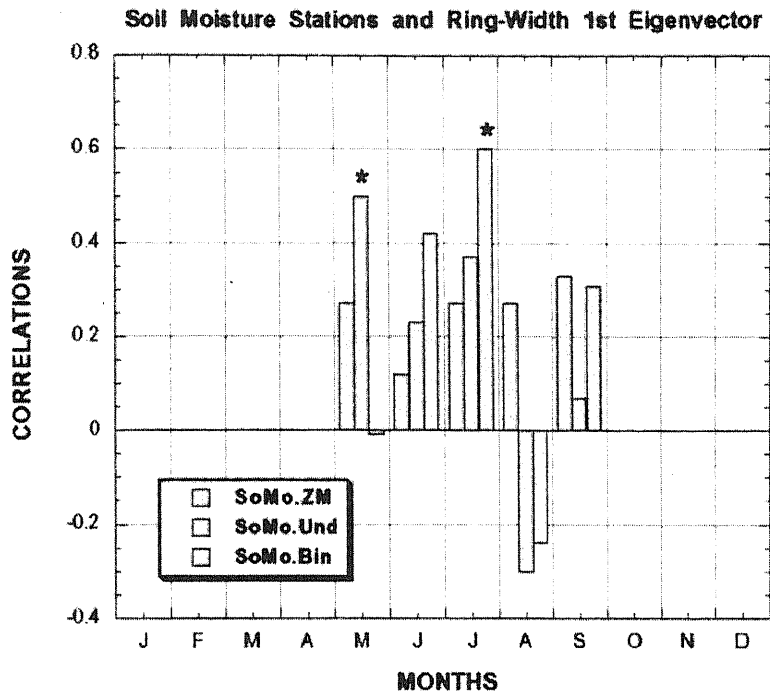


Figure 4b: Correlations between the tree-ring first eigenvector and individual station monthly soil-moisture values. Largely due to low n values, only two correlations are significant at the 0.95 level. The three stations are: ZM=Zuun Mod, Und=Underkhan, and Bin=Binder.

THE VEGETATION DYNAMICS IN ECOTONE ZONE OF MONGOLIA USING NDVI DATA IN THE PERIOD OF 1982 - 2001

P.D.Gunin*, A.N.Zolotokrylin**, S.N. Bazha*

*A.N. Severtsov Institute of Ecology and Evolution, RAS 119071 Moscow,
the Leninsky prosp., 33

** Institute of Geography, Russian Academy of Science

Abstract

In the present report the results of study of green phytomass dynamics having the ecotone character in zonal ecosystems are considered. They will be localized near to borders between discriminating by humidification of landscape-ecological regions and zonal - sub zonal strips. The purpose of investigation is revealing of zonal ecosystems, which the green phytomass, as a result of climate change and anthropogenic pressure on pastures decreases up to threshold value and becomes lower than it within the last decades. For this purpose digital maps of average parameter of green phytomass threshold for separate decades (1982-1991 and 1992-2002) and the difference of parameters between decades are developed.

Joint analysis of a map of landscape-ecological geographical zoning of Mongolia, maps of zonal ecosystems and geographic distribution of the season with green phytomass not of superior threshold volume ($NDVI \leq 0.07$) allows us to make the following conclusions:

- The ten years' phytomass changes close to its threshold value are dominant in a transitory strip between the Central-Asian and lying to the north Central-Mongolian-Dahuria-East-Mongolian landscape-ecological regions. The inter decade phytomass changes have zonal character.
- The territory with the lower than threshold volume phytomass notably has extended north in the season of 1992-2001, in comparison with the season of 1982-1991, which indirectly testifies to intensifying aridization per the last decade.

In the season of 1982-1991, the border with lower threshold volume of phytomass passed in limens of diffusion of very dry steppe ecosystems (semi dwarf shrub- tussock-cereals), and in the season of 1992-2001, it shifted to a southern strip of zonal dry steppe ecosystems (motley grass-tussock-cereals) and has come nearer to the southern border of diffusion of steppe ecosystems (tussock-cereals) on the east of Mongolia. Thus, the indicated zonal ecosystems can be considered as the ecotone with the most dynamical phytomass changes near to its threshold volume. These ecosystems can be considered as trigger, the phytomass change, which in connection with anomalies of deposits, can be as sustained by the aridization processes at the phytomass above threshold volume and constrain them at phytomass below than threshold volume.

The inter decade phytomass change, which lower than threshold volume is impure on the area: in next decade it grows in ecotone strip between regions and decreases in Inter-mountain depressions district of the Gobi-Altai Range.

1. Introduction

At the end of 20th century, satellite supervision over a condition of Earth surface become a source of the information on vegetation cover dynamics in different natural zones. Attempts of elaboration derivatives based on satellite given parameters, which represent special interest for the characteristic of a vegetation condition on the dry soils, are even more often undertaken. These parameters are rather useful to studying

desertification dynamics, especially in its early prevention. The appreciable place in research belongs to a satellite vegetation index (NDVI) which forms a basis for calculation, for example, the Vegetation Condition Index (VCI), describing a condition of vegetation from stressful up to good in relation to the norm (Kogan, 1987;1990), or threshold green biomasses, is lower for which the probability of aridization a climate grows (Zolotokrylin, 2002, 2003).

In the present report, results of investigations of green biomass dynamics in zonal ecosystems having the ecotone character is considered. They are located near to borders of landscape-ecological regions differing on humidifying, and it is zonal - sub zonal strips (Ecosystems of Mongolia, 1995). The purpose of study—revealing a zonal ecosystems in which green biomass, as a result of climate fluctuations and anthropogenic pressure on pastures, decreases up to threshold value and becomes lower than it, within last decades. For this purpose digital maps representing the mean parameter of threshold green biomass for separate decades (1982-1991 and 1992-2002) and differences of parameters between decades are calculated.

2. Methodological approaches on adaptation Vegetation index to arid zone

In arid regions with prevalence of perennial plants reflection in seen (K1, 0.58-0.68 microns) and in the nearest infrared (K2, 0.72-1.1 microns) ranges decreases in proportion as the vegetation' projective covering increases. It explains the fact that long-term deserted plants have a mix of green and dying off leaves that in aggregate reflect in a seen range more intensive, and more intensively absorb in infrared, than a vegetative cover in regions with more damp conditions. Besides, under low projective covering of plants in deserts, some deflection of an estimation is brought with the soils highly reflective ability in seen and in near infrared ranges of spectrum.

The week data of Vegetation index with the pixel 16x16 km have primary value for studying distribution the weather-induced variations of vegetation cover. However, strengthening of their variability, which reduction the need for additional special procedure of processing (Kogan, Sullivan, 1993) is connected to the high spatial and time sanction of these data. The monthly data of Vegetation Index with the sanction 1x1 ° in this case are more stable and are of interest for regional generalizations. In the given work, monthly values of a vegetative index with the sanction 1x1 ° for the period May - September, 1982-2001 (Distributed AAC ...) are used.

The monthly $NDVI \leq 0.07$ is applied as threshold biomass value. As shown in the previous works (Zolotokrylin, 2002; 2003), the aridization processes in dry lands are well expressed under domination of the radiating mechanism of heat exchange between land surface and atmosphere. This mechanism is shown in arid ecosystems with green biomass $\leq 0,5$ т/ha in dry weight that is equivalent to value $NDVI \leq 0.07$. Thus, the concept threshold biomass is convenient for using for monitoring aridization processes in ecosystems, bringing to desertification. It is necessary to note, that falling biomass up to threshold value in zonal ecosystems is observed as a result of the long-term droughts covering extensive territories more often. Besides, falling biomass becomes more appreciable in ecosystems, subject to human influence.

3. The threshold green biomass cartographical interpretation

For cartographical interpretation the parameter was entered – the period during of which the green biomass does not exceed threshold value. Maps of such parameter were elaborated as follows: on researched territory in everyone one-degree cell the sum of months for a vegetation season (May - September) with $NDVI \leq 0.07$ was determined. Further division of this sum into the sum of all years calculated average volume of a

parameter for May - September for two decades (1982-1991 and 1992-2001). The parameter has dimension of time and shows duration of conditions, in months, at which green biomass achieved or was below threshold volume. Zero an isoline a parameter it is considered as long-term border of distribution mainly aridization processes. The parameter grows in the direction of southern State border of Mongolia, and in extra-arid deserts it comes nearer to the maximum value – to five months.

For the analysis the maps of landscape-ecological division of Mongolia (Gunin, Vostokova, 1995) and zonal ecosystems (Ecosystems of Mongolia, 1995), and also the scheme of geographic distribution of a parameter have been used. Fig. 1A presenting the map on which in color, beginning from light-green up to violet, shows increasing the parameter for the period of 1982-1991. On same map the fat line allocates regions, and by thin lines - the areas corresponding to landscape-ecological division into districts (tab. 1).

Table 1. Scheme of landscape-ecological zones of Mongolia

Region	Province	District
A. Altai-Sayan	AI. Mongol-Altai	A I-1. Mongolian Altai
		AI-2. Ureg-Nuur
	A II. Hubsugul	AII-1. Ulan-Taiga
		A II-2. East Hubsugul
		AII-3. Darkhat
AII-4. Hubsugul		
	AII-5. Sangilen	
B. Transbaikal	BI. Middle-Selenga	BI-1. Buteiliin
		BI-2. Bureg-Nur
	BII. Khentii	BII-1. Baga-Khentii
		BII-2. Tuul-Onon
BII-3. West Khentii		
W. Daguria-East-Mongolian	WI. East-Mongolian	WI-1. Uldzin
		WI-2. Menengiintal
	WII. East-Khalkh	WII-1. Middle Kerulen
		WII-2. Dolongyn Gobi
		WII-3. Dariganga
G. Khyangan	GI. Sub-Hangai	GI-1. Middle Halhingol
		GI-2. Mondtoikhamar
D. Central - Mongolian	DI. Hangai	DI-1. North-Khangai
		DI-2. West-Khangai
		DI-3. South-Khangai
		DI-4. Khankhukhiin
		DI-5. Tesiin
	DII. West Halkh	DII-1. Orkhon
		DII-2. Burgetul
		DII-3. Darkhan
	DIII. Central Halkh	DIII-1. Mandal Gobi
		DIII-2. North Gobi

Region	Province	District
E.Central Asian	EI. Gobi - Altai	EI-1. Mountainous
	EII. Gobi - Tien Shan	EI-2. Inter-mountain depressions
		EII-1. Mountainous foothills
	EIII. Hollow-lake	EII-2. Piedmont
		EIII-1. Uvsunur
		EIII-2. Achitnur
		EIII-3. Lake
		EIII-4. Middle-mountain
	EIV. Walley-lake	EIII-5. Shargiin
		EIV-1. Khangai
	EV. Middle Gobi	EIV-2. Bontsagan-Orognur
		EV-1. Oigiingol - Saishand
EVI. Gobi	EV-2. Dalanzadgad	
	EVI-1. Dzhungarian Gobi	
	EVI-2. Transaltai Gobi	
	EVI-3. Alashan Gobi	
	EVI-4. Gashun Gobi	
	EVI-5. East-Gobi	

As shown on fig. 1A, the zero border of a parameter passes in the west territories between N 46 and 47°, approximately up to E 93°. Then it bends around Big Lakes Hollow from the north and further goes to the east up to E105°, migrating between N45.5 and 46.5°. On a site from Big Lakes Hollow up to the east terminal circuits of Khangai Ridge the border lays within the limits of the Central-Asian region, deviating from border between regions no more than on one hundred kilometers. To the east of E103 ° meridian the border of parameter has latitude direction between N45 and 46°, up to down to State border. Actually the border on this territory passes a little to the north of the Central-Asian region and divides North Gobi (DIII-2) and area Dolongyn Gobi (WII-2) districts almost half-and-half in latitude direction. As a whole the border does not leave for northern limits of very dry steppe ecosystems distribution (semi dwarf shrub-tussock-grasses) (fig. 2). As shown on fig. 2, the period with green biomass below threshold volume in ecosystems very dry steppes does not exceed 0.5-1.0 months.

The territory with green biomass not exceeding threshold volume has increased the next decade 1992-2001 (fig. 1B). The territory has extended due to Lake District (EIII-3), Khangai (EIV-1), and South-Khangai (DI-3.) The territory included completely North Gobi (DIII-2) and Dolodngiin Gobi (WII-2) districts, and significant part of Mandal Gobi (DIII-1). Thus, during 1992-2001 the border of parameter comes nearer to northern State border in a northwest part of Mongolia. In the central part of Mongolia it is stretched on southern slopes of Khangai Ridge. To the east of a ridge the border lays between N46 and 47°, and only in the east territories it falls to the south up to N45°. Thus, in decade of 1992-2001 the period with green biomass below threshold volume has exceeded one month in northern ecosystems of very dry steppes, and in the central part of Mongolia the period has come nearer to one month in ecosystems of dry steppes (tussock-grasses) (fig. 3), and to 0.5 months - in the most southern ecosystems of droughty steppes (tussock-grasses) (fig. 4).

Using the method of superposition for map of landscape-ecological zones and the period with green biomass, not exceeding the threshold volume, contains the information for areas in which changes of the period in compared decades are insignificant. To such areas we relate Transaltai Gobi (EVI-2) and Alashan Gobi (EVI-

3) (fig. 1). In this connection it is important to allocate zonal ecosystems in which there is a sharp change of the period on area. As shows fig. 5, the maximal change of the period is marked in a strip of south desert ecosystems. Here in direction from the north to the south, the period will increase from 1,5 months up to 4 (transition from yellow to dark-violet color). In spite of the fact that fig. 5 characterizes a situation of 1982-1991 decade, the zone of sharp change of the period in the next decade is observed in same ecosystems up to E 102° meridian, and to the east in a strip of middle desert ecosystems.

For study vegetation dynamics the zonal ecosystems revealing is interesting, where the greatest changes of the period with green biomass below threshold are marked. On fig. 6 and 7 colors shows change of the period in a decade of 1992-2001, in comparison with previous decade. Brown shades show increase in the period, and flavovirent – reduction. It is visible from figures; the appreciable increase in the period at 0,5-1 months last decade, in comparison with previous. It has taken place mainly in ecosystems of very dry steppes (semi dwarf shrub-tussock-grasses) and in ecosystems of deserted steppes.

Alongside with expansion of territory with green biomass below threshold to the north, last decade some reduction of the period with threshold biomass in a southwest part of Mongolia (especially in east part of a strip south desert ecosystems) (fig. 6,7) is observed. The area of reduction of the period lies between Mongolian State border - in a southwest, and E104° meridian. In some local places of this area the period has decreased almost for 1 month. Thus, last decade promotion of border with green biomass below threshold volume to the north and increase in its period to the greatest degree in a southeast of the Central - Asian region was marked. The given result testifies to aridization processes strengthening on this territory. Local reduction of the period with green biomass below threshold volume (aridization easing) in inters mountain-hollow areas of region were simultaneously observed.

4. Conclusion

The joint analysis of map of landscape-ecological zones of Mongolia, maps of zonal ecosystems and geographic distribution of the period with green biomass not exceeding threshold volume ($NDVI \leq 0.07$) allows to make the following conclusions:

Ten years' change in biomass near to its threshold value dominates in transition strip between landscape-ecological regions: Central - Asian and lying to the north Central - Mongolian and Daguria-East-Mongolian. Inter decade biomass changes have zonal character.

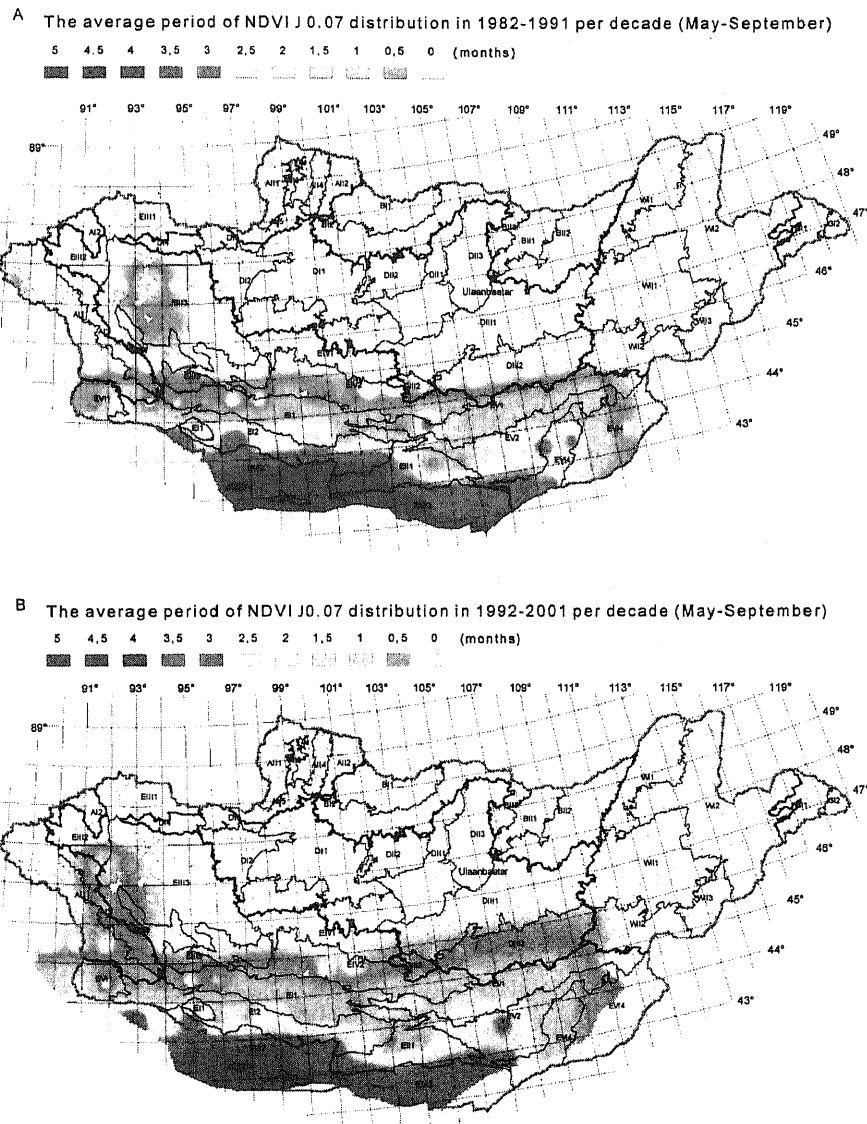
The territory with biomass below threshold volume during 1992-2001 has appreciably extended to the north, in comparison with the period of 1982-1991, that indirectly testifies to aridization strengthening last decade.

During 1982-1991 the border with in biomass below threshold volume passed within the limits of distribution ecosystems of very dry steppes (semi dwarf shrub-tussock-grasses), and during 1992-2001 it was displaced in a southern strip of zonal ecosystems of droughty steppes (motley grass-tussock-grasses) and has come nearer to southern border of steppe ecosystems distribution (tussock-grasses) in the east Mongolia. Thus, specified zonal ecosystems it is possible to consider as ecotone with the most dynamical biomass changes near to its threshold volume. These ecosystems can be considered as trigger, biomass changes of which in connection with precipitation anomalies can to support the aridization processes under biomass above threshold volume, and to constrain them under biomass below threshold volume as well.

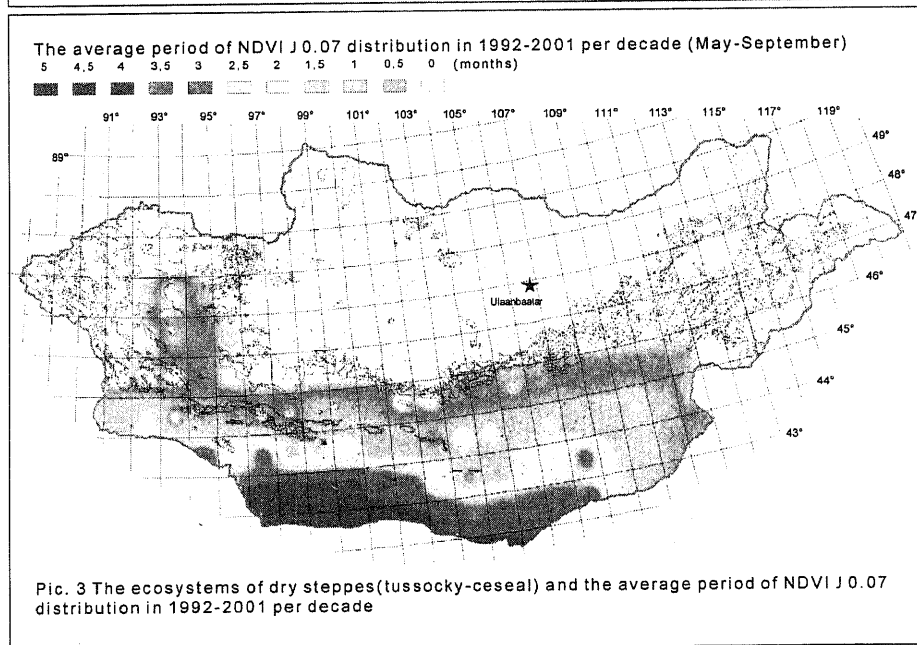
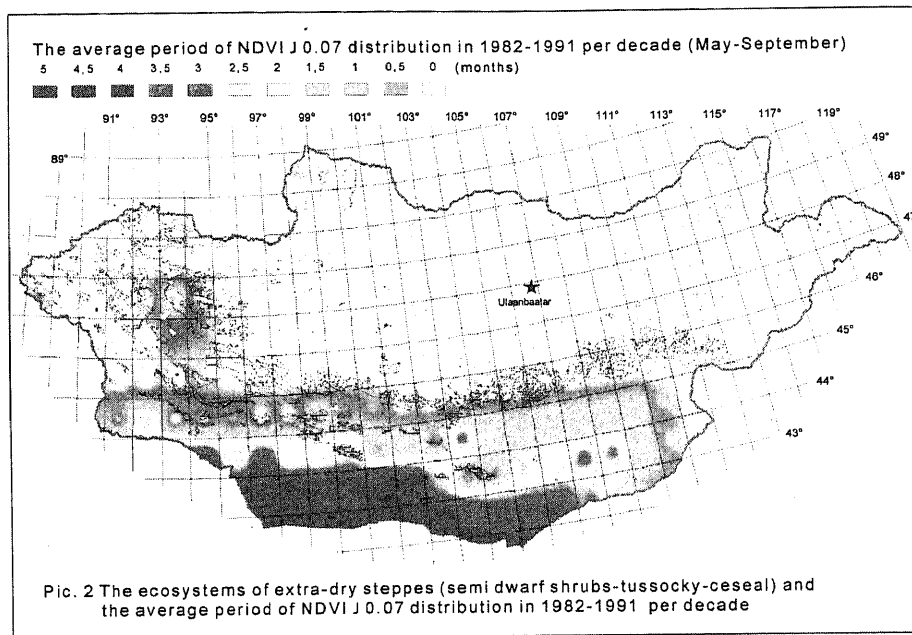
Inter decade biomass change below threshold volume is dissimilar in territory: during the last decade it grows in ecotone strip between regions and decreases in Mountainous district of Gobi Altai region.

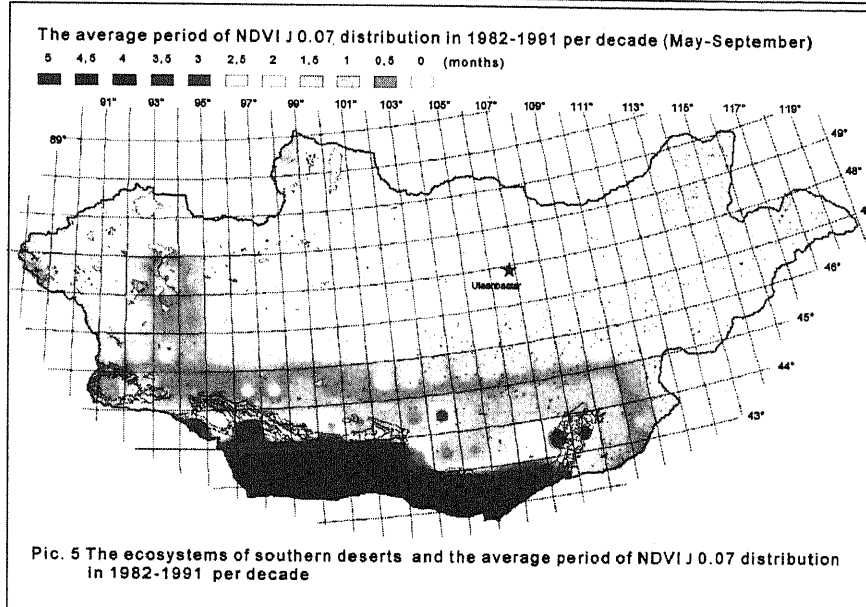
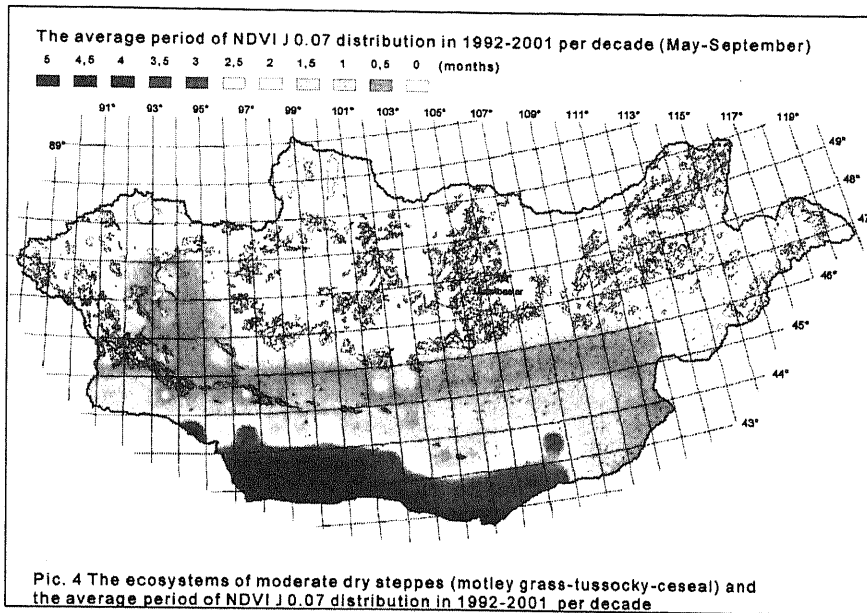
References

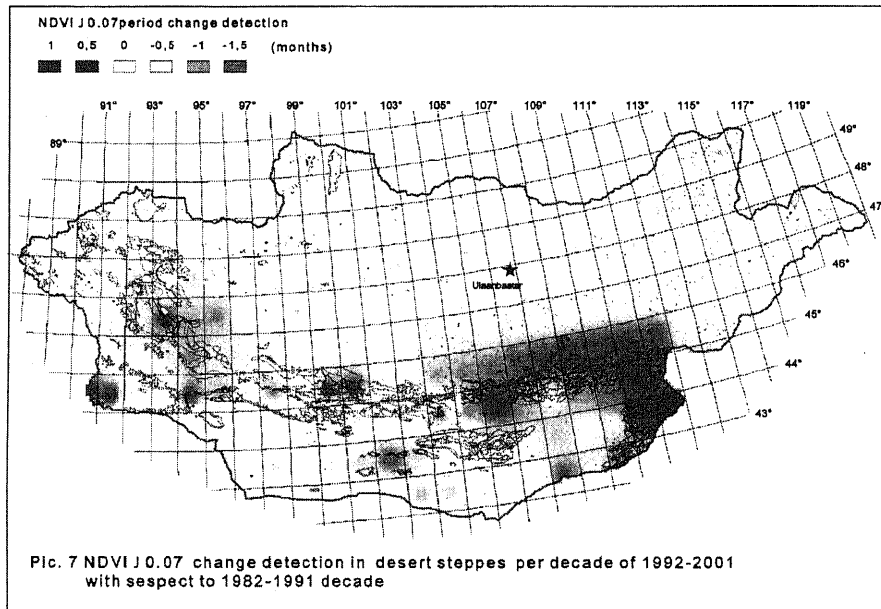
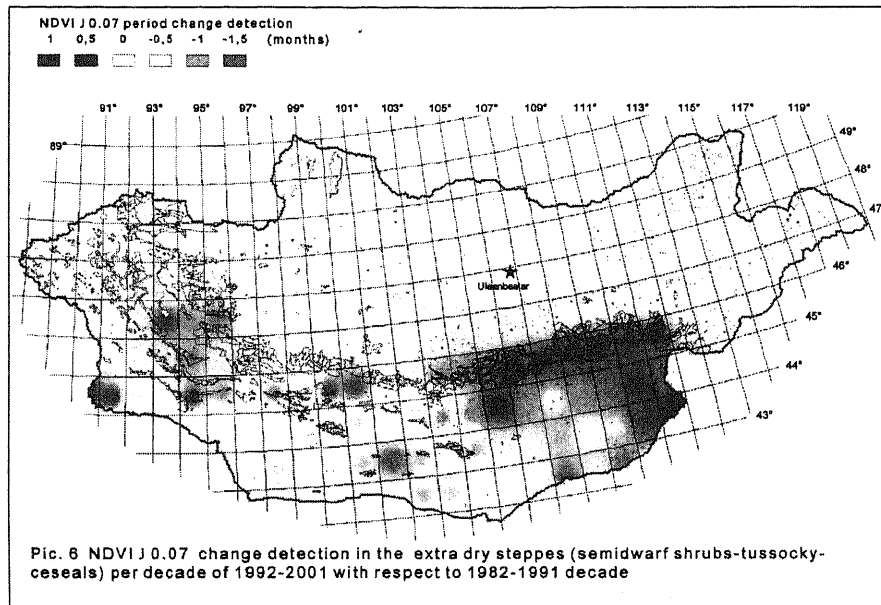
1. Zolotokrylin A.N. The climate aridity indicator // *Arid ecosystems*. 2002. T. 8, № 16, pp. 47-59.
2. Zolotokrylin A.N. *Climat desertification*. M.: Science, 2003. 246 p.
3. *Ecosystems Mongolia: distribution and a modern condition* // *Biological resources and an environment of Mongolia*. T. XXXIX. M.: Science, 1995. 219 p.
4. Distributed Active Archive Center. Pathfinder AVHRR Land Data. Internet: [htt: // daac/gsfc.nasa.gov/](http://daac/gsfc.nasa.gov/)
5. Gunin P.D., Vostokova E.A. *Ecosystems of Mongolia. The map*. Scale 1:1000000. 15 sheets, Moscow, 1995
6. Kogan F.N. Vegetation index for areal analysis of crop conditions. Preprints, Proc. 18th Conf. On Agricultural and Forest Meteorology, 1987. West Lafayette
7. Kogan F.N. Remote sensing of weather impacts on vegetation in non-homogeneous areas. *Int. J. Remote Sens.*, 1990.11, pp. 1405-1419.
8. Kogan F.N., Sullivan J. Development of global drought-watch system using NOAA/AVHRR data. *Adv. Space Res.*, 1993, 13 (5), pp. 219-222.



Pic. 1 The landscape-ecological zoning of Mongolia and the average period of NDVI J 0.07 distribution in 1982-1991 and 1992-2001 per decade







THE NEED OF GIS FOR NATURAL RESOURCES MANAGEMENT AND POLICY DEVELOPMENT IN MONGOLIA

Tsutomu Suzuki, Environmental Policy Adviser to MNE/JICA
Davaasuren Narangerel, Informatics &RS Institute, Mongolian Academy of Sciences

1. Introduction

Resources and environment are limited. For sustainable use of limited natural resources, there is need for agreement among stake holders environmental management. It is important and also effective to plan an environmental management have based on environmental information systems. GIS and its visual presentation are important communication tools for resources management planning.

2. Natural Resource Management Problems in Mongolia

Information availability is low. Data are scattered and difficult to find and obtain. Discussions using maps and visual presentations are poorly implemented in Mongolia. Few people use handouts and other materials in discussion.

3. Important Factors in Resource Management

For proper implementation of resource management, important factors include public participation, understanding of resources management and logical extension and transparency of planning process.

3.1. Public Participation

As the most of environmental issues concern land use, actual land users—the ordinary public—have to be involved in land production of resources management plans. Otherwise the management plan will be merely paper plan.

3.2. Understanding of Resources Management

Understanding of the needs of resources management and the awareness of the stakeholders are the most basic elements for effective implementation of resources management the plans. Therefore, the choice and use of the right communication tools are most important. Illustration and presentation on maps are effective communication tools for land use planning.

3.3. Logical extension and transparency of planning process

It is possible to view the environment as a structure by using environmental information system data. Also it is possible to handle simulation data. The nature of the planning process of resources management requires people with rationality to heap many others to understand the plan.

It is not a good idea for the planning process to be concealed in a black box. The thinking process of the planning must have transparency and all the information which used in the process must be accessible to everyone.

4. GIS

GIS as a scientific application in geology, environment and natural resources management, began to be used in Mongolia in 1990. But the applications of GIS and Remote Sensing information for environmental policy and decision-making process are quite very new and there needs to be more facilitation and development. For future development of Mongolian protected areas under the Ministry of Nature and

Environment, the applications of GPS, GIS and Remote Sensing are very important, especially if we consider that actual protected areas boundaries are not defined with GPS. Descriptions of protected area boundaries defined in terms of peak mountain points and centers of rivers often could lead to mismatches of these boundaries on produced maps. Establishing “hard”, precise GPS points for protected area boundaries, especially in “crucial” areas near mining-licensed areas and settlements, will help to avoid problems and issues of illegal mining, illegal hunting, logging and man-made forest fires inside the protected areas.

5. Environmental Policy

5.1. Characteristics of Mongolia

The great extent of the territory, small population and diverse natural ecosystem are the characterize of Mongolia. Therefore it is important to grasp the nature in the big scale and smaller cost.

At this moment in Mongolia, the mining industry and the special protected area system are contradicting sharply. There was plan to extend the protected area up to 30% of the territory by the year of 2030. In 2003, 70% of the territory already issued and covered by some of the mining licenses. Where will Mongolian people live in the future? Unless Mongolia sticks to the present policy, which does not allow mining inside the special protected areas, it must be the turning point not only for the protected area system but also nature conservation in this country. If one example of excluding special protected area approved in the parliament, it must occur a domino effect and disrupted the protected area system in Mongolia.

5.2. Applicable in many fields

GIS and satellite tracking systems help to understand and find the gap between the designated area and actual use area for migratory animals, such as the white-tailed gazelle. Wildlife conservation issue is also a matter of land use, how much resources we should allocate them to avoid conflict with domestic livestock.

GIS and environmental information system can be widely use these technologies to pasture land management, combating with the desertification, protected area, air quality and water quality management.

6. Needs and Advantages of Introducing GIS

6.1. Centralized GIS and environmental database systems

At present there is no existing centralized environmental database. A number of major components in whole geo-information infrastructure such as Geospatial data standard, solid policy for data quality are hardy missing.

In order to improve environmental information supply and information quality, standards and roles for data sharing and exchange should be given to centralized agencies of the Ministry for Nature and Environment.

6.2. Data quality

Many current policy makers of environmental information still do not have access to accurate GIS information. Most of the existing GIS data are not processed with adequate accuracy—and some basic operations with spatial data such as data entry, geometric and radiometric correction, geo-referencing, primary classification are not processed at a degree which suits users needs and by people with expert knowledge.

The issue of spatial data geo-referencing differs at organizations dealing with GIS information. Use of old Soviet system of projection and ellipsoid has been discussed many times, but still it is not clear and not considered from the Geodesy and Cartography department. Setting up standards such as national reference system,

Mongolian national standardized spatial data sets of geographical names, administrative boundaries, thematic information—soil, hydrology, underground and ground water resources, vegetation, population and meta-data sets will improve Geospatial data infrastructure in Mongolia.

6.3. Data processing

Processing spatial data with ARC VIEW GIS is quite popular in Mongolia. It is one of the cheapest ways of producing GIS maps in a “quick and dirty” way. Data processing could take place at specialized agencies that can directly communicate with users, substantially improving GIS data quality.

6.4. Data integrity

Many sources of GIS and environmental data agencies, organization operate separately without data and information exchange sharing. Situations commonly where organizations overlap work of others. Organizations arise working at Environment field have potential in policy decision making and therefore, data integration from different sources could influence decision and policy making process in a positive way.

6.5. Capacity building

In recent years in Mongolia demand for accurate GIS information on environmental issues is rapidly increasing. Many environmental experts working both outside and inside Mongolia are seeking support from the Ministry of Nature and Environment to share data at national, continental and global levels. The issue of building institutional capacity at both policy and technical levels will integrate planning, management, monitoring and decision policy making processes. The linkage between organizations, identification of training needs, personnel training should be developed and optimized.

One of the negative aspects concerning GIS training in Mongolia is the selection of the highest ranking people from ministries, without appropriate educational backgrounds on environmental subjects. The technical personnel dealing with environmental information from relevant organizations of the National Forest Management Center, the Water Resource Center and others do not have access to information on new technology on GIS and RS. Many are using old Soviet methodology to estimate forest and water resources. In very rare cases some Remote Sensing information with production of GIS maps without accuracy standards on ARC VIEW GIS systems in a “quick and dirty way” do not really meet international standards and do not encourage data exchange at international level neither at national level.

6.6. Project implementations with freedom of information

The issue of data information exchange sharing between different organizations should be one of the milestones in Mongolia. Setting up Mongolian national geospatial standards will substantially improve and it will welcome implementation of environmental projects into Mongolia. GIS information freedom in this context will be on appropriate data sharing, data exchange standards in a settled way without seeking illegal GIS data sources, without obtaining unreliable and not accurate GIS information from different sources and organizations.

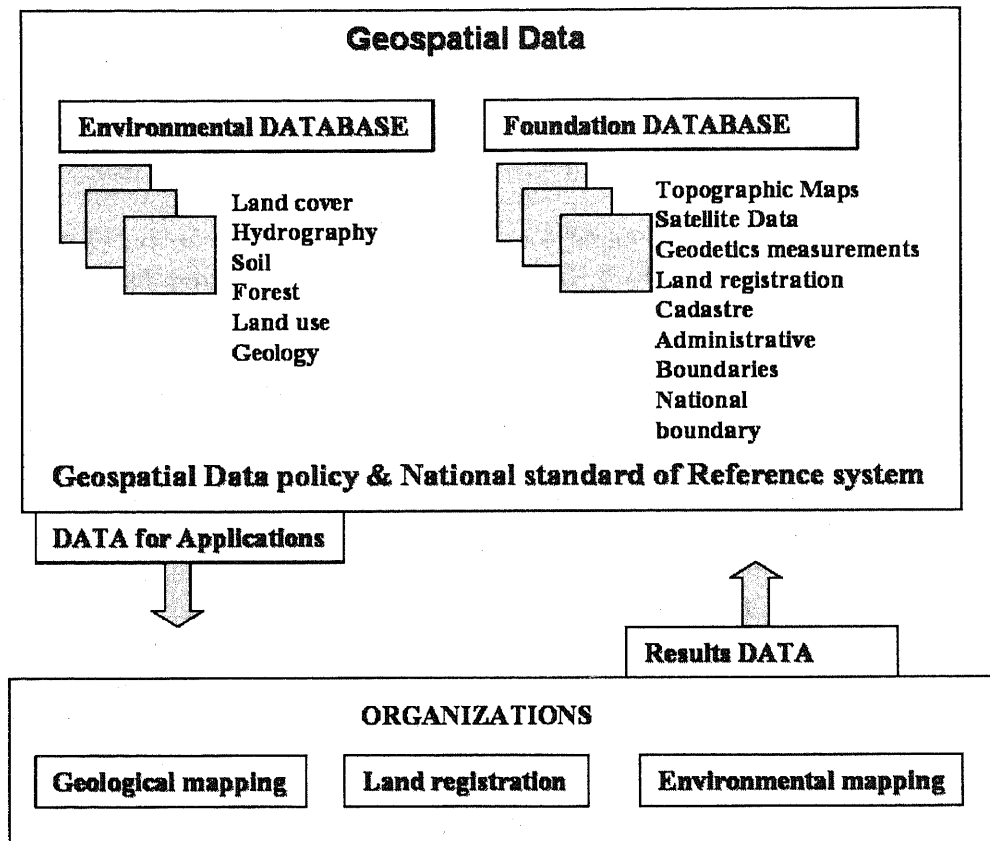
6.7. Maintenance and updating

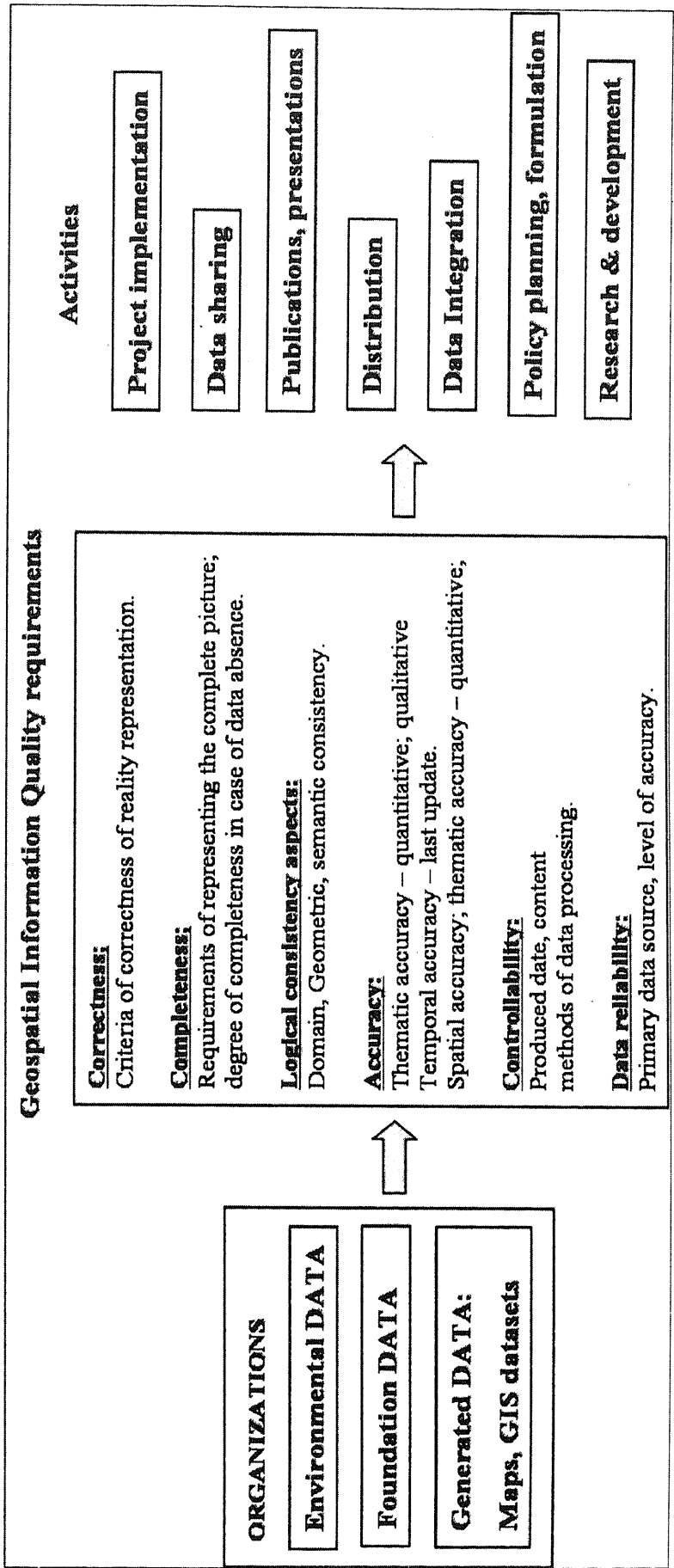
Any established GIS system needs regular updating of information. The information exchange and information flow between organizations working in environmental fields and organizational linkage should be optimized and further developed.

7. Conclusions

The idea and need to formulate a centralized environmental database at the Ministry of Nature and Environment and the development of a geospatial data infrastructure

framework at a national level is substantial. Efforts have to be made in terms of capacity building, establishing mechanisms for data exchange and sharing. Organizations working on environmental issues have to be involved. The Ministry of Nature and Environment should formulate and implement information strategy for sustainable environmental management. The process of geo-information flow between different agencies of the Ministry of Nature and Environment will need settled up information infrastructure framework and cooperation. Basic knowledge of GIS, GPS and RS technology applications for environmental purposes is one of the primary needs of the Ministry of Nature and Environment personnel.





LAND COVER CLASSIFICATION IN THE YELLOW RIVER BASIN USING MODIS DATA

Masayuki Matsuoka¹, Tadahiro Hayasaka¹, Yoshihiro Fukushima¹, Yoshiaki Honda²

1 Research Institute for Humanity and Nature, Japan

E-mail: matsuoka, hayasaka, yoshi@chikyu.ac.jp

2 Center for Environmental Remote Sensing, Chiba University, Japan

E-mail: yhonda@cr.chiba-u.ac.jp

Abstract

Land cover classification over Yellow River basin, China, by means of simple decision tree classification method using multi-temporal metrics derived from MODIS data is demonstrated in this paper. Since land cover is one of the input parameters in hydrological model, the critical feature of classification method is to control the classification result using threshold values. The tentative results show good correlations with existing digital land use map, though small overestimation or underestimation are uncovered in several categories and improvement is necessary in discriminating the single cropped agricultural field from natural grassland. Adjustments of the threshold values established in the decision tree would be done with the aid of higher resolution satellite data.

1. Introduction

The development of water resource management model in the Yellow River basin, China, is important because the stream of the river has not reached the Bohai Sea for many days in a year since 1970s as a result of climate change and human activities. The land cover and its change reflect the interactions between human activities, such as agriculture and urbanization, and nature as dynamics of water and energy, therefore, it is one of the essential parameters for the development of model. The purpose of this study is to analyze the land cover and its change for 20 years since 1980s over Yellow River basin using satellite data.

This study consists of four parts and three kinds of sensors. Terra/MODIS, NOAA/AVHRR, and Landsat/TM or ETM+ are utilized in each part according to its spatial and temporal resolutions. First part is land cover classification using MODIS. MODIS is a new sensor operated since 1999, and it has two 250 meters bands in visible and near infrared. MODIS view the entire Earth's surface every 1 to 2 days. The land cover classification map is generated from time series MODIS data in 2002 by supervised decision tree method. Second part is comparison of the land cover map with AVHRR data. AVHRR is operated over twenty years from the end of 1970s [1], and precious and long term seamless data are archived. The spectral and temporal characteristics of AVHRR data in 2002 are compared with each land cover category of the classification map. Third is the detection of land cover change since 1982 using time series AVHRR data. In fourth part, TM and ETM+ are utilized for validation and tuning of the land cover classification and change detection, and the detailed analysis intended for the drastically changed area.

2. Methodology

2.1 Data

The product named "Surface Reflectance 8-Day L3 Global 250m" (MOD09Q1) is used in this study. MODIS use 250m all over Surface Reflectance is a two-band product computed from the MODIS Level 1B land bands 1 and 2 (centered at 648nm and

858nm, respectively). The product is an estimate of the surface spectral reflectance for each band as it would be measured at ground level if there were no atmospheric scattering or absorption. The 45 periods of MOD09Q1 products in the whole of 2002 are re-projected to Equirectangular (latitude/longitude) projection by MODIS Reprojection Tool [2]. The spatial coverage is from 20⁰-50⁰ north, and 90⁰-150⁰ east, and the resolution is 7.5 arc seconds. Six multi-temporal metrics; annual maximum NDVI (NDVI_ann_max), annual minimum NDVI (NDVI_ann_min), annual amplitude of NDVI (NDVI_ann_amp), annual minimum band 1 reflectance (Ref1_ann_min), annual minimum band 2 reflectance (Ref2_ann_min), time series of monthly metrics (April minimum NDVI (NDVI_apr_min), June maximum NDVI (NDVI_jun_max), and August minimum NDVI (NDVI_aug_min) are derived from the time series scales MODIS data.

2.2 Algorithm

Land cover classification from regional to global scales has been implemented with the use of AVHRR data by means of a variety of classification methods as such clustering [3], maximum likelihood classification [4], decision tree classification [5], and hybrid algorithm of decision tree and neural network [6]. Running et al.[7] proposed a simple new logic for classifying global vegetation based on the structural characteristics of vegetation. Since the classification result in this study is the input parameter for the hydrological model, the critical feature of the classification method is to control the classification result using simple parameters.

The supervised decision tree classification method is selected in this study easiness in controlling the classification result. The decision tree classification algorithm has significant potential for land cover mapping problems [8], and its performance is acceptably good in comparison with that of other classifiers, except with high-dimensional data [9]. The scheme of the classification method in this study is shown in Figure 1. The eight threshold values are arranged in the each steps of the decision tree, and the result of the land cover classification is tuned by these threshold values. Ref2_ann_min is applied to extract water area since the spectral reflectance of water in near-infrared wavelength band is much lower than that of land surface. NDVI_ann_max represent the most active status of the vegetation in the year, hence it is applied to categorize the non-vegetation and less-vegetation from other vegetated land. NDVI_ann_min is applied to the vegetated area for the discrimination between evergreen and deciduous vegetation. Ref1_ann_min is also applied to the vegetated area to discriminate tree type and grass type vegetation based on the rough assumption that the tree type land surface is generally “darker” than grass type land in the visible wavelength. The time series of NDVI_apr_min, NDVI_jun_max, and NDVI_aug_min are jointly used to extract double cropped agricultural areas especially in the downstream of Yellow River basin. The first cropping season is from middle of February to end of May, and second season is from July to middle of November in this region. This phenological characteristic is unique compared with other natural grasslands or single cropped agricultural fields. Therefore, if NDVI_apr_min is greater than NDVI_jun_max and NDVI_jun_max is less than NDVI_aug_min, that pixel is categorized as double cropped agricultural field. NDVI_ann_amp and NDVI_ann_max are applied to deciduous grass type vegetation land to separate single cropped agricultural fields from natural grassland. These two categories have quite similar spectral and phenological characteristics. Therefore, this criterion (if NDVI_ann_amp is higher than threshold and NDVI_ann_max is higher than threshold, then it is categorized as single cropped agricultural field) has no supportive evidence and it is derived fully empirically by trial and error approach.

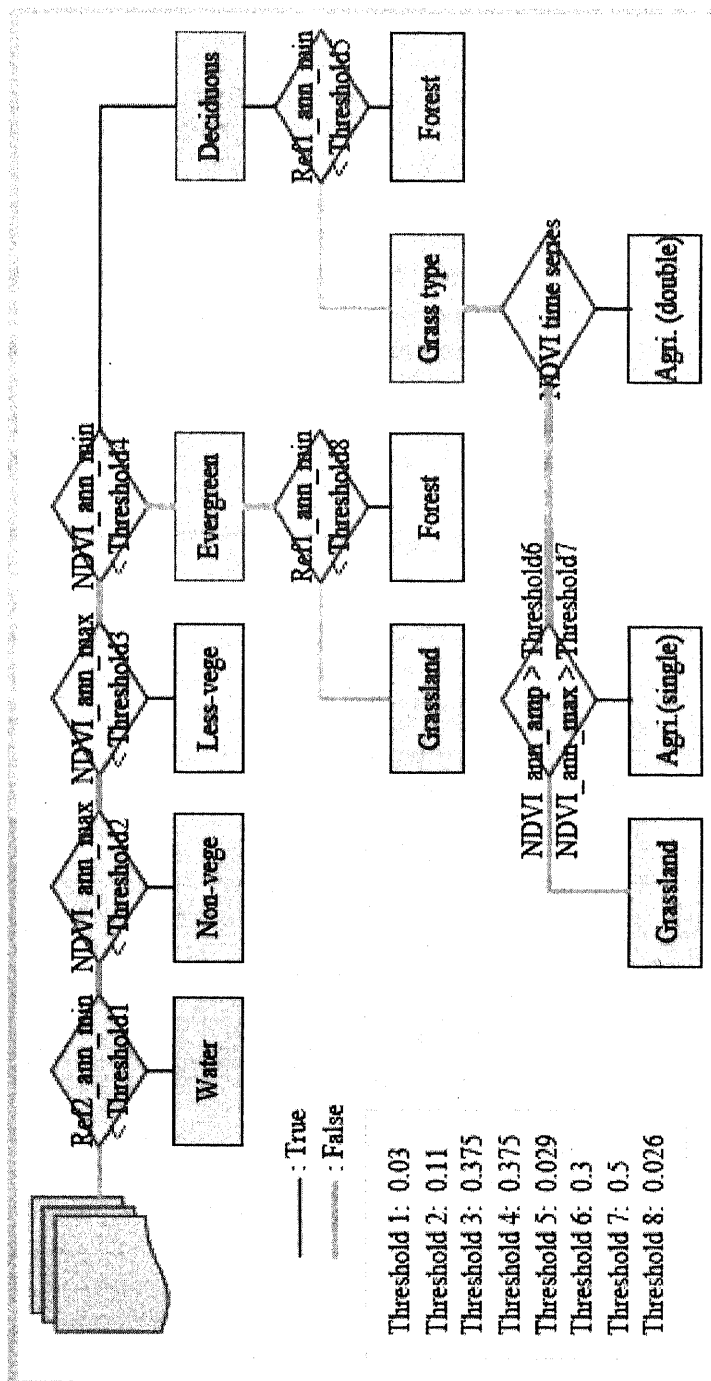


Figure 1. Flow of the land cover classification

Nine land cover categories (water, non-vegetation, less-vegetation, evergreen forest, evergreen grassland, deciduous forest, deciduous grassland, single cropped agricultural field, and double cropped agricultural field) are established from the viewpoints of the parameterization of the water balance model used in this study, and the accuracy of the land cover classification. In general, parameterization of the land surface properties in the physical model is expected to be difficult, and the accuracy of the land cover classification will deteriorate with increase in the number of classes. Therefore minimum numbers are established at this stage, and might be increased hierarchically with a focus on outcomes from the model.

3. Results and discussion

The land cover classification map is shown in Figure 2. The threshold values are determined manually using image processing software. According to the visual interpretation, non-vegetation, less-vegetation, evergreen forest, and double cropped agricultural field have relatively high agreements with existing land cover maps and satellite based classification maps, though the categories of land cover do not fully corresponded to each other. These categories have distinct characteristics in NDVI or reflectance. single cropped agricultural field is not sufficiently discriminated from grassland, and it is overestimated especially in the northern region from eastern Siberia to northeastern China, and southern region around Xizang (Tibet), Sichuan, and Qinghai provinces. In these regions, the multi-temporal metrics of grassland and agricultural field used in this study show the indistinctive characteristics as a result of the similarity in spectral reflectance in the two bands land, (and thus also in NDVI and phenology).

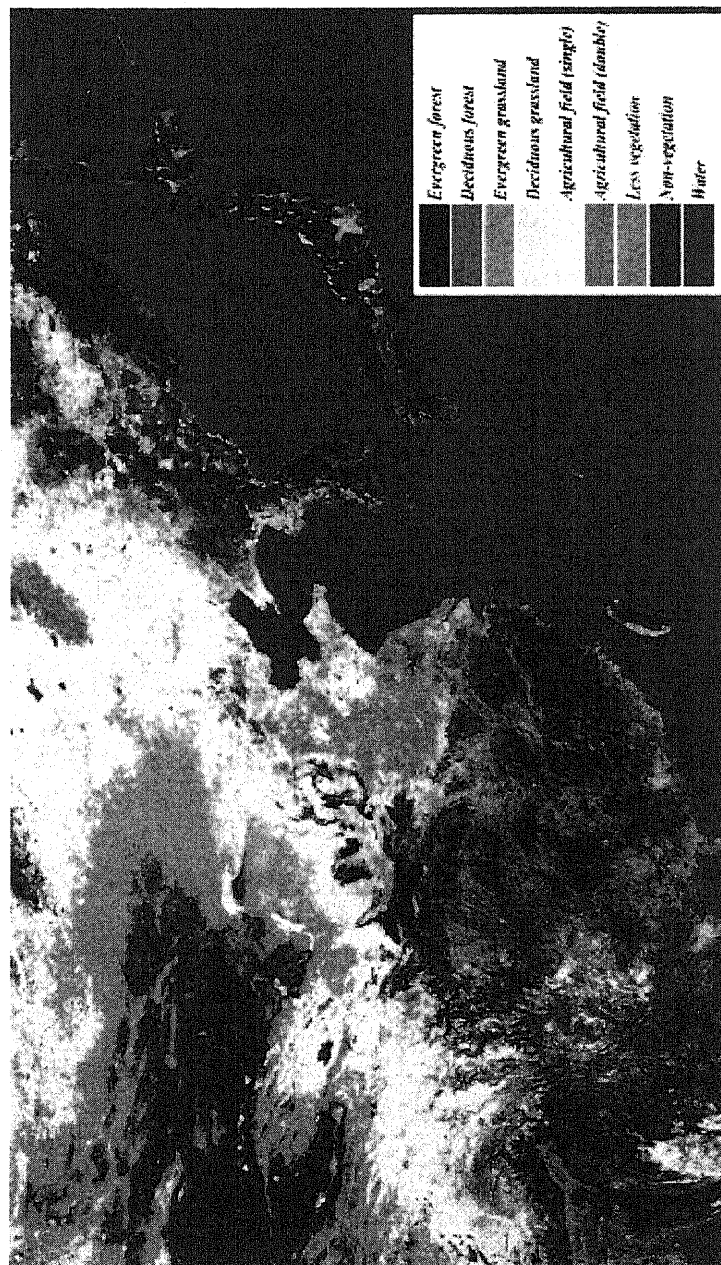


Figure 2. Land cover classification map

Areas of each land cover category are compared with the existing land use map “1 KM Grid Data of land-use and land-cover of China” (CASW). This map is about 1 km grid data of land use and land cover of China in 1996. The value of a grid in every land use layer is a percentage coverage of the land use in the grid (1 km²), derived from 1:100,000 land-use vector map of China.

The areas of five land use categories (forest, agricultural field, grassland, less-vegetation, and non-vegetation) are figured out for each province by aggregation of the grids and appropriate categories of each map. The results are shown in Figure 3. Good correlations occur in forest and non-vegetation, though classification result has the tendency to overestimate relative to the CASW data. In case of agricultural field, most provinces where there are small areas of agricultural fields resulted in underestimations. In contrast, grassland shows countertrend, that is, provinces with small grassland areas have trends of overestimation, but in provinces with larger grassland, underestimations. Comparison of total area of agricultural field and grassland is shown in Figure 3 (f). Total area has much better agreement than individual comparison. This might be because of the difficulty in discriminating the single crop agricultural field from natural grassland mentioned above. To overcome this insufficiency in performance, utilization of additional information such as other temporal metrics, fine resolution satellite data, and digital elevation model is recommended. The tuning of the threshold values will be implemented by means of TM and ETM+ data. These higher resolution image are geometrically overlaid to the MODIS image, and finer distribution of land use is interpreted manually and semi-automatically to get the appropriate threshold values.

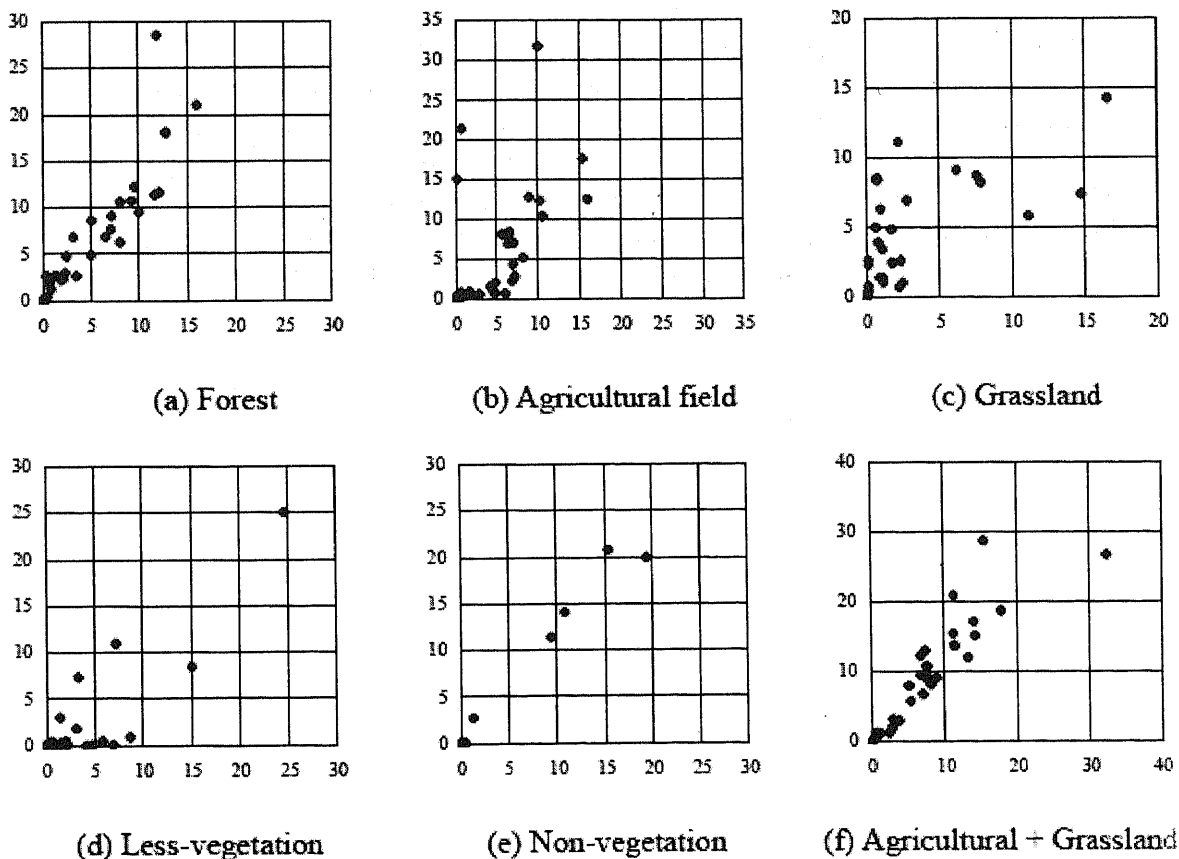


Figure 3. Comparison of land use area with CASW data
(horizontal axis: CASW data, vertical axis: this study, unit: 10000km²)

4. Conclusion

The land cover classification over Yellow River basin by means of simple decision tree classification method using MODIS data is demonstrated in this paper. This method is designed to control the classification result by tuning of threshold values, and to be applied to the multi-temporal metrics that represent the phenological characteristics of the vegetation. The classification result show basically good agreements with existing land cover map, though certain degrees of overestimation or underestimation are encountered. The tuning of the threshold values would be implemented by the aid of fine resolution satellite data. Potential of the additional data to get around the difficulty of discriminating of single cropped agricultural field from natural vegetation should be investigated.

References

- [1] Kidwell, K. B., 1998. NOAA polar orbiter data user's guide.
- [2] USGS - NASA Distributed Active Archive Center. MODIS reprojection tool distribution page. <http://edcdaac.usgs.gov/landdaac/tools/modis/index.asp>
- [3] Pan, Y., et al., 2003. An integrate classification of vegetation in China based on NOAA AVHRR and vegetationclimate indices of the Holdridge life zone. *International Journal of Remote Sensing*, 24(5), pp. 1009-1027.
- [4] Liu, J. Y., et al., 2003. Land-cover classification of China: integrated analysis of AVHRR imagery and geophysical data. *International Journal of Remote Sensing*, 24(12), pp. 2485-2500.
- [5] Townshend, J., et al. 1999. MODIS Enhanced Land Cover and Land Cover Change Product Algorithm Theoretical Basis Documents (ATBD).
- [6] Friedl, M. A., et al., 2002. Global land cover mapping from MODIS: algorithms and early results. *Remote Sensing of Environment*, 83, pp. 287-302.
- [7] Running, S. W., et al., 1995. A remote sensing based vegetation classification logic for global land cover analysis. *Remote Sensing of Environment*, 51, pp. 39-48.
- [8] Friedl, M. A., et al., 1997. Decision tree classification of land cover from remotely sensed data. *Remote Sensing of Environment*, 61, pp. 399-409.
- [9] Pal, M., et al., 2003. An assessment of the effectiveness of decision tree methods for land cover classification. *Remote Sensing of Environment*, 86, pp. 554-565.

AERIAL PHOTOGRAPHY INTERPRETATION OF VEGETATION IN THE FLOODPLAIN ZONE OF SHISHKHED RIVER VALLEY, MONGOLIA

E. Munguntulga¹, G. Punsalpaamuu¹, H. Nishida², Ts. Jamsran³

¹-Mongolian State University of Education,

²-Kanazawa University, Japan

³-National University of Mongolia

1. Introduction

Asia's continental watershed runs through Mongolia, splitting the country's more than 4,000 rivers and streams into three drainage basins. Roughly a quarter of Mongolia's territory belongs to the Arctic drainage basin. This area includes the Selenge river watershed which is a major tributary of Siberian's famous Lake Baikal, the Shishkhed (west of Khovsgol Lake) and Bulgan rivers.

The rivers in a smaller area in northeastern Mongolia make up the Pacific drainage basin; including the Onon, Uldz, Kherlen and Khalkhiin gol rivers, which flow east via Russia's mighty Amur River.

The majority of Mongolia's territory, however, drains to no ocean. In the northwest, the basin encompasses the depression of the Great Lakes, including Uvs, Khar Us, Khar, and Khyargas lakes. In central Mongolia, the basin includes the Valley of the Lakes in the Gobi region. The lakes, rivers, streams, marshes, oases and other wetlands in each of the six preceding natural zones support their own distinctive flora and fauna.

Wetlands provide crucial habitat for the waterfowl and water-frequenting birds that make up a majority of Mongolia's migratory bird species. Especially important to biodiversity are the huge reedy marshes bordering lakes in the Shishkhed watershed and in the Depression Great Lakes and the dynamic floodplains of Mongolia's larger rivers.

Though they occupy a relatively small area of the country, riparian areas have great importance to the nation. Wetlands are both vital to nomadic livestock husbandry and vulnerable to impacts of high concentrations of people and animals near water.

2. Materials and methods

Our investigation area is located in the Shishkhed River Valley of the Darkhad depression centred at 99° 23' 650" east 50° 57' 650" north. Study the summer season from August 2002 to July 2003. In the floodplain zone we choose 5 study areas, which we classified by plant species. Aerial photographs from each study area were taken by a motor paraglide and CCD camera, ORYNPUS CAMEDIA 2500L which has 200,000 pixels resolution. During the research work, aerial photographs were interpreted with ground plant association using the ArcView 3.2a and Orima packet program.

3. Research results:

1. The Shishkhid River Valley has 3 types of vegetation: forest, steppe and meadow. In this place we chose 5 research areas. These included sedge meadow, steppe meadow, stipa steppe, mixed forest, and formations (picture 1).
2. In sedge meadow formations; hippuris – sedge, sedge – calamagrostis, sedge – forb associations and simulates yellow green color dominated. The center of the sedge meadow formations has water, which is shown in black.
3. In steppe meadow formations; kobresia – sedge, sedge – grass, grass – forb, bush – dasiphora associations and simulates general green color dominated.
4. In stipa – steppe formation; elymus – stipa, grass – forb, grass – artemisia associations and simulates grey color dominated.

5. In mixed forest formation; larix – bush, bush – dasiphora associations dominated.

Table 1 – Shows dominant do species

Area	Species
Sedge meadow	1. Hippuris vulgaris 2. Carex rostrata 3. Carex caespitosa /захаар / 4. Beckmania 5. Agrostis 6. Calamagrostis epigeios 7. Potamogeton 8. Polygonum viviparum 9. Sanguisorba officinalis 10. Vicia cracca 11. Kobresia Bellardii 12. Salix 13. Pedicularis rubens /довон дээр/
Steppe meadow	1. Carex 2. Kobresia Bellardii 3. Parnasia palustris 4. Cirsum 5. Potentilla anserina 6. Potentilla dealbata 7. Potentilla bifurica 8. Sanguisorba officinalis 9. Thalictrum 10. Taraxacum 11. Silene repens 12. Galium verum 13. Gentiana decumbens 14. Elymus dahuricus 15. Artemisia 16. Koeleria macrantha 17. Calamagrostis epigeios
Stipa steppe	1. Elymus secalinus 2. Artemisia frigida 3. Artemisia boreale 4. Heteropappus biennis 5. Potentilla acualis 6. Potentilla bifurca 7. Aster alpinus 8. Leontopodium ochroleucum 9. Ephedra monosperma 10. Amblynotus 11. Thalictrum minus 12. Bupleurum scorzonerifolia

	13. <i>Oxytropis glabra</i> 14. <i>Kobresia Bellardii</i> 15. <i>Heteropappus biennis</i> 16. <i>Stipa</i> 17. <i>Agropyron cristata</i>
Mixed forest	1. <i>Larix sibirica</i> 2. <i>Salix</i> 3. <i>Dasiphora fruticosa</i> 4. <i>Pedicularis resupinata</i> 5. <i>Ptilagrostis mongolica</i> 6. <i>Anemone sylvestris</i> 7. <i>Sanguisorba officinalis</i> 8. <i>Equisetum arvense</i> 9. <i>Potentilla anserina</i> 10. <i>Gentiana decumbens</i>

4. Conclusions

1. Though they occupy a relatively small area of the country, riparian areas have great importance to the nation. Wetlands are both vital to nomadic livestock husbandry and vulnerable to impacts of high concentrations of people and animals. The floodplain plant association and formation conditions in particular seasons of the year and their growth dynamism are very essential in ecological assessment of the region. Especially in wide areas of research, aerial photography application procedures are useful. On the basis of aerial photography, we interpreted different kinds of plants in the floodplain zone of the Shishkhed River. The aerial photographs give a different color simulation according to the soil temperature and moisture distribution.
2. In the future, application of aerial photography with actual ground interpretation of plant will become one of the priority research subjects in the Darkhad Depression.

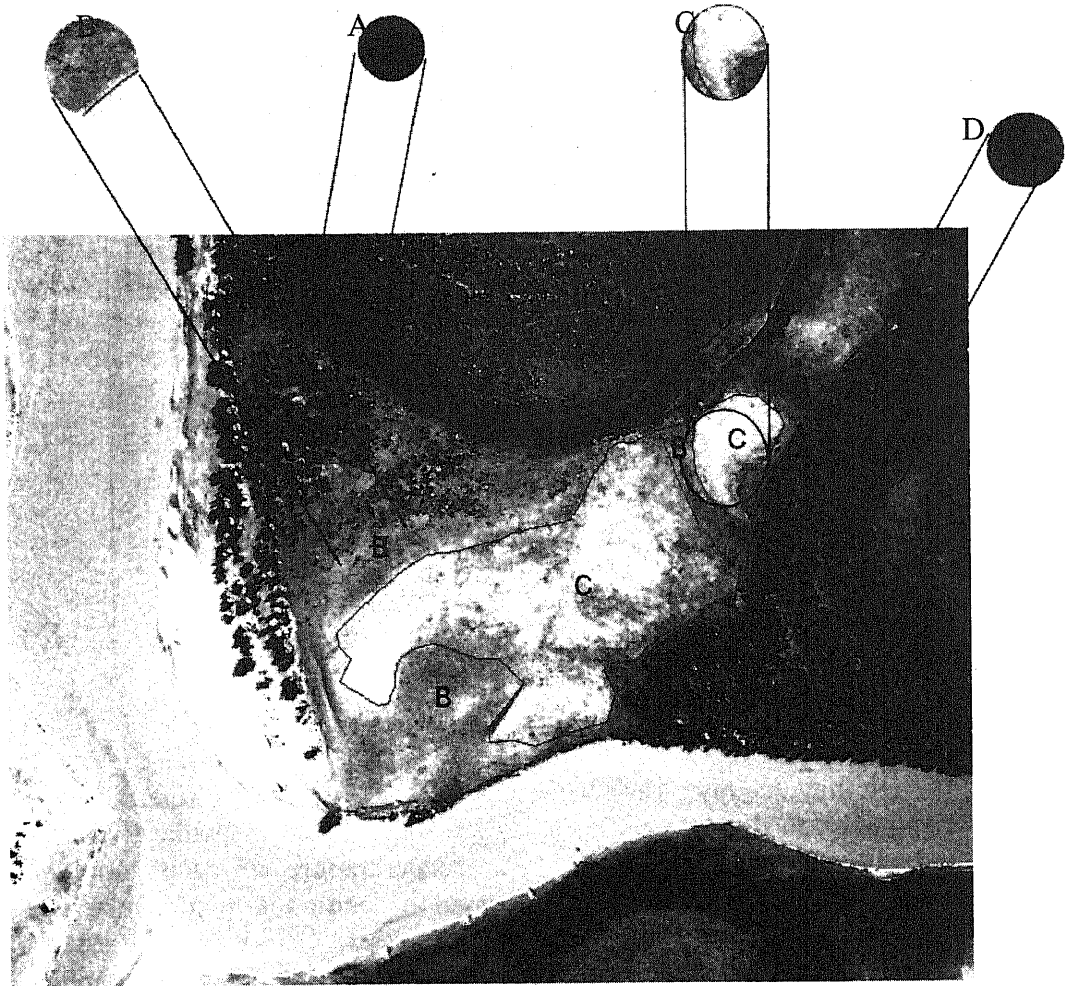


Figure 1 Vegetation types

- A:** Sedge meadow
- B:** Steppe meadow
- C:** Stipa steppe
- D:** Mixed forest

References

1. Grubov V.I. *Opredelitel sosudistiih rastenii Mongolii*. L., 1982
2. Dash D. *Mongol ornii landshaft – ekologiin zarim asuudluud*. UB., 2000
3. *Khuvsgul orchmiin baigaliin nukhtzul, nuuts bayalag*. UB., 1996.
4. *The research Papers of Darhadyn Wetland in Mongolia*. Japan., 2004

MULTI-TEMPORAL ANALYSIS OF VEGETATION INDICES FOR CHARACTERIZING VEGETATION DYNAMICS IN MONGOLIAN GRASSLAND

Ts. Javzandulam¹, R. Tateishi¹ and R. Tsolmon²

¹Center for environmental Remote Sensing, Chiba University, 1-33, Yayoi, Inage, Chiba 263-8522 Japan.

E-mail: javzaa@graduate.chiba-u.jp, tateishi@faculty.chiba-u.jp

Tel: +81-290-3965; Fax: +81-290-3857

²Remote Sensing Laboratory, Center for Geophysics, National University of Mongolia

Abstract

An attempt has been made in this study to delineate the characteristics of spectral signatures of vegetation in terms of various vegetation indices (VIs), particularly the Normalized Difference Vegetation Index (NDVI), Modified Soil Adjusted Vegetation Index2 (MSAVI2) and Enhanced Vegetation Index (EVI) to manifest their ability to discriminate vegetation biomass over a large area. Multi-temporal SPOT-4 VEGETATION data from 1998 to 2002 have been used for the analysis. The correlations between the vegetation indices observed at various degrees of vegetation coverage during different stages of growth were examined. All of the VIs have shown qualitative relationships to variations in vegetation. Apparently, the NDVI and MSAVI2 are highly correlated for all of the temporal changes, representing the different stages of phenology.

Keywords: Vegetation Indices, Vegetation dynamic, and Mongolia

1. Introduction

VIs are indicators of spectral transformations of two or more bands of satellite-derived data, employed to enhance the contribution of vegetation properties. They provide reasonable and reliable inter-comparisons of spatial and temporal information of terrestrial photosynthetic activity and canopy structural variations over a wide range of empirical observations. Investigations have shown that the use of VIs is highly useful in deciphering the characteristics of phenological stages of vegetation. The seasonal variability of the vegetation dynamics can be estimated easily with the availability of the present database allowing for a rational correlation with the empirical observation and controlling of bio-geo-physical parameters. The most of the VIs are called broadband VIs because they are based on algebraic combinations of reflectance in the red and the near infrared spectral bands (Bannari, 1995). These algebraic combinations are designed to minimize the effect of external influences such as solar irradiance changes due to the atmospheric effect or variations in soil background optical properties on the vegetation canopy spectral response. VIs is calculated based on the various functions and roles played by the vegetative cover in regards to degradation processes.

In this study, we attempted to delineate the characteristics of the spectral signatures of vegetation in terms of the above VIs, such as NDVI, MSAVI2 and EVI and to manifest their ability to discriminate vegetation biomass over a large area. We explored multi-temporal SPOT-4 VEGETATION (VGT) data for the analysis.

2. Study area

Our experiment was conducted in grassland area of Mongolia, which is geographically located between 41°35'N to 52°09'N and 87°44'E to 123°00'E. Total area is 1,565,000 km². The territory of Mongolia is divided into several natural zones such as mountain, mountain steppe, plain steppe, desert steppe and the Gobi-desert. Mountain steppe, plain steppe and desert steppe are the most significant and large for livestock and agriculture.

The climate of country is characterized by short, dry summer and long cold winter season. The mean annual precipitation is 200-300mm. The growing season lasts from end of May to the end of August.

3. Data

1) Multi-temporal SPOT-4 VGT sensor data

VGT-S10 data from April 1, 1998 to September 21, 2002 (time series of observations). The VGT sensor belongs to a new generation of space-borne optical sensors that were designed for mainly observations of vegetation and land surfaces (Saint, 2000).

2) Ground truth

Biomass measurement is determined by cutting all the grass inside an area of 1m². The wet grass weight, dry grass weight and grass height were measured. In this study, we used biomass measurement data from middle of June 1998 to middle of September 2001. Prior to sampling, we determined the number of samples necessary to detect differences in vegetation indices. 17 sample points were adequate for all the vegetation indices examined:

- 2 points from mountain steppe, which is widespread in central, north and western regions of Mongolia and usually has dark brown and brown soil. Common grasses in this area are *F. lenensis*, *F. sibirica*, *Polygonum angustifolium*, *Coluria geodes*, *Crossularia acicularis* and *Pentaphylloides fruticosa*.
- 10 points from plain steppe, which is abundant between the small mountain and valleys. The prevailing herbs and plants in this area are *Stipa capillata*, *S. decipiens*, *S. grandis*, *Cleistogenes squarros*.
- 5 points from desert steppe, which is located in the southern section Mongolia. Soil is grey-brown and desert steppe brown with pebbles. Plants abundant in this area are *Stipa gobica*, *S. glareosa*, *Cleistogenes squarrosa*, *S. klemenzii* and *C. songorica*, and less abundant plants are *Kochio prostrate*, *Allium polyrrhizum* and *A. mongolicum*.

4. Methodology

4.1 Vegetation indices

NDVI, MSAVI2 and EVI were calculated for each of the VGT-S10 products.

1. NDVI is a normalized ratio of the NIR and red bands;

$$NDVI = \frac{NIR - Red}{NIR + Red} \quad (1)$$

2. Huete (Tomoaki Miura, 2001) suggested a new vegetation index which was designed to minimize the effect of the soil background, which he called the soil-adjusted vegetation index (SAVI). Huete (1988) developed an iterated version of this vegetation which is called MSAVI2:

$$MSAVI2 = \frac{2NIR + 1 - \sqrt{(2NIR + 1)^2 - 8(NIR - Red)}}{2} \quad (2)$$

3. EVI was developed to optimize the vegetation signal with improved sensitivity for high biomass regions and improved monitoring through de-coupling of the canopy background signal and reduction in atmospheric influences.

$$EVI = G \frac{NIR - Red}{NIR + C_1 Red - C_2 Blue + L} \quad (3)$$

where L is the canopy background adjustment that addresses nonlinear, differential NIR and Red radian transfer through a canopy, and C_1 , C_2 are the coefficients of the aerosol resistance term, which uses the blue band to correct the aerosol influences of the red band. The coefficients adopted in the EVI algorithm are, $L=1$, $C_1=6$, $C_2=7.5$, and G (gain factor)=2.5 (Qi, 1994 , Huete, 1994)

4.2 Analysis

Relationships between vegetation indices and observed at various degree of vegetation coverage during their different stages of growth were analyzed using regression analyses. The relationships between VIs and biomass were investigated using ground measurement data. The accuracy of the estimated biomass by vegetation index was measured using a standard error of estimate, SE;

$$SE = \sqrt{\frac{1}{N-2} \sum_{i=1}^N (\hat{y}_i - y_i)^2} \quad (4)$$

where \hat{y}_i and y_i are the predicted and ground measured value of biomass respectively, and N the number of samples. Sensitivity analysis consists in computing derivatives of one or more quantities (outputs) with respect to one or several independent variables (inputs). The sensitivity of vegetation indices to vegetation density was evaluated using finite-differences method. Finite-differences method for sensitivity analysis is calculated as follows;

$$\frac{df}{dx_i} \approx \frac{f(x_i + h) - f(x_i)}{h} + O(h) \quad (5)$$

where h is the finite-difference interval, the truncation error is $O(h)$, and hence this is a first-order approximation and $f(x_i + h)$, $f(x_i)$ is the value of function at x_i and $x_i + h$ points.

5. Results

Vegetation indices were calculated from SPOT-4 Vegetation data of April to September from 1998 to 2002 and relationships across the various VIs between indices for each 10 day series were investigated. In the early stages of the growing season, EVI is less correlated to the NDVI and MSAVI2. Apparently, the NDVI and MSAVI2 are highly correlated for all of the temporal changes and in different natural zones. Correlation coefficients between vegetation indices for study area are shown in the table1.

The relationships between biomass and each vegetation index for each natural zone are shown in figures 1, 2, and 3. Equations (6), (7) and (8) give empirical relationships between biomass and vegetation indices for mountain steppe, plain steppe and desert steppe, respectively.

Table 1 Correlation coefficients between vegetation indices study area during the growing season

	EVI & MSAVI2	EVI & NDVI	MSAVI2 & NDVI
April	0.55	0.58	0.98
May	0.88	0.91	0.98
June	0.96	0.91	0.98
July	0.96	0.98	0.99
August	0.94	0.97	0.98
September	0.91	0.96	0.98

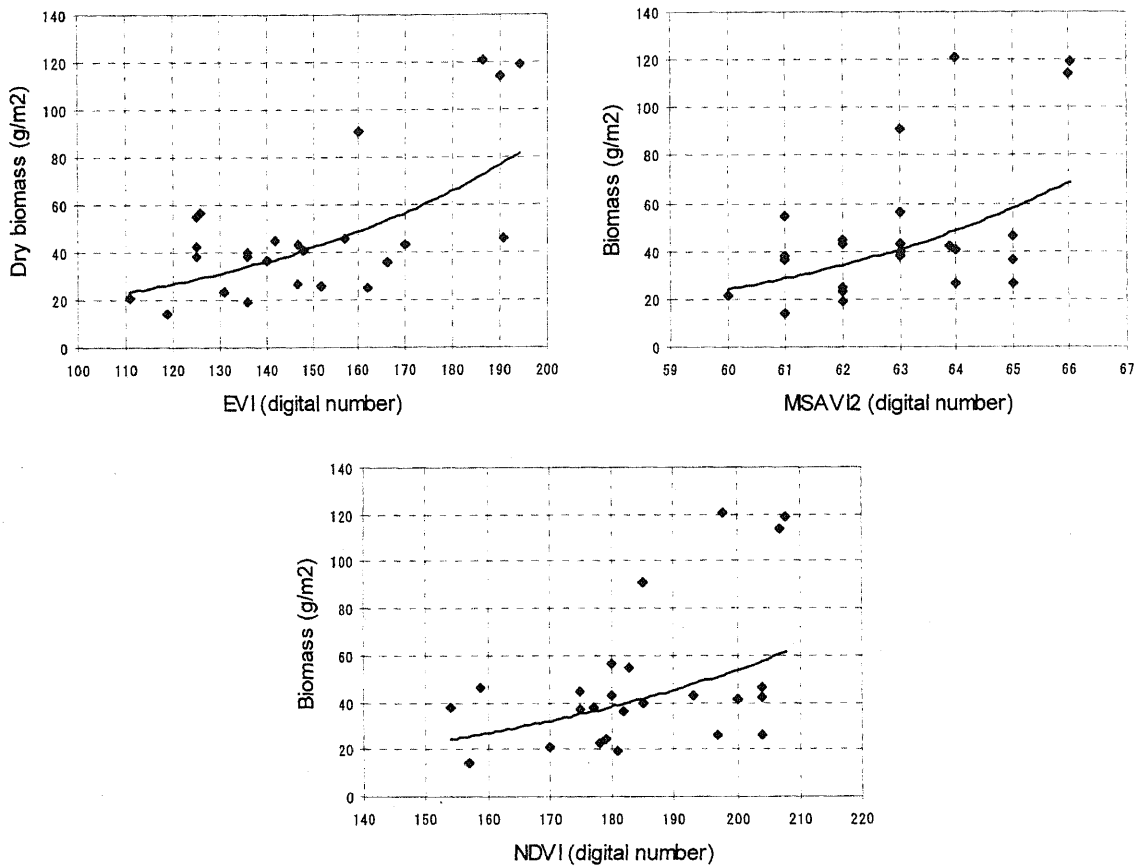


Figure 1 The relation between biomass (g/m²) and vegetation indices in mountain steppe

Table 2 Correlation coefficients between each vegetation index and biomass in different natural zones

Natural grassland zone	EVI	MSAVI2	NDVI
Mountain steppe	0.64	0.53	0.53
Plain steppe	0.65	0.59	0.56
Desert steppe	0.48	0.50	0.41

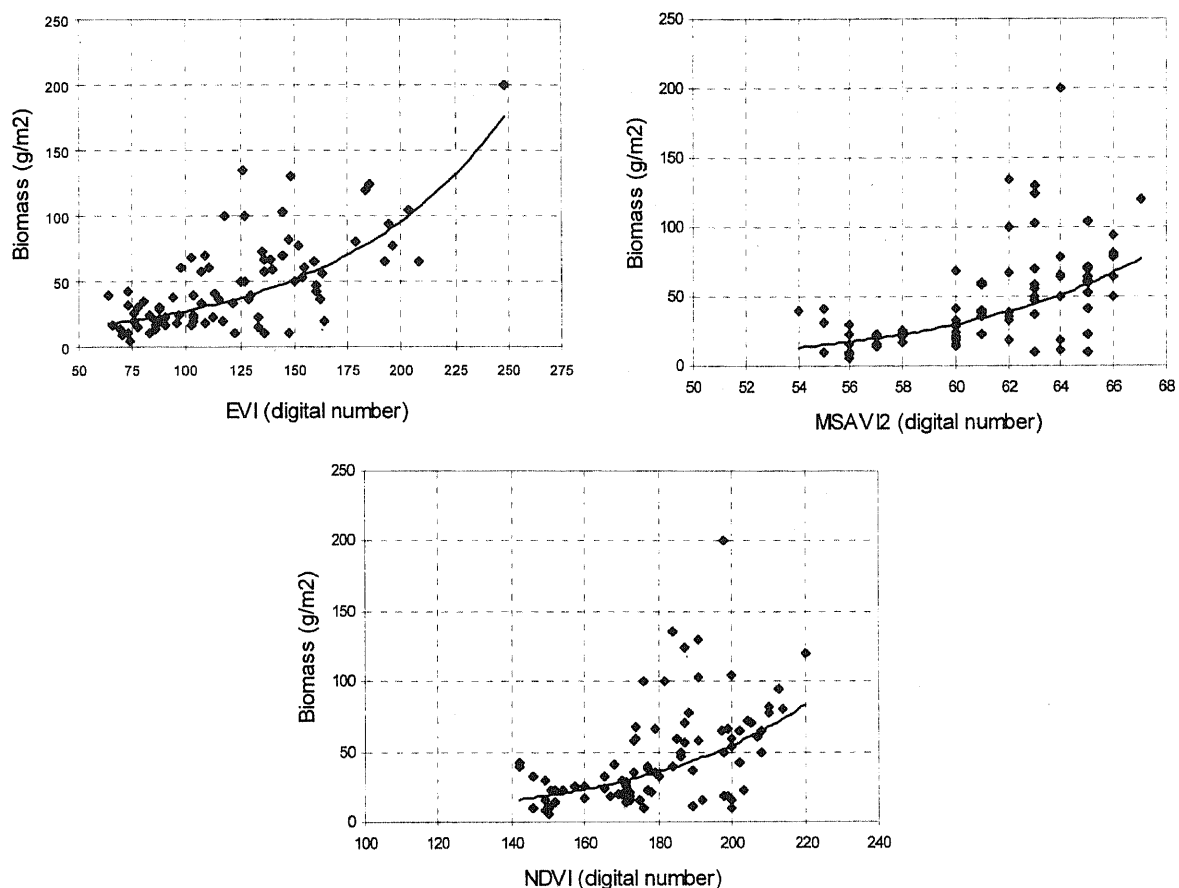


Figure 2. The relationship between biomass (g/m²) and vegetation indices in plain steppe

In mountain steppe and plain steppe zone EVI and biomass are correlated better than the other indices. The biomass and EVI are exponentially related; as vegetation index increases, biomass becomes saturated. MSAVI2 and biomass are correlated well in desert steppe zone. Table 2 shows the correlation coefficient for the relationships between biomass and vegetation indices for different zones in growing season. In desert steppe zone, MSAVI2 was better correlated to biomass. The standard error of estimate for biomass in the different grassland zones for all vegetation indices is shown in table 3.

Table 3 Standard error of estimates of biomass for various vegetation indices in different natural zones

Natural grassland zone	EVI	MSAVI2	NDVI
Mountain steppe	7.64	11.70	14.47
Plain steppe	17.56	13.45	13.57
Desert steppe	6.68	9.48	5.47

$$biomass = 4.4088e^{0.015EVI}$$

$$biomass = 0.0007e^{0.1752MSAVI2} \quad (6)$$

$$biomass = 1.7528e^{0.0171NDVI}$$

$$biomass = 7.7796e^{0.0126EVI}$$

$$biomass = 0.0091e^{0.1350MSAVI2} \quad (7)$$

$$biomass = 0.7714e^{0.0213NDVI}$$

$$biomass = 0.1407e^{0.047EVI}$$

$$biomass = 2E-06e^{0.2682MSAVI2} \quad (8)$$

$$biomass = 0.0017e^{0.0537NDVI}$$

The purpose of the sensitivity analysis was to demonstrate the sensitivity of the VIs to vegetation density. In this study, sensitivity of vegetation indices to vegetation density is evaluated in different zones separately. The sensitivity results are shown in figure 4. In desert steppe zone MSAVI2 is more sensitive to vegetation density. In plain steppe zone sensitivities of the vegetation indices are similar. In mountain steppe EVI is more sensitive to vegetation density.

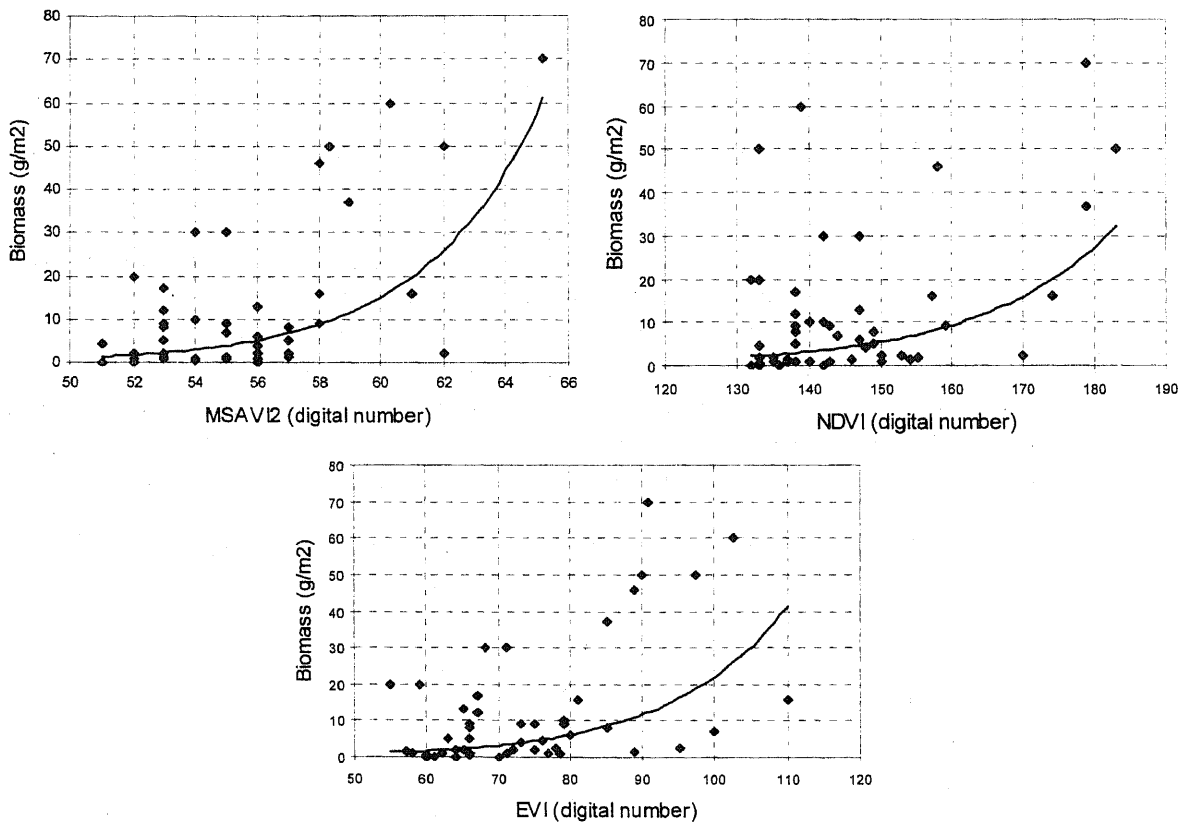


Figure 3. The relation between biomass (g/m²) and vegetation indices in desert steppe

6. Conclusions

The objective of this study was to examine the relationships between vegetation indices, to compare vegetation indices to manifest their ability to estimate vegetation biomass. The results show that in Mongolian desert steppe zone MSAVI2 is the best, while in mountain steppe and plain steppe zone EVI is found to discriminate biomass well. EVI was the more sensitive to high vegetation density.

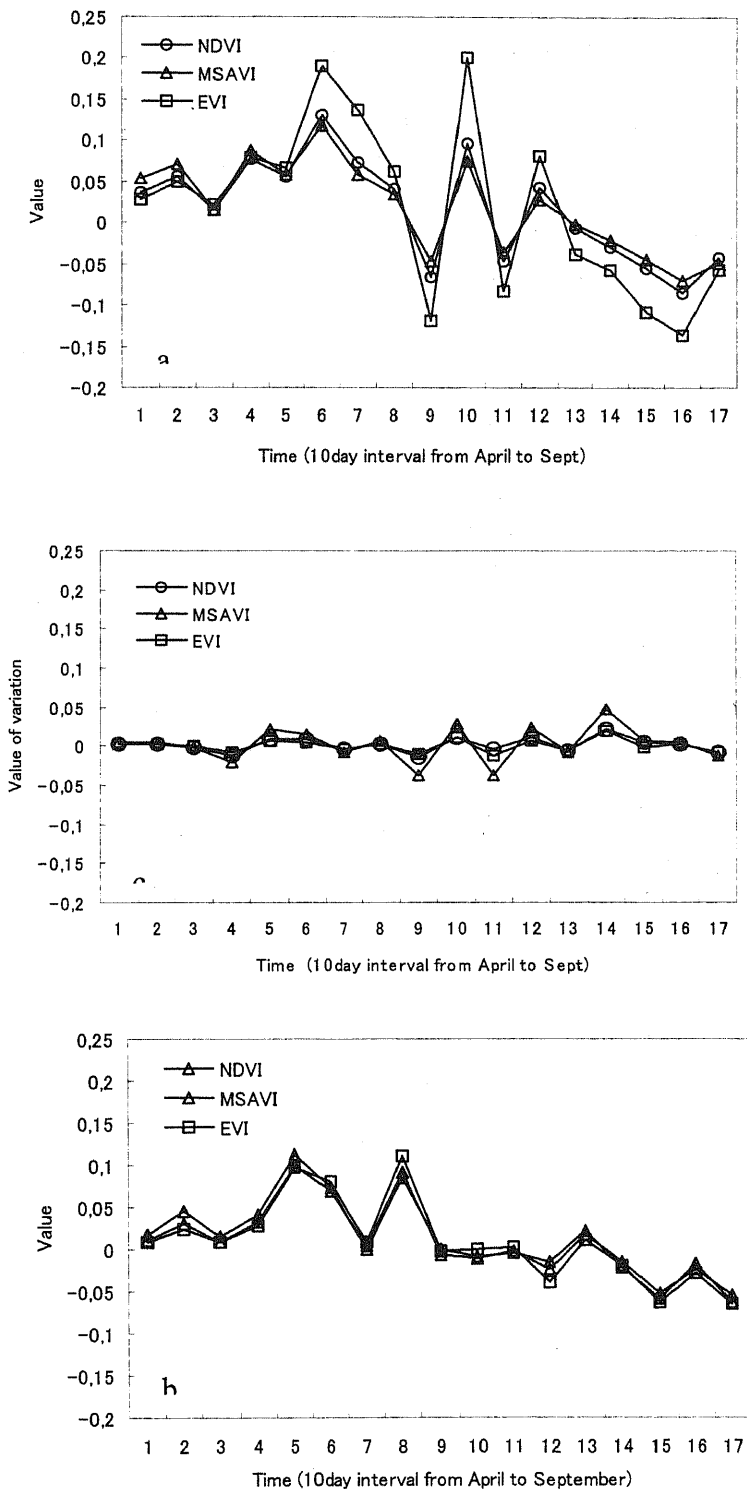


Figure 4. Sensitivity analysis of VIs at 10-day interval over the period April-September in different natural zones: a. mountain steppe, b. plain steppe c. desert steppe

References

1. Bannari et al., 1995. A. Bannari, D. Morin, F. Bonn and A.R. Huete , A review of vegetation indices. *Remote Sensing Reviews* 13, pp. 95–120.
2. Saint, G. 2000. Proceeding of VEGETATION 2000: 2years of operation to prepare the future. International Conference of VEGETATION 2000, April 3-6, Lake Maggiore, Italy.
3. Tomoaki Miura, Alfredo R. Huete, Hiroki Yoshioka and Brent N. Holben, December 2001. An error and sensitivity analysis of atmospheric resistant vegetation indices derived from dark target-based atmospheric correction, *Remote Sensing of Environment* 78, pp.284-298
4. Huete,A.R., 1988. A soil-adjusted vegetation index *Remote Sensing and the Environment*, 25, pp.53-70
5. Qi, J., Chehbouni A., Huete, A. R., Kerr, Y. H., and Sorooshian, S., 1994. A modified soil adjusted vegetation index, *Remote Sensing and the Environment*, 48, pp. 119-126
6. Huete, A.R. and Liu, H.Q., 1994. An error and sensitivity analysis of the atmospheric- and soil-correctingvariants of the NDVI for the MODIS-EOS. *IEEE Transactions on Geoscience and Remote Sensing* 32 4, pp. 897–905
7. Huete, A.R., Liu, H.Q., Batchily, K. and van Leeuwen, W., 1997. A comparison of vegetation indices over a global set of TM images for EOS-MODIS. *Remote Sensing of Environment* 59, pp. 440–451
8. Xiangming Xiao, Bobby Braswell, Qingyuan Zhang, Stephen Boles, Stephen Frolking and Berrien Moore. 2003 Sensitivity of vegetation indices to atmospheric aerosols: continental-scale observations in Northern Asia, *Remote Sensing and the Environment*, 48 pp. 385-392

MAPPING SNOW COVERAGE USING LINEAR MIXING MODEL ON MODIS/TERRA SATELLITE DATA

L.Ochirkhuyag¹, R.Tsolmon²

¹ Information and Computer Center of NAMHEM, The National Remote Sensing Center
Juilchiny street-5, Ulaanbaatar 210646, Mongolia

Tel: 976-11-329984, Fax: 976-11-329968, E-mail: lochir@yahoo.com

² Remote Sensing Laboratory, Center for Geophysics, National University of Mongolia,
E-mail: tsolmon@num.edu.mn

Abstract

Snow coverage map is one of the sources of information for livestock and human activities. The study aimed at determining the relative proportions of snow coverage and other components in a mixed pixel. For this purpose a linear mixing model was used for snow coverage mapping in Mongolia. In this paper, reflective bands 1 and 2 of the Moderate Resolution Imaging Spectroradiometer (MODIS)/TERRA satellite data was used to map three land components. MODIS data may greatly enhance the operational success of satellite based snow coverage monitoring, in providing multi-spectral data on parameters of the environment.

1. Introduction

To obtain knowledge of how snow coverage is scattered within Mongolia, it is necessary to use remotely sensed data. Lack of tools and methods to manage and monitor snow coverage in large area is a problem. Linear mixing model previously developed is applied to the study area to generate regional estimates of snow coverage and other land components over Mongolia. Snow coverage plays a crucial role in this area. Main types of snow coverage change in the study area are conversions between forest and steppe, steppe and Gobi.

Recently, remote sensing technology has been an efficient and helpful tool to monitor snow coverage and plantation in large area. Remote sensing technology has capability to monitor and understand how existing snow coverage areas are presented on the ground especially for the snow coverage estimation in the study areas. This indicates that identification and mapping snow coverage are important to manage actual information about snow coverage map in developing countries such as in Mongolia.

2. Study area, snow data

The study area is located in including Mongolian general natural zones, within 40° - 53° N and 90° - 117° E.

The Precipitation is low in wintertime of year because in winter dominates weather condition of anticyclone over Mongolian region. (Only 10 to 15% from annual precipitation) In Mongolia we use snow ruler and doing measurement of snow cover. But it is difficult to determine real snow cover depending on the relief and land, river, and population density. (B.Jambaajamts 1989) For Mongolia, we used snow cover and depth maps from Institute of Meteorology and Hydrology (IMH). The snow cover and depth maps from IMH are based on synoptic measurements as well as visual interpretation of MODIS images.

In this study, MODIS/TERRA data of 19th January 2004 were used. This image was processed at level 1b (HDF format data projected on Geography, WGS 84 system) by the EOS Data Gateway, Land Process Distributed Active Archive Center (LP DAAC) of NASA.

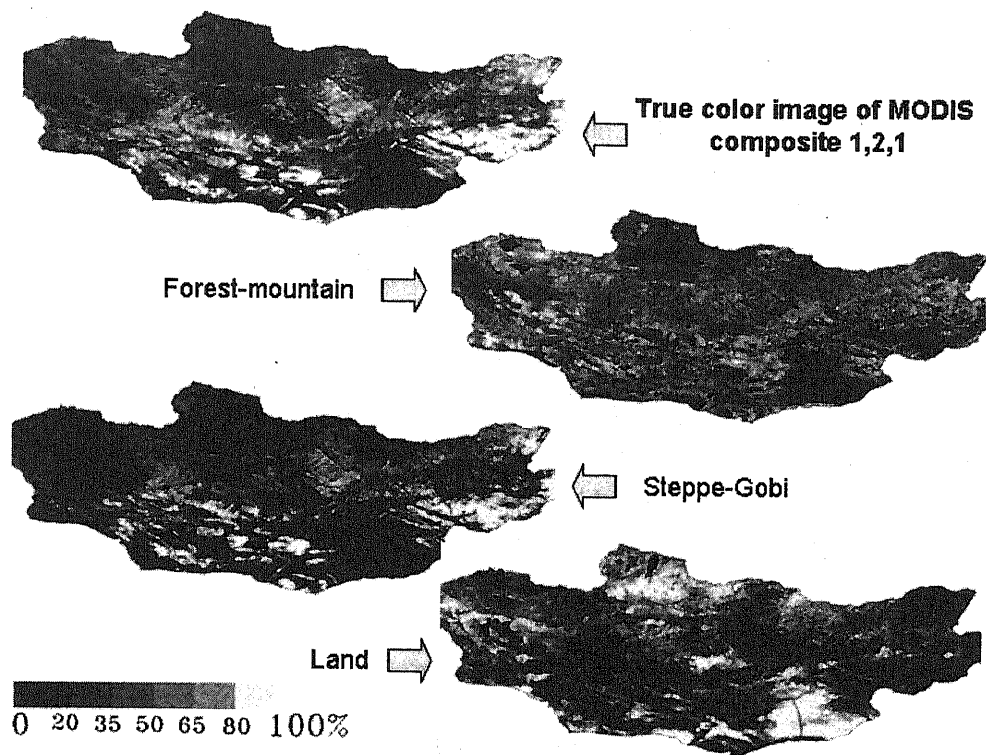


Figure 1. Fraction images of three end-members

5. Results and Discussion

Classification results indicate that pine can be classified with an acceptable accuracy. The snow cover fraction image seems to be useful for snow coverage map since it contains cover percentages information about forest proportion within the pixels. The procedure produced maps showing percentages of components within pixels of size 250m (for MODIS). The output fraction images were compared with 10-day composite the snow map from IMH and true color images (RGB) of MODIS. Application of the method to higher resolution data to test its potential was hindered by lack of high-resolution data sets. Further work should test the robustness of the approach, when applied to large areas by using multi-temporal data to detect environmental changes resulting from anthropogenic activity. The main problem in monitoring was clouds. The study had considered not only the forest cover components but also cloud as cover components. The advantage of fraction images is that they contain physical information such as amount of each component within the pixel.

Acknowledgments

The authors are grateful to EOS Gateway of LP DAAC/NASA for supplying MODIS/TERRA Level 1b data. We also would like to thank Institute of Meteorology and Hydrology for their assistance in collecting ground truth data.

References

B.Jambaajamts, 1989, Climate of Mongolia, HEVLEL, Ulaanbaatar

Adams, J.B., and Adams, J.D., 1984, Geologic mapping using Landsat MSS and TM images: removing vegetation by modeling spectral mixtures. Proceedings of the Third

Thematic Conference on Remote Sensing for Experimental Geology, Colorado Springs, Colorado, (Michigan: ERIM), pp.615-622.

Cross, A.M., Settle, J.J., Drake, N.A., and Paivinen, R.T.M., 1991, Sub pixel measurement of tropical forest cover using AVHRR data. *International Journal of Remote Sensing*, 6, 1159-1177.

Gillespie, A.R., Smith, M.O., Adams, J.B., Willis, S.C., Fischer, A.F.III, and Sabol, D.E., 1990, Interpretation of residuals images: spectral mixture analysis of AVIRIS images, Owens Valley, California. *Proceedings of the Airborne Science Workshop: AVIRIS, JPL, Pasadena, CA, (JPL Publication 90-54), pp.243-270.*

Smith, M.O.Johnson, P.E., and Adams, J.B., 1985, Quantitative determination of mineral types and abundances from reflectance spectra using principal component analysis. *Journal of Geophysical Research*, 90, 792-804.

Shimabukuro, Y.E., 1987, Shade images derived from linear mixing models of multispectral measurements of forested areas. Ph.D. Dissertation, Colorado State University, Fort Collins, CO.

Tsolmon R., R.Tateishi "A Linear mixture model for land cover classification using 8km and 1km AVHRR data," *Proceeding of Japan Society of Photogrammetry and Remote Sensing Symposium, Japan, pp.213-216, 17 November 2000 (Tottori: JSPRS).*

TEXTURE BASED SEGMENTATION OF REMOTELY SENSED IMAGERY FOR IDENTIFICATION OF GEOLOGICAL UNITS

Tsolmongerel Orkhonselenge¹, Arko Lucieer², Alfred Stein²

1. GeoInformatics Center, Mongolian University of Science and Technology
tsolmongerel@must.edu.mn , tsolmongerel@alumni.itc.nl
2. International Institute for Geo-Information Science and Earth Observation
lucieer@itc.nl stein@itc.nl

Abstract

This paper explores the potential of a newly developed spatial segmentation based on Local Binary Pattern for geological unit identification. Spatial homogeneity of pixels plays an important role in spatial segmentation. In this study, homogeneity is defined using the concept of texture. This leads to the Local Binary Pattern Operator, based on a rotation invariant texture model. Multivariate case of this approach helps in spatial segmentation with a reasonably good performance for information extraction. Segmentation has been carried out on remotely sensed images from Landsat TM and Aster for the Southern Mongolian arid region. Appropriate band combinations for multivariate Local Binary Pattern have been used in delineating geological units of the region.

Closest Distance Metric, an edge validation algorithm has been implemented. It finds possible matchings between two images in relation to distances between edges. Segmented images have been assessed using reference data from a geological map. The algorithm is highly sensitive for over-segmentation, which leads to a low similarity value. However, another accuracy measure, Boundary Fit Index results in 52% of boundary fitting. It shows that image segmentation if done properly could improve geological maps.

Keywords

Segmentation, Local Binary Pattern, Edge Matching, Geological unit

1. Introduction

The application of remote sensing for geological mapping and/or exploration in Mongolia has been rapidly increasing during the last decade. An explanation is the availability and accessibility of satellite images with high spatial and spectral resolution, together with RS and GIS tools. Remote sensing techniques are highly useful for mapping large and remote areas in which collection of ground observation is very difficult. On the other hand, because of geographical and political reasons, the geological preservation is in a good condition in Mongolia. For example, steppe outcrops are, at the moment, very well preserved in Mongolia, in contrast to many other countries. Mongolia is one of the largest countries in the world in terms of its territory. This territory is geologically not studied very well, and has only partially been studied in detail. Efficient geological mapping and exploration requires identification of geological units from satellite images. This can be viewed as a segmentation process that takes into account the spectral and spatial characteristics of an image. Assessment of segmentation result will be carried out on both Landsat TM and Aster images segmentation results. An illustration is taken in the southern Mongolian arid area. The paper is organized as follows. The methodology, multivariate Local Binary Pattern operator, the segmentation, and a validation technique; the Closest Distance Metric is

described in Section 2. Some experimental results are presented in Section 3. Discussion is included in Section 4, and Section 5 concludes the paper.

2. Methodology

The study consists of three parts. The first part contains segmentation and edge detection. It considers a supervised segmentation using multivariate Local Binary Pattern measurements based on band combinations of Landsat TM and Aster imageries. From these, edges are derived. The second part concerns ground truth data as reference data. It handles selection, digitization, and rasterization of thematic data. The third part addresses, validation to assess segmentation results with edge comparison techniques.

2.1 Texture based segmentation

Typically, the term segmentation describes the process, both human and automatic, that separates zones or regions in an image showing some characteristics with respect to a certain evaluation function [2]. These characteristics could be, for example, similar brightness or color, roughness, and texture. Recent studies [8], [9] show that complementary information of local spatial pattern and contrast, which is called the Local Binary Pattern (LBP), plays an important role in texture discrimination. It is supported by some studies on human perception that analyzes images in terms of objects with similar characteristics, including texture orientation, coarseness, and in contrast to perceptually important textural properties [9]. Lucieer et al. proposed a multivariate extension of the standard univariate local binary pattern operator to describe color texture. Segmentation differs from classification, as spatial contiguity is an explicit goal of segmentation whereas it is only implicit in classification [7]. Segmentation is the division of an image into homogeneous regions or categories, which correspond to different objects or parts of objects. Pixels in the same category have similar gray scale or multivariate (spectral) values or belong to a similar pattern and form a connected region.

Since the pixel-by-pixel approach ignores potentially useful spatial information between pixels, object-based approaches have become popular with the increase of high resolution imagery in remote sensing. The spatial homogeneity of pixels plays the most important role in spatial segmentation, and this is widely used in remote sensing. In contrast to the pixel-based approach, objects or segments are formed because of their spatial correlation, not only because of their thematic similarity. Lucieer et al. used a top-down hierarchical segmentation process. They mentioned it offers a very suitable framework for classifying image regions based on texture.

2.1.1 A multivariate texture model

The $LBP_{c,j}$ texture measure gives a texture description of a single band [7], [9]. Due to the necessity of using multiple bands of remote sensing images, Lucieer et al. [7], propose a new texture measure LBP_{mc} , based on $LBP_{c,j}$, describing color texture or texture in three bands. It considers the spatial interactions of pixels within not only one band, but also the interactions between bands. Hence, the neighborhood set for a pixel consists of the local neighbors in all three bands.

The local threshold is taken from these bands. It makes up a total of nine different combinations. This gives the following operator for a local color texture description:

$$LBP_{mc} = \sum_{j,k=1}^{nb} \sum_{l=0}^{P-1} s(g_{i,j} - g_{c,k}), \quad (2.1)$$

where nb is the number of bands, here $nb=3$, s is sign function of difference of the two gray values, and summation is done over the different bands. A central pixel in a particular band is compared with neighborhood pixels in all the different bands. A total of nine LBP values (when, $nb=3$, where an LBP value is calculated based on the

threshold of a center pixel in one of the bands with a set of P neighbors in one of the bands) are obtained and summed to derive LBP_{mc} . The histogram of LBP_{mc} occurrence is computed over an image or a region of an image, and describes the binary color pattern feature. It contains $P \times 3^2$ bins, e.g., $P=8$ results in 72 bins. This measure is completed with contrast and variance, including the color histogram, RGB-3D. Each 8-bit band is quantized into 32 levels by dividing the pixel values by 8, resulting in a three-dimensional histogram with 32^3 entries.

G-statistic is used as a similarity measure for the LBP_{mc} and RGB-3D histogram. The similarity sum of the two G-statistic values in the top-down hierarchical splitting process of the segmentation algorithm to obtain image block class labels and uncertainty values is applied. Interested readers for more detailed information referred to [7]. They concluded that, overall, the color texture operators perform well.

2.1.2 Segmentation for geological unit identification

We are interested in segmentation that takes into account the spectral and spatial characteristics of the ground in the remotely sensed imagery for identification of geological units. To do so, multispectral LBP segmentation was chosen, this was because this operator is assumed to have good performance on segmentation based on texture. To have more information about geological units in the imagery, different band combinations of Landsat TM and Aster data are explored and studied. For the Landsat TM data, bands giving more information on geological units are band 7, 5, and 1. In this study, band combination 7 and 5 are usually taken with one of the other bands for multiband segmentation. Out of Aster bands SWIR bands are more interesting for the geological unit identification, which ranges from $1.60\mu\text{m}$ – $2.43\mu\text{m}$. This range falls in the quite similar and closer range as Landsat TM band 7, and 5.

2.1.3 Decorrelation stretching

The decorrelation stretch has found increased usage, primarily for multispectral imaging systems that have closely spaced channels in the spectral region, and thus, extremely high inter-channel correlation [2]. The decorrelation stretch reduces the inter-channel correlation and stretches the dynamic range to the full extent, which enhances the color variation and improve visualization for interpretation [4], [3]. Decorrelation stretch is applied to both the Landsat TM and Aster data. It is expected to give higher accuracy segmentation because color enhancement is done which is an important factor for multivariate LBP operator.

2.2 Edge validation - Closest Distance Metric

Since we obtained edge maps from the segmentation, appropriate validation techniques were adopted to assess the segmentation results. We implemented the Closest Distance Metric (CDM) to assess the similarity between edge images.

2.2.1 CDM algorithm

CDM builds a one-to-one matching between edge pixels obtained by a segmentation and edge pixels of the reference. It allows small shifts of edge pixels. First, for each reference edge pixel, the segmented image is inspected to find possible matches within neighborhood set of an a priori defined window. In this study, a 5×5 window, with a neighborhood set of 2 pixels in all directions is taken. For the reference edge pixel, all possible matches within the neighborhood in the detected image are taken and ordered based on the distance to the reference edge position. If in the ordering an exact match occurs, i.e., at the same position as the edge pixel in the reference image, there is an edge pixel in the detected image, we then assign a value 0 to that order. If we find a match in orthogonal neighbors in the distance of 1 pixel then it is assigned as a 1st order.

Next, diagonal neighbor match in the distance of 1 pixel is then assigned a 2nd order. In this way, 3rd, 4th, and 5th orders are assigned according to the edge pixel position in the detected edge for the match of the reference edge pixel.

The reason to order these positions during match finding, is to assign a preference during the process of finding possible matchings. If we can not find any match between the reference pixel and the detected edge pixel, that pixel is left unmatched, and taken into account as such later on in the overall metric.

After taking all possible matches for each edge pixel in the reference, including their order, reference pixels are ordered again with match according to their first possible matching order. Thus, we have an ordered set of reference pixels with ordered possible matches. From here, a one-to-one match finding starts. First, we will take the first possible match of the first reference pixel. Next, we check the first possible match of the second reference pixel, determining whether its position as a detected edge pixel is already chosen for the matching or not. If it is not chosen the most ahead possible match is taken. If this is already chosen then the next possible match is inspected. If we can not find any match for the reference pixel then it is left out and we continue for checking of the next reference pixel. By this way, we can find the first possible one-to-one matching between reference edge and detected edge. Besides this matching, a cost function is introduced to evaluate the costs for matching. For exact match, the cost is 0. The cost is introduced as 0.1; 0.21; 0.22; 0.31; 0.44 for 1st–5th order match respectively. For unmatched pixels in both the reference edge and detected edge images, the cost is 1. Since matching between two images cannot always find a pair for every pixel, a cost of matching should take into account the cost of every match included in it and cost of all the pixels left unmatched from both images [11]. The Cost is calculated by summation of the number of unmatched pixels (number of unmatched pixels times 1), and the cost of a matching between reference edge and detected edge pixels.

By calculating the cost of the matching, a similarity between the edge images is estimated:

$$CDM_{\eta} = 100 \times \left(1 - \frac{C(M(f, g))}{|f \cup g|} \right), \quad (2.2)$$

where η is the maximum pixel distance for the matching, $C(M(f, g))$ is the cost of the found matching, and $|f \cup g|$ is the total number of edge pixel in f or in g , i.e., union of f, g images. Interested readers for more detailed information in [12].

3. Experimental results

3.1 Segmentation results

Segmentation has been carried out on Landsat TM and Aster images of the southern Mongolian arid region. It is located in the Dundgovi aimag (province). The total area is 1415.58 km². The geological map of this area, which is visually interpreted on remotely sensed imagery based on field experience, is illustrated in figure 1. The following geological units occur on the geological map:

1. Sedimentary rocks

- Cenozoic deposit
 - Q4 — Quaternary Lakes sediments
 - Q — Quaternary sediments
 - E2 — Eocene (middle Palaeogene)
 - E1 — Miocene (lower Palaeogene)
- Paleozoic and Mesozoic deposit
 - P-T — Permian & Triassic formation

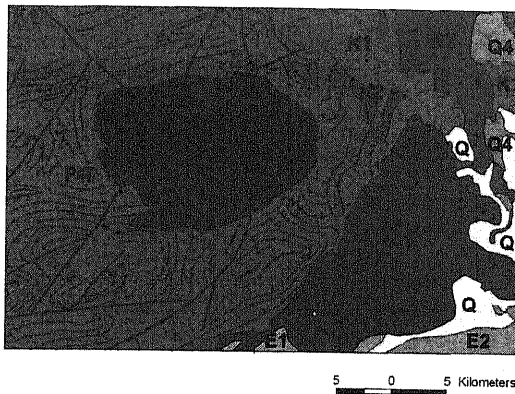


Figure 1. Geological map of the Baga Gazar area

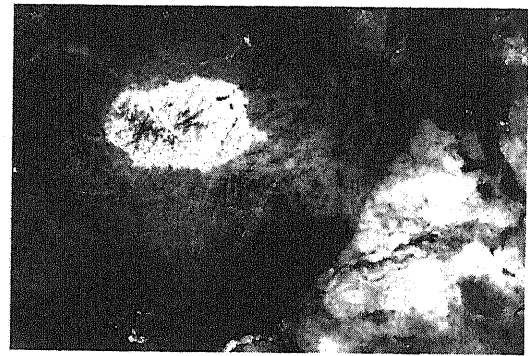


Figure 2. Aster SWIR bands 964

2. Volcanic rocks

K2 — Upper Cretaceous basalt

K1 — Lower Cretaceous basalt

aT3-J1 — Upper Triassic & Lower Jurassic andesite

3. Intrusive rocks

yT3-J1 — Upper Triassic & Lower Jurassic granite

yPR — Proterozoic granite

3.1.1 Landsat TM

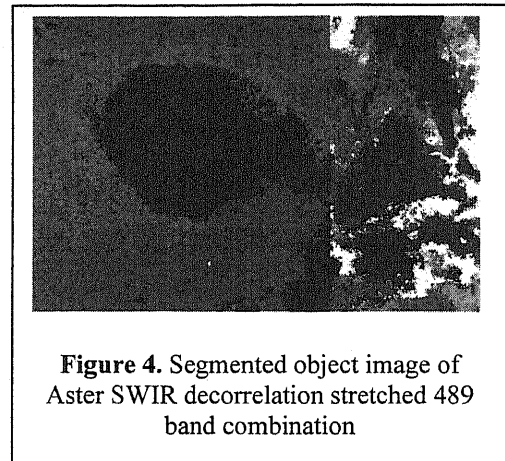
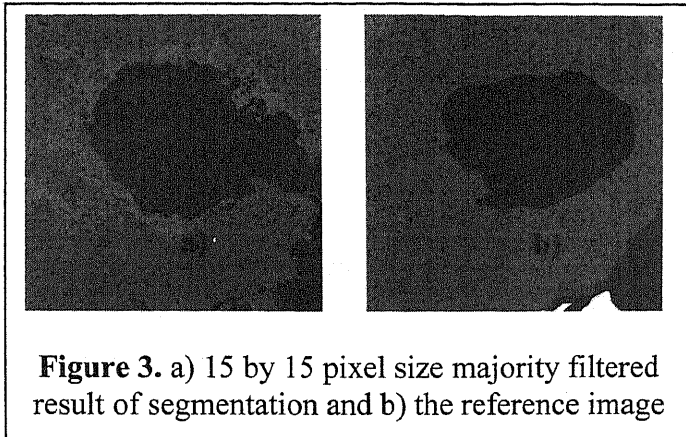
Landsat TM bands 751, and bands 754 segmentations are done. Visually, in the segmentation of Landsat TM 751 combination, Q4 units are very well identified, almost uniquely identified without any noise. It is because of Landsat TM band 1 penetrates water body, thus, Q4 is identified well. Also, yT3-J1 and yPR units are identified well and less noisy than the segmentation of Landsat TM 754 combination. K2 unit is better identified in the segmentation of Landsat TM 754 than the segmentation of Landsat TM 751.

In general, geological units are clearly identified though they are differently identified in different parts. In some cases those do not match exactly because of the partial processing. De-correlation stretch is used to reduce inter-channel correlation, and increase the color separation. De-correlation stretched images with output of byte data enables segmentation.

3.1.2 Aster SWIR

The Aster SWIR data has 6 bands. As we used Landsat bands 7, 5, 4 for the segmentation, we have chose bands 9, 8, 4 of SWIR for segmentation. The Aster image bands 964 combination is illustrated in figure 2. Aster SWIR 4 covers basically the same spectral region as Landsat TM band 5, Aster SWIR bands 5–8 are within the range of band Landsat TM 7, and Aster SWIR 9 is out of Landsat spectral region, but it is very close to Landsat band 7. Since decorrelation stretched bands discriminate the units well, we have done segmentation of the stretched bands. Aster SWIR segmentation is smoother and better than the Landsat TM segmentation, especially for the aT3-J1 unit is well determined. The P-T unit is determined very smoothly. However, noise occurs in the surroundings of yT3-J1 and aT3-J1. This is because of weathering process, P-T is covered by loose soil from the hill, and that part is determined as K1 unit. The

segmentation results of Aster SWIR decorrelation stretched bands 489 combination is illustrated in figure4.



3.2 Validation

3.2.1 Edge images

The edge image is derived from the object image, which is the result of segmentation. Object edges represent well the geological unit boundaries in comparison with reference edge and detected edge images, although too many small object edges occur. These small objects not occur in reference edge image.

3.2.2 Results

Validation carried out using CDM for the object edge images of both Landsat TM and Aster SWIR. CDM has found possible edge matching between the edge images and estimates the similarity of those edge images. The final metric gives similarity of 3.55% for Aster SWIR result and reference edge in western part of the study area (part1). The question rises why the overall result has a very low value of similarity. First, the number of detected edges is too large. Second, displacement between detected edge and reference edge is farther than 2-3 pixel difference. The reasons related to this are discussed in the following section. As mentioned above, the main reason why the overall percentage of the metric is much lower for the comparison of segmentation result and reference image in this study is that too many small objects are detected, i.e., over-segmentation occurs in segmentation results compared to the reference edge. Since the image segmentation has a large over-segmentation as compared to the reference image, we need to find a proper way to evaluate segmentation.

3.2.3 Comparison on validation

Boundary Fit Index

To improve validation, different approaches have been applied to compare edges. The Boundary Fit Index is an accuracy measure that does not take into account the number of edge pixels [6]. A scan window was used to find an edge match between segmented image and reference image. The scan window was 21 pixels in size.

The CDM1 a version of CDM, using the same formulae as CDM, but not taking into account that an edge pixel in the segmentation result can represent multiple matches. The weights are also determined by the distance. First, the clump operator applied to reduce the amount of small objects in the edge image part1 by three clump versions. Clump window sizes were 0, means no clump, i.e., original segmentation result, 15 and 50 pixels. Second, the different accuracy measures applied to compare the detected edge image and reference edge image. The result of CDM was CDM=5.9%, on the edge map with Clump window of 15 pixels. The result of Boundary Fit Index was 51.98%, while

CDM1 was 8.52% on the edge map with Clump window of 0, which is the original edge images without any change.

The results show that the bigger clump window size the smaller the number of exact matching pixels. Though the clump operator reduces the smaller objects when the clump window increases, it decreases the accuracy measures. Hence, without changing the major segmented objects, the elimination of small objects, i.e., merging into larger objects could be the way to increase accuracy measure. For this reason, Edge merging applied to detected edge image. It inspects edge image by different window size, whether the window includes small objects, i.e., that small objects is completely inside the window or not. If the window has small objects inside, it deletes the edges. Numerically, it reduces number of edge pixels by thousands. We observed that the edge map derived from reference image has 1 pixel width. Therefore, in contrast to previous edge image used for the validation, we derived 1 pixel width edge map. This has almost twice as few of the edge pixels than edge images of 2 pixels width. On edge map of 1 pixel width of part1, elimination of small objects is applied. CDM result was CDM=5.19% on this.

Confusion matrix

The segmented object image of part1 of Aster SWIR de-correlation stretched 489 band combination is validated by the confusion matrix using reference object image. The overall accuracy is 71.0%. A majority filter reduces number of small objects in an image. The majority filter of 15 by 15 pixel size window is applied to the segmented object image. After this, the overall accuracy is 71.4%. It improves little bit compared to the original image validation. The majority filtered segmentation result and a reference are illustrated in figure 3.

4. Discussion

The current study explores a multivariate texture segmentation based on multivariate LBP operator for geological unit identification in Landsat TM and Aster SWIR images. The multivariate LBP complemented by RGB-3D color histogram is identifying the objects accurately. For the geological mapping, it provides a first sketch of the study area automatically.

Segmentation could give an important division of units otherwise invisible. Though segmentation results show smooth and accurate object identification, it detected too many small objects. Landsat TM and Aster SWIR are related to the solar reflection region, which brings information only from the top few microns-thick surficial features (soil, surface coatings, encrustations, dust).

The thermal infrared (TIR) data, in contrast, is related to a few centimeters-thick top surface zone and its emitted radiation. Since this is somewhat deeper, it may be better for geological application. Therefore the spectral features of the bedrock material are observable even if surficial coatings, encrustations are present. Further, the mineral spectra are basically additive in this region [5], and therefore rock spectra are interpretable in terms of relative mineral abundance. Although spatial resolution is low, TIR image segmentation could be applicable to various geological applications. Aster TIR image segmentation, its band combinations in TIR region, or image fusion with the SWIR region are out of the scope of the current study.

In geological mapping we need to map bedrock, ignoring the type of surface cover. In addition, some surface cover may cross bedrock unit boundaries, and therefore obscure them from the sensor's view, for example vegetation, alluvial fans (loose soil from a hill), loose debris from steep slopes (talus slopes).

Therefore, some geological unit boundaries can not be identified by the segmentation using different bands from solar reflection region and/or thermal infrared region. Accurate interpretation needs help from geophysical measurements to penetrate the surface and reach the bedrock. Such limitations are not so serious in Mongolia or in some other regions, considering that most of the area of Mongolia has sparse vegetation, outcrops are often well exposed, so that segmentation is expected to be useful for accurate geological mapping. For good geological unit identification, exploring different band selections is important.

For quantitative validation of the segmentation result, CDM was used. CDM was implemented with different weights based on the distance between detected edge pixel and reference edge pixel locations. CDM validation finds possible matching within neighborhoods in a certain window, and estimates the cost based on the matching. Finding possible matching is based on all possible matching between reference edge pixel and detected edge pixel.

As discussed in the Results, many small objects were identified in the segmented image. This is probably the main reason that only 2.5%-3.6% of the edges correctly matched between detected edge and reference edge images. This raises the question of how we can evaluate the obtained results properly. Visually, the segmentation results have good correspondence with geological units, but this is not reflected in the edge correspondence. There are two ways to have better matching, such as once there is too much displacement between reference edges and detected edges, we could allow a bigger window, and many neighbors for the matching. In this study, we allowed only 2 pixel difference in all directions, i.e., 5x5 window. The other way comes from the following question. Can we merge small objects all surrounded by only one class of object into larger object? The answer is yes because those edges are not occurring in the reference image. This should make a great difference in the overall result. But the elimination of small objects was not implemented in this study. It is obvious that the 1:200 000 scale of the geological map that we use as a reference makes a difference in validation.

Despite the structural information on geological map, geological boundaries between different units, those bedrock and superficial deposits are of our interest in this study. We used a geological map that was made for this study on the basis of a visual image interpretation and on the field knowledge at a scale of 1:200,000. It is generally acknowledged that geological maps are subjective and based on different concepts. The concepts (conceptual model-inference) of the mapping are outside the scope of the study. Data quality is an important issue, since RS and GIS tools enable integrity of different types of data and further for data sharing, for instance, geological map could be used as a base map for other applications and mapping. Can the geological map be updated using image segmentation? Yes, segmentation results give more detailed information. Depending on scale, we could use it for better detailed mapping.

A geologist can benefit from an enhanced remote sensing product and suitably interpret the image data, considering the various surficial features like dry channels [5]. Obviously, ground truth data is required for optimum geological mapping and lithological discrimination.

According to the development and daily use of GIS and geo-databases, we are required and allowed to have more accuracy to coordinate the information. Though spectral enhancement followed by visual interpretation is generally preferred for geological-lithological discrimination purposes, as compared to the automatic approaches, we argue that automatic approach gives accurate detection (improve accuracy of

delineation) in one hand, and the other hand, it gives more information to geologists about surface elements which need ground observation.

5. Conclusions

- In this research work, multivariate texture segmentation has been successfully used for geological unit identification. The segmentation accurately identifies different objects on the images. Overall accuracy is 71% in part1 segmented image, using Confusion matrix, which is standard technique to assess classification. It also detects many small objects, which make it difficult to compare the segmented image with reference image that does not contain those small objects.
- A selection of proper band combinations for segmentation is important. In this study, the VNIR and SWIR spectral regions are used for segmentation with different range combinations. Segmentation of de-correlated Aster SWIR band combinations results into smooth and accurate geological object identification.
- The discrepancy measure, CDM, is implemented for validation of segmentation. According to Zhang's evaluation, two properties of validation are the abilities to evaluate the segmentation results in a quantitative way and on an objective basis [13]. CDM is both an objective and a quantitative discrepancy measure. From the experimental results, it is shown that CDM is too sensitive for over-segmentation. For this reason, we have a very low similarity metric in the overall comparison between segmented and reference edge images. This discrepancy measure concerns an application that needs both reference image and segmented image. Small scale geological map which does not have small objects, is used as a reference in this study. It was the reason why we have low value of accuracy measure in the validation, in other hand.
- We used different accuracy measures and validation technique. From these, it becomes clear that the whole validation procedure is subject to uncertainty.
- Since more detailed object information and much more edges were obtained by segmentation, existing geological maps could be updated to have more accuracy based on the segmentation. Moreover, a large scale geological mapping, this segmented image can be used in the initial phase.

Bibliography

- [1] ALLEY, R. E. Algorithm Theoretical Basis Document for Decorrelation Stretch, 2.2 ed. Jet Propulsion Laboratory, 4800 Oak Grove Drive, Pasadena, CA 91109, August 1996.
- [2] GELSEMA, E. S., AND KANAL, L. N., Eds. Pattern Recognition in Practice IV: Multiple Paradigms, Comparative Studies and Hybrid Systems (1994), Elsevier.
- [3] GILLESPIE, A. R. Enhancement of Multispectral Thermal Infrared Images: Decorrelation Contrast Stretching. *Remote Sensing of Environment* 42 (1992), 147–155.
- [4] GILLESPIE, A. R., KAHLE, A. B., AND E., W. R. Color Enhancement of Highly Correlated Images. I. Decorrelation and HSI Contrast Stretches. *Remote Sensing of Environment* 20 (1986), 209–235.
- [5] GUPTA, R. P. *Remote Sensing Geology*. Springer-Verlag, Springer-Verlag Berlin Heidelberg, 1991.
- [6] LUCIEER, A., AND STEIN, A. Existential uncertainty of spatial objects segmented from remotely sensed imagery. *IEEE Transactions on Geo-science and Remote Sensing* 40 (2002), 2518–2521.

- [7] LUCIEER, A., STEIN, A., AND FISHER, P. Multivariate Texture Segmentation of High-Resolution Remotely Sensed Imagery for Identification of Fuzzy Objects. In review, 2003.
- [8] OJALA, T., AND PIETIKÄINEN, M. Unsupervised texture segmentation using feature distributions. *Pattern Recognition* 32 (1999), 477–486.
- [9] OJALA, T., PIETIKÄINEN, M., AND MÄENPÄÄ, T. Multiresolution gray scale and rotation invariant texture classification with local binary patterns. *IEEE transactions on pattern analysis and machine intelligence* 24, 7 (July 2002), 971–987.
- [10] PONOMAREVA, N. I., ROZOV, B. S., AND SHEVELEVA, N. I. Geological regions of Delgertsogt and Ukhtal sums, Dundgovi aimag, People's Republic of Mongolia, Results from the 1:200 000 scale geological mapping and surveying of section no. 155, in 1954. Tech. Rep. 815, Geological Information Center of Mongolia, Ulaanbaatar, 1956.
- [11] SEGUI PRIETO, M., AND ALLEN, A. R. A Similarity Metric for Edge Images. *IEEE Transactions on Pattern Analysis and Machine Intelligence* 25, 10 (October 2003), 1265–1273.
- [12] TSOLMONGEREL, O. Texture based segmentation of remotely sensed imagery for identification of geological units, MSc thesis, ITC, 2004
- [13] ZHANG, Y. J. A Survey on Evaluation Methods for Image Segmentation. *Pattern Recognition* 29, 8 (1996), 1335–1346.

LAND TENURE, ROADS AND BIODIVERSITY; AN INTERCONTINENTAL COMPARISON

Dr. Hein van Gils
gils@itc.nl

1. Introduction

Recent research on the impact of land tenure regimes and road development on biodiversity conservation is presented for discussion. International experience shows that major land reform and new roads are both likely to impact on biodiversity, an impact heightened by their combination. Mongolia will soon start implementing its Land Law of 2002 providing novel land tenure regimes for individuals and groups and concomitantly considers to construct the Millennium Road providing improved access to the Mongolian steppes. However, if unmitigated, new farm fences and road reserve fences could become barriers for the migrating wildlife.

Remote sensing and GIS have proven to be indispensable tools for detecting and monitoring the impact of both the developing land tenure regimes and such road developments on the biodiversity resources.

Parallels between the Millennium Road in Mongolia and the Trans-Kgalagadi-Road (TKR) in Botswana are discussed first. Both roads cut across extensive unfenced pastoral land that doubles as the habitat for the last regional migratory herds of their part of the Asian and African continents. Both roads are principally international: the TKH connects the economic heart of South Africa with the Atlantic in Namibia, the Millennium Road will connect China and Russia.

Next we explore two areas in Bolivia respectively South Africa each with 4-5 contrasting land tenure regimes found in close proximity under identical environmental conditions. In both areas biodiversity is threatened, in Bolivia by deforestation and in South Africa by invasion of alien weeds. On the world level conversion of tropical forest into non-forest cover types and invasion of alien weeds are considered major causes of biodiversity decline.

2. Trans-Kgalagadi-Highway EIA in Botswana

Need for a Trans-Kgalagadi-Highway (TKH) as a shorter international connection between the heartland of South Africa and the Atlantic Ocean (Walvisbay harbour, Namibia) have been considered for decades. Within Botswana the TKH connects the western rural periphery with the main cities in east. The TKH supplies the western cattle industry with road access to the export abattoir in Lobatsi, replacing cattle treks of several hundreds kilometres on the hoof.

The African Development Bank (AfDB) offered a loan for the TKH to the Government of Botswana (GoB) in 1991. An Environmental Impact Assessment (EIA) was an AfDB loan conditions. At the time Botswana lacked national EIA legislation. A consultant carried out the EIA. An ITC MSc undertook a re-engineering of the EIA using GIS.

3. TKH Environmental Impacts

The screening and scoping phase of the EIA identified the *barrier effect* on the migratory of herds of herbivores (Wildebeest, Hartebeest, Gemsbok, Springbok) as

potentially the dominant impact. The barrier effect could apply to the road itself, to a fenced road reserve and the development of fenced cattle farms along the TKH.

The TKH had three alternative routes in the Ghanzi District: the northern (Ghanzi cattle trek), the middle (Okwa valley) route and the southern cattle trek. For all practical purposes the three alternative routes had the same length. The northern and the southern treks served the beef industry best.

The Ghanzi District is about the center of the Kgalagadi Ecosystem in Botswana. The Kgalagadi extends further across internationally boundaries in all directions. The Kgalagadi is an extended sand-plain, lacking permanent surface water. Hunter-gatherers (San; Bushman) were the only inhabitants of the central Kgalagadi prior to the import of borehole technology about a century ago, which allowed permanent settlement of Afrikaner cattle ranchers and African cattle pastoralists. Ten thousands of large wild herbivores move through the wider Kgalagadi ecosystem reacting to the episodic availability of green grass, seasonal rivers and pans.

Two aerial wildlife surveys or censuses are available in shapefile format (ESRI; ArcView/ARCGIS). The survey of 1979 represents the data from 4 consecutive aerial censuses in 1978-1979 of the Kgalagadi area aggregated into blot-shaped polygons. The 2002 census has been carried out in the dry season and covers the entire country in grid-shaped polygons of sizes varying with wildlife densities.

The challenges in the EIA of the TKH alternatives were how to assess herbivore presence over seasons and drought years and how to weigh one animal species against another. The economic valuation of the three alternative TKH routes took stock of numbers of cattle farms, heads of cattle and number of people served by each route. The northern alternative was finally selected as combining the minimum barrier effect with the best access for the beef industry. However even the environmentally best route presents potentially a barrier for the moving herds. The TKH EIA proposed two major mitigations to reduce the barrier effect: (1) unfenced road reserve and (2) gradually sloping banks. Both mitigations have been accepted and have been implemented in road design and road construction. Further mitigations for the TKH, or similar roads like the Millennium Road, are suggested.

4. Land tenure regimes and roads in Bolivia

The most important proximate cause of biodiversity decline on world level is the conversion of tropical forest into non-forest cover types. With four nearly cloud-free LANDSAT-TM satellite images from 1986, 1990, 1996 and 2002 conversion of forest was quantified for an ITC research area in Bolivia. Geometric correction, normalisation, enhancement, pre-classification, classification and overlaying of the four images have been carried out with the ILWIS 3.1 software.

Conversion of Closed Forest (CCF) into other cover types, mainly Grass, Crops and Open Forest, occurs between 1986-2002 in the ITC research area of Cochabamba, Bolivia at an annual rate of 3.1%. CCF into non-forest cover types shows a rate of 1.5%. The land tenure regime and the distance from roads can largely explain the CCF, each with high significance ($p < 0.001$). Soil texture, as proxy for soil fertility and soil suitability for farming, shows no predictive powers for CCF. Distances from settlements and topography have minor predictive powers for CCF, although at a relative low level (low LRT and low to intermediate significance).

Closed Forests in the Colonies & Syndicates, National Park (NP) and Untitled Land have been converted into Non-Forest (Table 4) in similar proportions (62-64%). At the

other end of the scale the Closed Forest in the University Reserve proved to be nearly immune to conversion. On Indigenous land CCF shows an intermediate level (32%).

The CCF seems to be driven by road extension and by land tenure regime, both facilitating agricultural expansion. What a positive message for biodiversity resource management. Both the number of roads and their alignment are manageable. Furthermore land tenure arrangements are at the discretion of society. Tenure and management by indigenous people and by NGO's appear more effective than state ownership, even if the latter is with the explicit goal of conservation such as the NP. Of course I am aware that here in Mongolia we have steppes rather than forest. But it seems better for (forest) nature conservation that indigenous people own and manage land. And the NGO (university) seems to be a better owner and manager of their nature reserve than the government is of their National Park.

5. Land tenure regime and alien weeds in South Africa

Invasion by alien plants is considered to be a main cause of biodiversity decline. Field sampling of alien weed invasion in the uncharted forest reserve required high-resolution satellite imagery. The Aster satellite image (8 June 2002, band 3, 2 and 1) has been geo-referenced, re-sampled, classified (Maximum Likelihood) for land cover with ground control points and its accuracy assessed (confusion matrix) with ILWIS 3.1 Academic. The digitising of analogue cadastral maps and the plotting the GPS based ground sampling of the weed *Chromolaena* was done with ILWIS 3.1. ArcView 3.3 was used for generating the land tenure regime map.

Across four land tenure and land management regimes in South Africa the tropical "weed" *Chromolaena* was abundant in the State Forest Reserve (19.2%). Weed abundance in corporate plantation forest (9.4%) was less than half of that in the Reserve. Both the private cane farms (2.1%) and the Communal Land Trust grasslands (2.9%) show a substantially lower abundance of the weedy invader.

6. Land tenure regimes and biodiversity

In both Bolivia and South Africa the state owned and state managed conservation areas (respectively National Park and Forest Reserve) showed to be the least effectively protected against biodiversity resource degradation. Biodiversity resources were best conserved in the indigenous (communally), institutionally and corporately owned and managed land across research areas. The privately held farmland performed in between.

7. Issues for Mongolia

How to go about an EIA of the Millennium Road? How to mitigate a barrier effect of a Millennium Road? Can the EIA be done with GIS? Are alternative road alignments available for EIA?

What land tenure regimes, state, group (communal), private individual, private corporate or institutional (NGO) would be optimal for biodiversity conservation in Mongolia?

References

- Laletsang, G.T. (1997). Impact assessment of the Trans-Kgalagadi Highway on wildlife. MSc thesis ITC, Enschede: 108 pp.
- Loza, A.V.A.U. (2004). A spatial logistic model for tropical forest conversion. MSc thesis ITC, Enschede: 74 pp.
- Mwanangi, M.M. (2003). Spatial distribution of invasive species and land tenure. MSc thesis ITC, Enschede: 60 pp.

USE OF REMOTE SENSING (RS) AND GEOGRAPHIC INFORMATION SYSTEM (GIS) TECHNOLOGY FOR IMPROVING SPECIAL PROTECTED AREAS MANAGEMENT: CASE STUDY; UVS LAKE BASIN, WESTERN MONGOLIA.

Byamba Tsend-Ayush,
Senior officer, Protected Areas Management division, Ministry for Nature and
Environment.

Post box 1107, Ulaanbaatar 13, Mongolia. Email: tsend@mobinet.mn

1. Introduction

The Uvs Nuur Basin is located in the heart of Central Asia and it covers neighboring territories of the northwestern part of Mongolia and part of the republic of Tuva located on the southern frontier of the Russian Federation (figure 1). «The Uvs Nuur Basin» site includes territories of two nature preserves - «The Ubsunur Hollow» in Russian Federation and «Uvs Nuur» in Mongolia. The Mongolian «Uvs Nuur» preserve consists of four clusters with the following coordinates:

- | | |
|---------------------|--------------------|
| 1. «Tsagan shuvuut» | 91° 09'E; 50° 19'N |
| 2. «Turgen» | 91° 22'E; 49° 46'N |
| 3. «Uvs Lake» | 92° 53'E; 50° 20'N |
| 4. «Altan els» | 95° 00'E; 49° 50'N |

The Uvs Nuur Basin contains 6 ecological zones: cold desert, desert-steppe, steppe, boreal forest and deciduous forest, taiga, alpine tundra within an ancient central Asian lake basin 160 km from North to South and 600km from East to West.

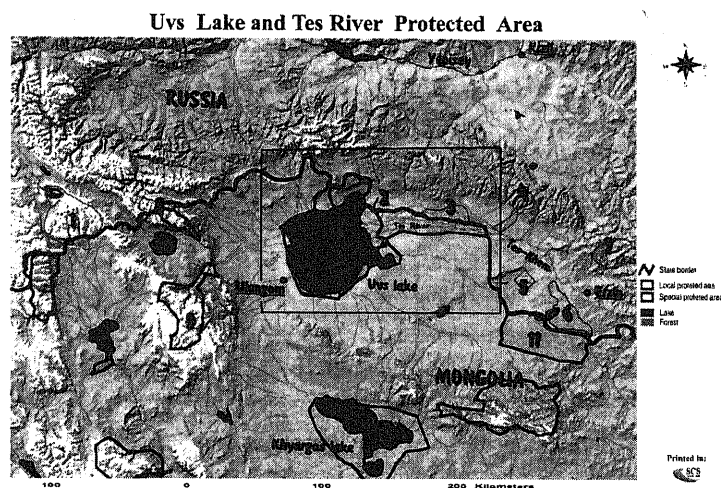


Figure 1- Location of Uvs Nuur SPA.

This basin is an extraordinary place in regards to the diversity of ecosystems and species present within such a small, enclosed basin. This provides an excellent opportunity for the study of watershed basin dynamics within many different biomes. Uvs Nuur (the largest salted lake according to surface area in Mongolia), several tall peaks, 20% of Mongolia's glaciers, Mongolia's second tallest waterfall and many high altitude lakes are all within the protected areas.

With regard to significant habitats for threatened species, Turgen Uul, Tsagaan Shuvuut and Mongun-Taiga strictly protected areas contain essential habitat for snow leopards.

2. The strategy for nature conservation:

A classical method for nature conservation is to ensure pristine nature and keep the ecological balance by expanding Protected areas network and inclusion of new areas for protection. The Mongolian Protected Areas' Network has been established following such a concept. In order to expand the protected areas network, it is required to take into account the vulnerability of the particular species and characteristics of biodiversity of this region.

The Protected areas system in Mongolia consists of two main parts: Strictly Protected Areas (SPA) and National Parks (NP). There are 14 Protected Areas' (PA) administrations under direct management from the Ministry of Nature and Environment (MNE). In addition, there are two more classification: Natural Reserves and Monuments. These are under direct management of local Governor's administration. In Mongolia in 1992, approximately 6 million ha. of land constituting 13 Protected areas existed. Today the total number has increased to 21 million ha. (Figure 2) and it represents 56 protected sites, which is 13.5% of the entire country. The Mongolian Parliament passed the 'Law on Special Protected Areas' in 1994 and the 'Law on Buffer Zones of SPA' in 1997, and approved the National Program on Special Protected Areas in 1998. The National program has around 30 separate rules and regulations.

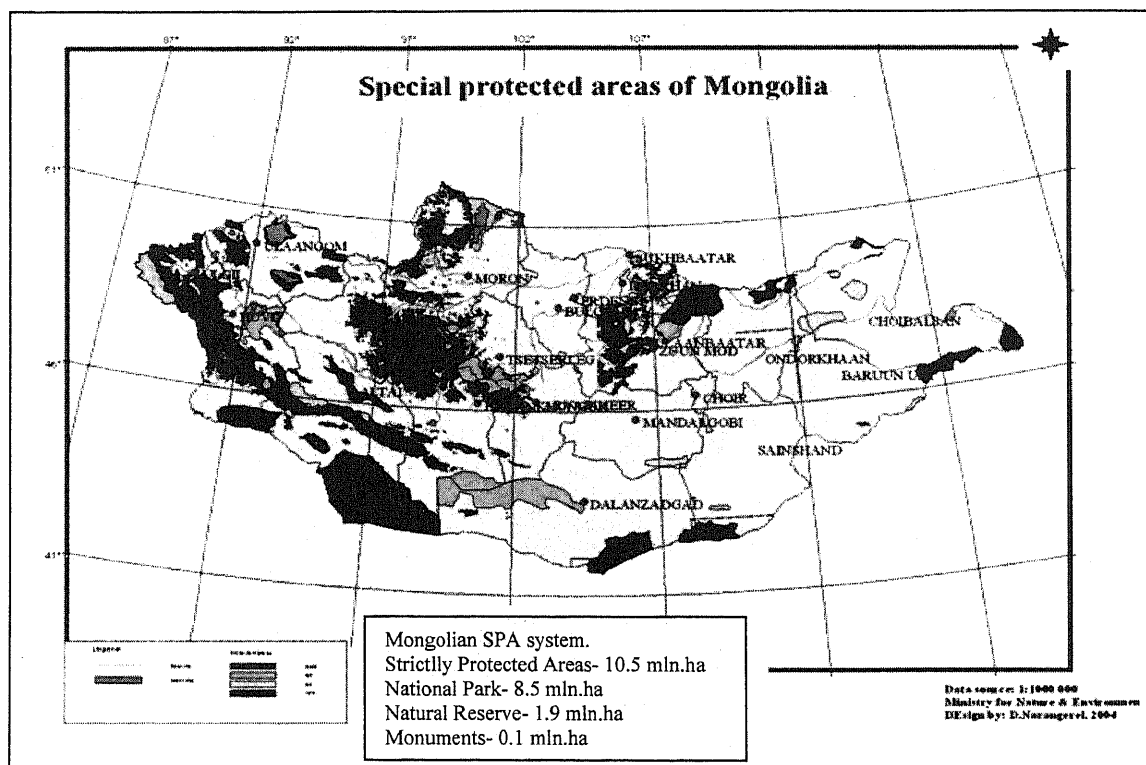


Figure 2. Mongolian Protected Areas' network.

The new conservation strategy adopted by the World Wide Fund for Nature (WWF) and by other international conventions and programs has an objective to concentrate conservation efforts on key ecological regions.

The Altay-Sayan eco-region within Uvs lake basin has been determined by the environmental community as a key ecoregion, and it is characterized by a distinct set of species and ecological conditions. According to the resolution of Mongolian Parliament,

approved on October 12, 1993, the Uvs lake-basin was included into the Mongolian Special Protected (SPA) areas system.

The main criteria for the selection of Uvs lake basin into the SPA system of Mongolia and the UNESCO World Heritage list in 2001 carried the following arguments:

(I) The property contains examples of the major stages of earth's history and outstanding geological features. Glacial activity, slope erosion and mobile sand dunes are significant and many geomorphological processes continue in this area.

(II) The basin contains examples of on going ecological and biological processes. The property contains a wide range of natural ecosystems in close proximity to each other, and is thus ideally suited for ecological research.

(III) The basin contains natural phenomena and areas of exceptional natural beauty and aesthetic importance.

(IV) The basin contains the most important and significant natural habitats for several endangered species. This property supports a high number of biodiversity, including a high number of relic and threatened species.

3. Trends in nature conservation

All management activities, policy and strategy objectives within the SPA system requires regular use of up to date information on natural resources, their status and succession dynamics. Due to the large size of the Uvs Nuur SPA and lack of socio economic development inside the region the existing problems could be described as follows:

1. Lack of Technology:

- Urgent needs for accurate up to date geo information.
- Lack of basic equipment and funding for inspection and monitoring activity.
- Most of management plans exist only on paper.
- Absence of information and monitoring system about forest fires in the region.

2. Poor Management and limited Human resources capacity

- Environmental monitoring and inspection system needs to be improved.
- Insufficient involvement and weak participation of rural population and existing communities in conservation programs and policy formulation.
- Weak cooperation within local administration both at sum and aimag level with park administration and ministry.
- The area is large, therefore up to date monitoring and inspection of forest, river basins and watershed regions are difficult.
- Human capacity building of the rangers and park staff is one of the main issues.

At present the Mongolian Protected areas system has had limited research, and lacks up to date mapping. The RS/GIS application has been used for conservation projects at Hustai National Park (wildlife and biodiversity conservation) and several projects from the German Technical Cooperation (GTZ) organisation. WWF successfully used GIS for visual representation of the protected areas network on selected cites, including Altay-Sayan ecoregion.

4. Remote Sensing/GIS contribution

The integration of Remote Sensing and GIS technology in Protected area management will support management and planning processes. Mapped information is important in designing plans for protection of rare and very rare species, their habitats

and biodiversity itself. At this moment, all management activities and strategy planning include limited use of detailed geo information.

A basic step for using RS and GIS technology on SPA management is cooperation and information exchange between different ministries, international projects, Agencies and NGO's. The obtained information could be linked and stored within a special database for serving as supportive tool on environmental management and planning. Such information is especially important for long term planning and monitoring activities.

The proposal of process modeling for such tasks using RS and GIS information for SPA management is shown in figure 3.

Table 1 shows possible contribution of RS information and GIS technology into Protected area management activities.

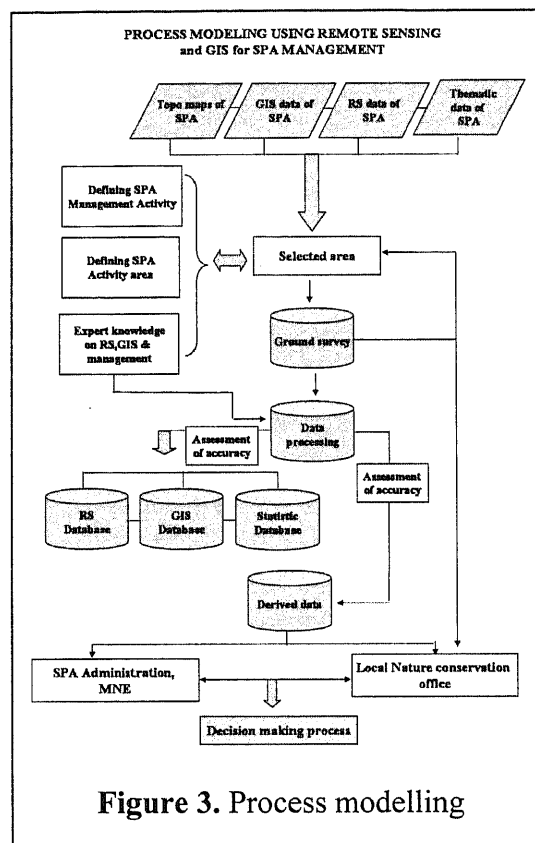


Figure 3. Process modelling

Table 1.

Planned activities	The main objective of the activity	Implementing institution	Proposed contribution from RS and GIS
1. Protection of biodiversity within selected sites	1.1.1 Determining of the location of rare and very rare species which are needed to be protected from human impacts.	Research organizations, local PA administration	Mapping of species habitat closely located to settlements and infrastructure (pasture camps; roads). Overlapping with rangers monitoring areas.
2. Basic activities on pasture management	Estimation of pasture carrying capacity	PA administration relevant organizations	Large scale pasture- land cover/land use.

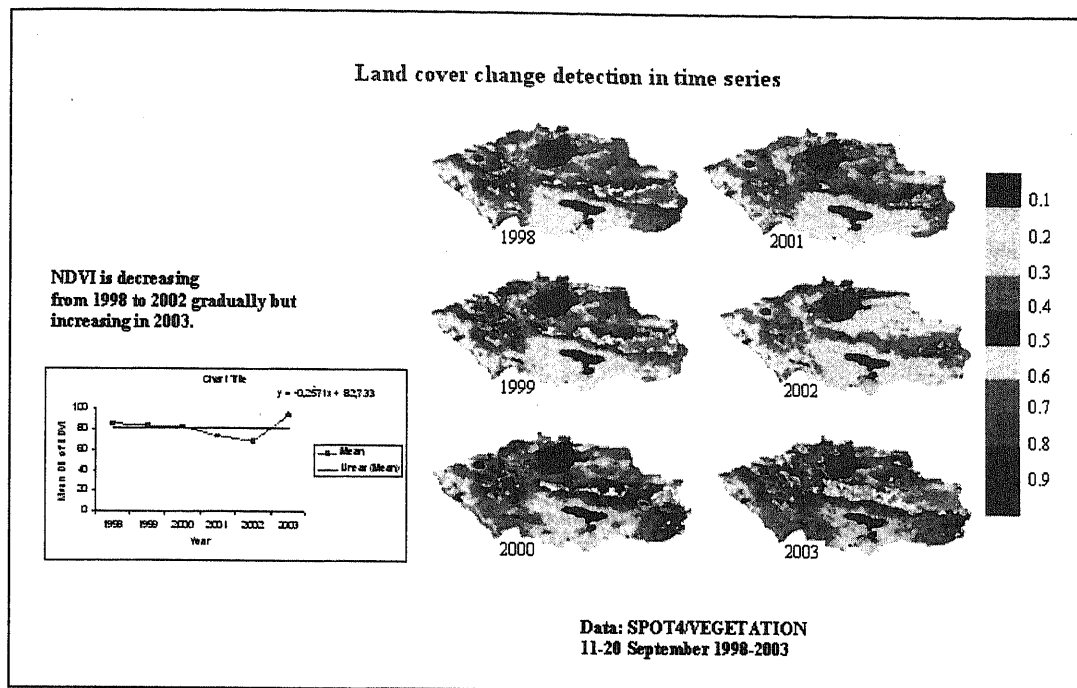


Figure 4. Land cover change detection.

5. Summary and conclusions:

- All management activities and strategies should rely on up to date information, including that available today through RS and GIS technologies.
- Considerable information has been collected by few professionals with limited budget.
- This information needs to be incorporated into a useful database, and additional information, collected using modern equipment and trained professionals.
- RS and GIS are modern tools. They need to be applied to the Protected Areas System.
- In order to make RS and GIS work for the Protected Areas' System and natural resources, it is crucial to cooperate with related ministries, agencies as well as appropriate NGO's.

References:

1. Uvs lake basin SPA management plan, prepared by B.Tsend-Ayush, Ministry for Nature & Environment, Ulaanbaatar, Mongolia, 25.04.2003
2. Long-term conservation of the Altai-Sayan eco-region, WWF, 2004.
3. "Nomination Uvs Nuur Basin", Mongolia and Russian Federation, 2001. Prepared by: Ubsunur Int.Center, Russia; Geography Institute, RAS; Geology, Geoecology Institute MAS. Sponsored by Greenpeace Russia, Federal Agency for Nature Conservation, BFN Germany.
4. S.Pradhan, 1999, Integration of GIS and RS for Crop Average Estimation: An information system development Approach, ICIMOD.
5. Multi-purpose geographic database guidelines for Local governments, 1999, ACSM-ASPRS Geographic Information Management System (GIMS) Committee, Remote Sensing and Photogrammetry, USA.

ANALYSIS OF DYNAMIC CHANGE ON LAND USE IN EAST TWO ALLIANCES AND TWO CITIES IN INNER MONGOLIA

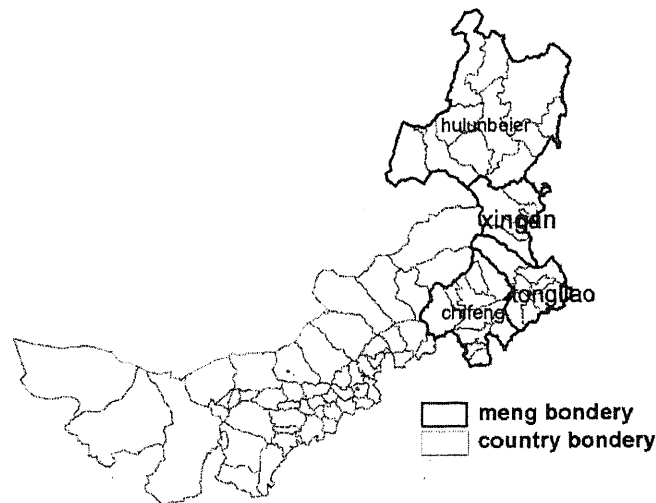
Bao-yu-hai¹ A-la-ten-tu-ya² Sa-re-na¹ A-mu-gu-leng¹

1 Inner Mongolia Autonomic Zone Key Lab of Geographic Information System

2 Institute of Geography Science Inner Mongolia Normal University, Huhhot, China

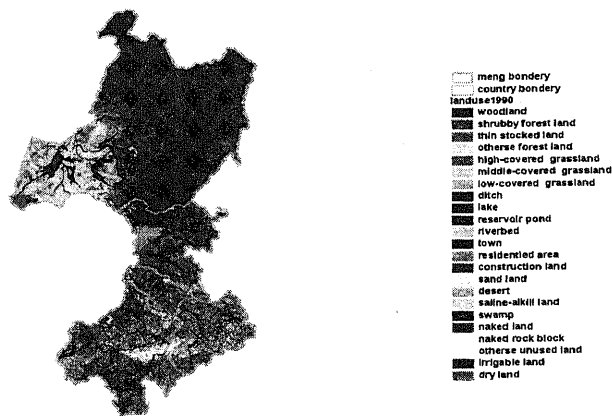
Abstract

The east two alliances and two cities in Inner Mongolia are the main body of the agriculture, forest and animal husbandry interlaced zone, have obvious transitive character, and are also one of the most sensitive area for the reaction to global change. Making use of TM data of 1990s and 2000 year as information source through synthesis, enhancement, correction, mosaic and man-computer interactive, and giving priority to farmland, the situation of land use change on this region is analyzed, and sustainable use countermeasure is put forward in this paper.



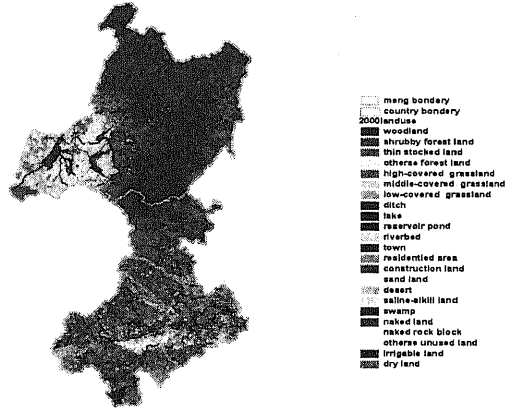
Map 1. Position of east part in Inner Mongolia

The East Zone of Inner Mongolia Land Use Map(year1990)



Map 2. Land use of east part in Inner Mongolia in 1990s

The East Zone of Inner Mongolia Land Use Map(year 2000)



1 Cultivated land

1.1 Omni-amount changes of cultivated land

From 1990 to 2000, the area of cultivated land in east two alliances and two cities in Inner Mongolia increased, amounted to $104.84 \times 10^4 \text{ hm}^2$. In which, the area of increased cultivated land in Hulunbeier alliance was the most, came to $33.46 \times 10^4 \text{ hm}^2$; Secondly, Chifeng city, came to $27.66 \times 10^4 \text{ hm}^2$; The least was in Xingan alliance, only $20.33 \times 10^4 \text{ hm}^2$. However, by comparing the expansion of cultivated land in every alliance and city to its whole land and scale of agricultural population, the expanding speed of Cultivated land in Xingan alliance is fastest, reclamation is most intense.

1.2 Regional distinction of alteration

1.2.1 Newly reclaimed land

From 1990 to 2000, the area of newly reclaimed land in east two alliances and two cities in Inner Mongolia amounted to $136.35 \times 10^4 \text{ hm}^2$. In which, the area in Hulunbeier alliance was the most, came to $58.39 \times 10^4 \text{ hm}^2$; Secondly, Chifeng city, came to $29.69 \times 10^4 \text{ hm}^2$; The least was in Xingan alliance, only $21.30 \times 10^4 \text{ hm}^2$.

The newly reclaimed land in Hulunbeier alliance mostly distributed in its southeast and northwest woodland and grassland region. Within more than ten years, the total area of forest reclamation and meadow reclamation respectively came to $21.19 \times 10^4 \text{ hm}^2$ and $35.39 \times 10^4 \text{ hm}^2$. The area of newly reclaimed land in Arong banner, Molidawa banner, Eerguna city, Elunchun autonomous banner and Ewenke autonomous banner was the most, the newly reclaimed meadow and forest were all more than $1.00 \times 10^4 \text{ hm}^2$. Especially Molidawa banner and Elunchun autonomous banner, their reclaimed area respectively came to $12.80 \times 10^4 \text{ hm}^2$ and $14.58 \times 10^4 \text{ hm}^2$.

The distribution of newly reclaimed land in Xingan alliance was comparatively homogeneous. It distributed in other four banners except Wulanhaote city, respectively came to $7.73 \times 10^4 \text{ hm}^2$, $4.85 \times 10^4 \text{ hm}^2$, $5.86 \times 10^4 \text{ hm}^2$ and $2.67 \times 10^4 \text{ hm}^2$. The reclamation was mainly grassland reclamation, which occupied 85.22% of the whole reclaimed land. For Keerqin banner, there was only $1.36 \times 10^4 \text{ hm}^2$ forest reclamation.

The newly reclaimed land in Chifeng city focused on grassland, its area occupying 86% of the whole. In the whole city, except Linxi county and Kalaqin banner, other banners all had different area of grassland reclamation.

Tongliao city also focused on grassland reclamation, occupied 87.7% of the whole city. Likewise, every banner of the city all had reclamation, the most reclaimed area lied in Zhalute banner, occupied 35.9% of the whole grassland reclamation in this city

1.2.2 Returned cultivated land

From 1990 to 2000, the total area of returned cultivated land in east two alliances and two cities amounted to $31.51 \times 10^4 \text{ hm}^2$. The area of returned cultivated land in Hulunbeier alliance was the most in it, came to $24.94 \times 10^4 \text{ hm}^2$; Secondly, Tongliao city, came to $3.56 \times 10^4 \text{ hm}^2$; The least was in Xingan alliance, only $0.98 \times 10^4 \text{ hm}^2$.

For Hulunbeier alliance, the returned cultivated land was mostly in the southwest Hulunbeier sandy land. Within more than ten years its returned cultivated land into grassland came to $24.3 \times 10^4 \text{ hm}^2$, occupied 97.4% of the whole. Ewenke autonomous banner, Xinbaerhu left banner, Chenbaerhu banner which lied in sandy land respectively had returned cultivated land 7.78 hm^2 , 3.21 hm^2 and 11.7 hm^2 .

For Xingan alliance, the returned cultivated land was very scattered, and its strength was not enough, too. For Chifeng city and Tongliao city, the distribution of de-cultivated land was very concentrated. The banners returned cultivated land into grassland and forest were almost Alukeerqin banner, Keshiketeng banner, Wenniute banner and Aohan banner which lied in Keerqin deserts. At the same time, the area of returned cultivated land to forest in Chifeng canton was larger, occupied 36.2% of the whole area of returned cultivated land. In Naiman banner of Tongliao city, the area of returned cultivated land to forest came to $1.14 \times 10^4 \text{ hm}^2$, occupied 52.8% of the whole returned cultivated land to forest.

2 Forest

2.1 Changes of omni-amount

From 1990 to 2000, the area of forest in east two alliances and two cities in Inner Mongolia decreased, nearly $81.04 \times 10^4 \text{ hm}^2$. About $52.98 \times 10^4 \text{ hm}^2$ forest in Xingan alliance decreased in it, the amount was the first of the four alliances and cities; Secondly, Hulunbeier alliance, forest decreased $24.70 \times 10^4 \text{ hm}^2$; The changes of forest in Chifeng city and Tongliao city were not obvious, respectively decreased $1.15 \times 10^4 \text{ hm}^2$ and $2.21 \times 10^4 \text{ hm}^2$. According to the forest changes, within more than ten years the forest destruction and land reclamation in Xingan alliance and Hulunbeier alliance had obvious influences on the forest changes of the two alliances.

2.2. Regional distinction of alteration

2.2.1. Forest destruction

From 1990 to 2000, the area of forest destruction in east two alliances and two cities was $84.48 \times 10^4 \text{ hm}^2$. The area of forest destruction in Xingan alliance was the most in it, the forest decreased $53.28 \times 10^4 \text{ hm}^2$; Secondly, Hulunbeier alliance, decreased $24.88 \times 10^4 \text{ hm}^2$; The least was in Chifeng city, only $1.85 \times 10^4 \text{ hm}^2$.

For Xingan alliance, forest primarily became grassland, mostly distributed in Keyou before banner, occupied 98.57% of the whole changes. At the same time, forest destruction led to $1.36 \times 10^4 \text{ hm}^2$ land reclamation in this banner.

For Hulunbeier alliance, the decrease on forest mostly resulted from large scale of forest destruction and land reclamation. From 1990 to 2000, $2.12 \times 10^3 \text{ km}^2$ forest decreased because of forest destruction and land reclamation, occupied 85.17% of the whole decrease on forest in this alliance. Land reclamation was mostly concentrated on Arong banner, Molidawa banner, Elunchun autonomous banner and Chenbaerhu left banner. The area of forest destruction and land reclamation was respectively up to $3.09 \times 10^4 \text{ hm}^2$, $10.61 \times 10^4 \text{ hm}^2$, $6.19 \times 10^4 \text{ hm}^2$ and $1.03 \times 10^4 \text{ hm}^2$.

2.2.2 Forestation

At the same period, the total area of forestation in the east two alliances and two cities was $3.44 \times 10^4 \text{ hm}^2$. At this point, the area of forestation in Tongliao city was the most, within more than ten years amounted to $2.26 \times 10^4 \text{ hm}^2$, accounted for 65.7% of the whole forestation in east two alliances and two cities, the other three alliances and cities had certain forestation, too.

3 Meadow

3.1 Omni-amount changes of meadow

From 1990 to 2000, the area of meadow in east two alliances and two cities in Inner Mongolia decreased, nearly $49.03 \times 10^4 \text{ hm}^2$. However, changes differed from each other. The area of

meadow in Chifeng city, Tongliao city and Hulunbeier alliance all decreased, respectively $22.81 \times 10^4 \text{ hm}^2$, $21.17 \times 10^4 \text{ hm}^2$ and $9.59 \times 10^4 \text{ hm}^2$. On the contrary, the area of meadow in Xingan alliance increased $4.53 \times 10^4 \text{ hm}^2$.

3.2 Regional distinction of alteration

3.2.1 From meadow to non-meadow

From 1990 to 2000, $104.44 \times 10^4 \text{ hm}^2$ meadow in east two alliances and two cities in Inner Mongolia became non-meadow and reclamation became the main factor for the decrease on the area of meadow. Within more than ten years meadow reclamation led to the decrease on the area of meadow $102.76 \times 10^4 \text{ hm}^2$, accounted for 98.39% of the whole decrease on meadow, in the meanwhile, $1.68 \times 10^4 \text{ hm}^2$ meadow completely degenerated into land difficult to use because of desertification or becoming salty land.

Meadow reclamation and meadow degeneration were quite popular in east two alliances and two cities. Owing to reclamation, $35.39 \times 10^4 \text{ hm}^2$ meadow in Hulunbeier alliance decreased; $25.56 \times 10^4 \text{ hm}^2$ in Chifeng city; $24.16 \times 10^4 \text{ hm}^2$ in Tongliao city and $18.28 \times 10^4 \text{ hm}^2$ in Xingan alliance.

3.2.2 From non-meadow to meadow

At the same period, barren put-down or forest felling resulted in $55.41 \times 10^4 \text{ hm}^2$ increase on the area of meadow in east two alliances and two cities. Forest felling led to $24.17 \times 10^4 \text{ hm}^2$ increase on meadow in it; Returning cultivated land led to $26.77 \times 10^4 \text{ hm}^2$ increase on meadow.

However, changes and changing breadth of the area of meadow in every alliance and city differed from those of entire east region. In the two alliances and two cities, the increasing breadth of meadow area in Hulunbeier alliance and Xingan alliance was larger, respectively $26.01 \times 10^4 \text{ hm}^2$ and $22.81 \times 10^4 \text{ hm}^2$, respectively occupied 46.94% and 41.17% of the whole meadow increase in east region in Inner Mongolia.

In the meanwhile, the factors for the area changes of meadow were various. For the increase on the area of meadow in Hulunbeier alliance, the main factor was returning cultivated land; for Xingan alliance, mainly resulted from forest felling.

4 Problems in land use and countermeasures to land resource sustainable use

4.1 farm belt

The present main problems in land use includes that land secondary salinization is serious, drain and irrigation system is not perfect enough, and water resource use rate is low. In mountainous and upland area, the nature condition is very bad, and a great deal of reclaim had resulted in fearful loss of soil and water.

It is necessary to take some countermeasures that include that to take de-cultivation policy to change the situation of dry land super advantage step by step in bad nature condition area; to build more farmland irrigation works, to develop irrigable land, paddy field and vegetable land, and to build and develop bases that produce commercial foodstuff, fat, fruits and sub-foodstuff in wellspring area.

To develop save-water agriculture. With little drainage area as unit, Basing on save-water agriculture, the demonstration projects that treat desertification synthetically would take effect on improvement of farm belt environment and sustainable use of land resource.

4.2 pasturing area

The main problems include that matching between water and grass is not suitable; environment is frangible; use of grassland is not balanced; long-term excess browsing; a great deal of grassland had salinized; construction level of grassland is low; ability of counterdisaster is puny.

Countermeasures and suggestions to land resource sustainable use include that: to enforce constructing of grassland; to develop and utilize water resource reasonably; to ban assarting grassland in disorder; to build natural protection zone; to take the policy of "double contract" in pasturing area

4.3 agriculture and pasture interlaced zone

The main problem is that the phenomenon of salinization, loss of soil and water and desertification are the most serious.

Countermeasures to land resource sustainable use include that: □by planning together, distributing reasonably, and optimizing the structure of land use, to heighten land use rate and economical effects; □regarding water as importance, forest and grassland as root, implantation as center, to take agriculture synthetical development policy. By improving production condition and environment, integrating economical effects, environment effects and social effects, to lead agriculture to a sustainable stable harmonious development road; □to add devotion to land, to heighten land use level and intensive degree; by exerting strength of state, group and individual, integrating measures of biology and project, to quicken synthetical treatment of little drainage area. It is necessary not only now but also in the future that to increase green vegetation, to defend wind and rivet sand, to improve environment.

4.4 Forest zone

The main problem is that a great deal of freeze-thaw erosion zone has come up because of air temperature increasing, forest over-cutting and etc. This does harm to not only forest cutting but also forest resource rebirth. Of course, there are others bad phenomenon including that cutting exceeding foresting, fall exceeding growth per year, forest resource decreasing year by year, forest quality decline step by step.

Countermeasure to forest land resource sustainable use is basing present condition, taking the policy of “integrating cutting and foresting, sustainable use” to develop forest resource and protect forest advantage.

STUDY OF ELECTRIC POWER CONSUMPTION AND CARBON DIOXIDE EMISSION BY USING DMSP/OLS DATA

Husiletu¹ Masanao Hara² Fumihiko Nisio¹

¹Center for Environmental Remote Sensing, Chiba University, Japan

²VisionTech Inc, Japan

1. Introduction

The 21th century is the environmental century. Cause of CO₂ discharged by burning large amount fossil fuels such as petroleum and coal has led to green effect resulting in global warming.

In this paper CO₂ emission from electric power consumption and relation of human activity from the nightlight, estimate the CO₂ emissions with the time series data for one year of DMSP/OLS. In order to increase the monitoring accuracy of DMSP/OLS, a gain revising model is to be developed, and then an advanced model to extract the stable light will be made. Based on the above development of technology, local analysis could be done. analyze the Satellite image of the study areas and estimate the CO₂ emission and electric power consumption of all provinces and cities. At last I will confirm statistical data of electric power consumption and the amount of CO₂ emission. It spreads the estimate method with the amount of electric power consumption by the analytic data of DMSP /OLS and the amount of CO₂ discharge. Purpose grapples with the problem of global warming due to the discharge of CO₂.

This paper is on the monitoring, by DMSP/OLS, to forest fire and the wide shutoff of electric power. On the other hand, this paper will introduce the dataset and the future research.

2. Background

On the research of OLS/VIS concerning the light from land, Elvidge et al. exacted the stable light in city region by time-scale data. On the other hand, using the unstable light, they also studied the method by which to induce the forest fire. As regards of the releasing of CO₂, Elvidge et al. observed that there is a relationship between the light in a region and the energy associated with CO₂. Doll et al. confirmed the relation is linear between the exponent of area of the light distribution and the exponents of the GDP and the release of CO₂. At the same time, they are making the releasing map of CO₂. Using DMSP/OCS data, Hara et al. analyzed the relationship between the consumption of the electric power and the release of CO₂ in some parts of Japan, China and Korea. Their research suggested that the light relate closely the consumption of electric power and the release of CO₂.

3. Research content and the future research topics

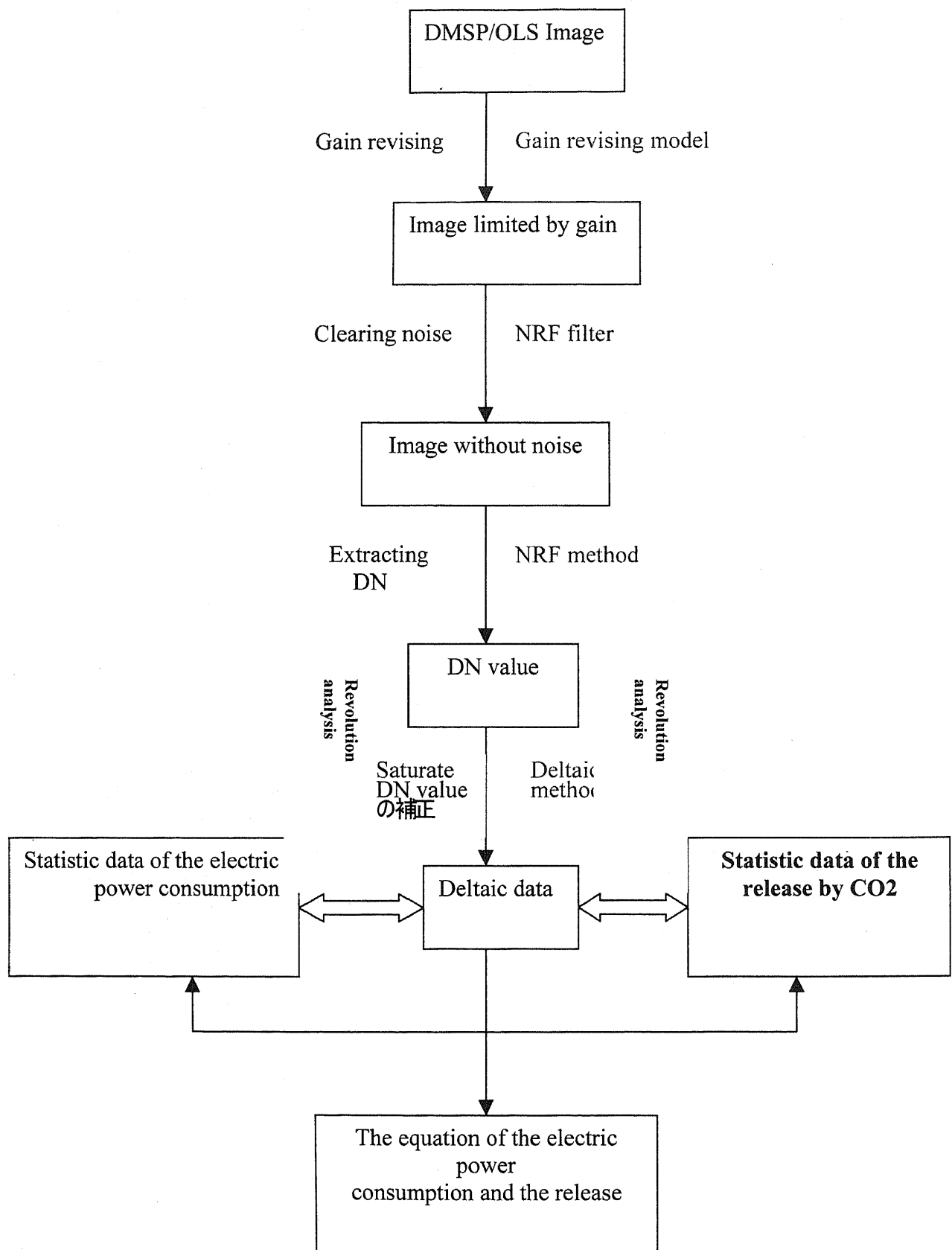


Fig 1. Flowchart of research procedure

After gain revising, the DMSP/OLS image without the limiting of gain 補正 is obtained. Using the NRF filter developed by Hara et al., clear the noise, after that the image without noise will be gotten. Extracting the DN value from image by use of the NRF method, we can get the DN value in each region. revising the saturate DN value by the Deltaic method modified newly, the Deltaic data, statistic data for the electric power consumption and the statistic data for the release of CO2 are gained. From the above data, to induce the formula of the power consumption and the release of CO2.

3.1 Development of the Gain Revising model

Owing to the limitation by the gain, though the body, which emits light, is same, the light valve in different image scene is different. This phenomenon will impact on the extracting stable light exactly. So it is necessary to develop the Gain revising model to delete the limitation due to gain.

3.2 Development of the model to extract the stable light

Figure 2 and Figure 3 are the results of the correlation between the deltaic data and the power consumption and the release of CO2. As seen from the figures, the correlations of the power consumption of Tokyo, Kansai, Tohoku and Hokkaido are low.

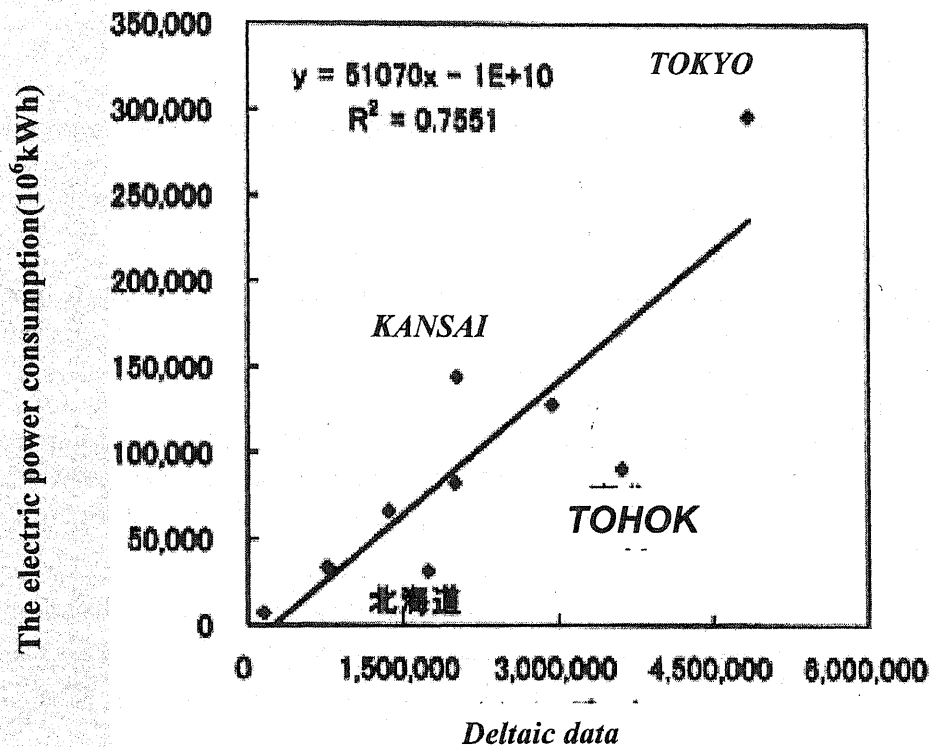


Fig 2. Correlation between the deltaic date and the power consumption

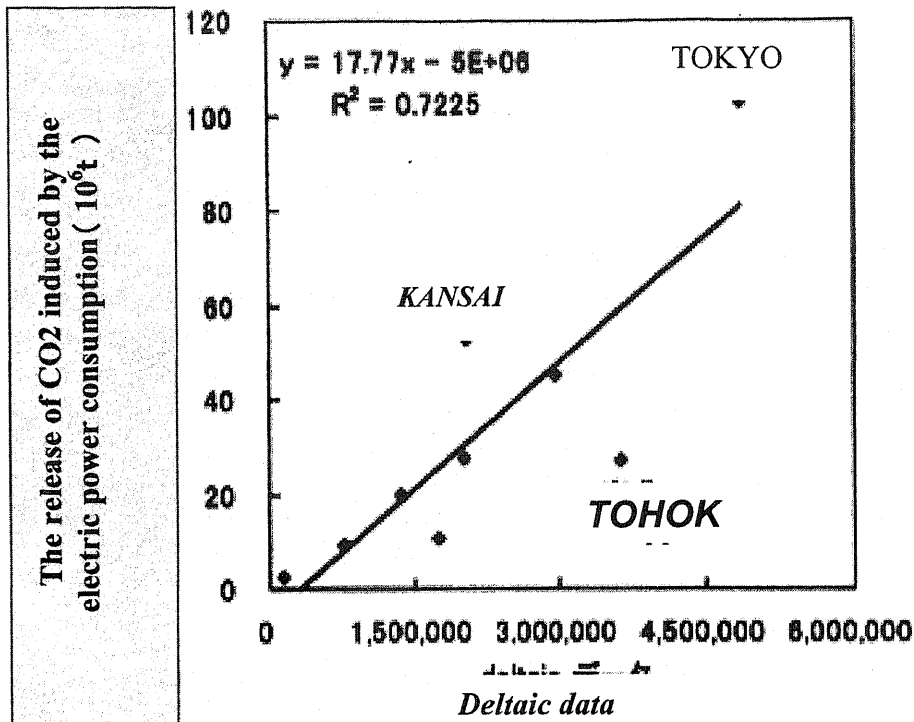


Fig 3. Correlation between the deltaic date and the CO² emission due to the power consumption

believe that the accuracy to infer the saturate revise will increase. Modifying the above problem, we can correct the deviation of the city, for example, , Kansai, Tohoku and Hokkaido, from the line. On the other hand, the new model developed will be used even more widely.

3.3 Extending the width of research

Hara et al., however, studied on the whole Japan and some parts of Korea and China, my Doctor thesis will focus on the developing of the model to increase the monitoring accuracy and to use it to Pacific Eastern coast, Japan, Korea, China, Taiwan and Indian of southern Asia.

4. Dataset

Firstly, the data of VIS and TIR were downloaded. The data are from the homepage of AGROPEDIA. This data include the 1999's archive data from DMSP-F13 and DMSP-F14.

References

Masanao Hara, 2003. Study of electric power consumption and Carbon Dioxide emissions by using the data of DMSP/OLS. Dissertation, Ph.D thesis, Chiba university, Chiba.,16-20,37-39,150-167.

Doll,C.N.H,Muller,J.-P.and Elvidge,C.D,2000.

Night-time Imagery as a Tool for Global Mapping of Socioeconomic Parameters and Greenhouse Gas Emission .Ambio,29(3),150-165.

Elvidge,C,D,Baugh,K.E,kihn,E.A,Kroehl,H.W.and Davis,E.R,1997a

Mapping city lights With Nighttime Data from the DMSP Operational Linescan System
Photogramm .Eng. Remote Sens.,63,727-734.

Elvidge,C,D, Baugh,K.E, kihn,E.A, Kroehl,H.W., Davis,E.R and Davis,C.,1997b.
Relation between satellite observed visible-near infrared emission, population and
energy consumption., Int. J. Remote Sens.,18,1373-1379.

COMPARISON OF VEGETATION PHENOLOGY BETWEEN MONGOLIA AND KAZAKH STEPPES BY USING REMOTELY SENSED DATA VEGETATION INDEX

Rikie Suzuki¹ and Tomoyuki Nomaki²

¹Frontier Research System for Global Change; E-mail: rikie@jamstec.go.jp

²Remote Sensing Technology Center of Japan; E-mail: nomaki@restec.or.jp

Abstract

The phenology of the vegetation covering mid-latitude Asia, that includes Mongolia and Kazakh, and its spatial characteristics were investigated using remotely sensed data Normalized Difference Vegetation Index (NDVI). The analysis used weekly averaged NDVI over 5 years (1987 – 1991) using the second-generation weekly Global Vegetation Index dataset. In the seasonal NDVI cycle, three phenological events were defined for each pixel: green-up week (NDVI exceeds 0.2), maximum week, and senescence week (NDVI drops below 0.2). Generally, there was a Kazakh-early/Mongolia-late feature in term of those events. In the zonal transect between 45°N and 50°N that covers Mongolia and Kazakh steppes, the timing of green-up, maximum, and senescence over Kazakh area was about 3.4, 8.7, and 13.4 weeks earlier than that over Mongolia area, respectively. It has been suggested that vegetation near Kazakh only flourishes during a short period when water from snow melt is available from late spring to early summer. In Mongolia, abundant water is available for the vegetation, even in mid-summer, due to precipitation.

1. Introduction

Vegetation covers, spreading over global terrestrial area, are remotely monitored from space by satellites. From the 1980s, global vegetation data have been provided by the measurements by Advanced Very High Resolution Radiometer (AVHRR) of the satellite NOAA. NDVI, which is the most well-known vegetation index, is computed as $NDVI = (Ch2 - Ch1)/(Ch2 + Ch1)$, where *Ch1* and *Ch2* are land surface reflectance of AVHRR Channels 1 and 2, respectively. Vegetation phenology, which is strongly characterized by the climate of a region, is one of targets of NDVI-related studies.

Suzuki *et al.* (2003) established a west-east transect over Siberia and some surrounding areas, and compared the vegetation phenology in western and eastern areas using the weekly NDVI on an annual basis. They discussed the west-east phenological contrast in relation to seasonality in the surface air temperature, precipitation, snow depth, and soil moisture, and found interesting vegetation-climate relation in those regions. The present paper highlights a part of their results regarding the phenological contrast between Kazakh steppe and Mongolia steppe. This study will lead to a better understanding of the essential climatological implications of seasonal vegetation change in both regions.

2. Data and analyses

This study analyzed the weekly NDVI and hydrometeorological measurements made at surface stations, averaged for 1987 to 1991 (5 years). We regard the 5-year mean values for these five years as representative of the normal values of those parameters. For some datasets, however, time spans other than 1987 to 1991 were selected because of the unavailability of data for 1987 to 1991.

Weekly NDVI values from 1987 to 1991 were obtained from the second generation weekly Global Vegetation Index data (0.144 × 0.144 degree spatial resolution) (Kidwell,

1990). This study carried out horizontal and temporal smoothing processes for the weekly NDVI data. As for the horizontal smoothing, (1) the NDVI value at a pixel (NDVI-a) was compared with the mean NDVI (NDVI-m) among the 8 pixels around NDVI-a pixel, (2) if the difference between NDVI-a and NDVI-m was over 0.1, NDVI-a was replaced by NDVI-m. As for the temporal smoothing, the highest NDVI value among three weeks of week “n-1”, week “n”, and week “n+1” was adopted for the NDVI value of the week “n” for each pixel.

Surface air temperature and precipitation data from 1987 to 1991 were obtained from the CD-ROM “Global Daily Summary (GDS)” that was provided from the National Climate Data Center (NCDC) of the National Oceanic and Atmospheric Administration (NOAA) (National Climatic Data Center, 1994). Stations distribution is shown in Fig. 1.

Snow depth values at surface stations from 1987 to 1991 were obtained from the CD-ROM of the Historical Soviet Daily Snow Depth (HSDSD) version 2.0 (Armstrong, 2001) which includes daily snow depth at 284 WMO station (Fig. 1). As for the snow depth in Mongolia part, where the HSDSD does not cover, an alternative snow depth information from 1994 to 1996 was obtained from Federal Climate Complex Global Surface Summary of Day Data (GSSD) Version 6 (<ftp://ftp.ncdc.noaa.gov/>) (Fig. 1).

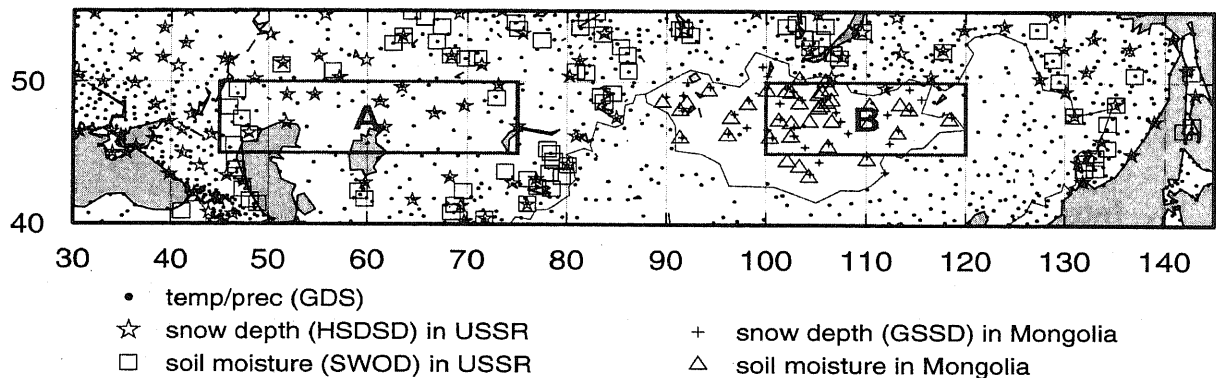


Figure 1 The study area (A: Kazakh area, B: Mongolia area), the distribution of GDS (dots), HSDSD (stars), GSSD (crosses), SWOD (squares) stations, and the soil moisture in Mongolia (triangles).

Gravimetric soil moisture data covering USSR by 115 surface stations (so-called SWOD) were used (Fig. 1). The observations were executed 3 times per month on 8th, 18th, 28th from April to October. Since the data from 1988 to 1991 are not available in the SWOD, the data of the SWOD from 1985 to 1987 were used as an alternative. The total soil moisture values (volumetric) in 0 – 10cm depth layer were utilized for the analysis. In Mongolia, soil moisture data at 42 stations are available on 7, 17, 27th of every month from April to October for the period from 1964 to 1993 (Robock *et al.*, 2000; *see* Fig. 1). This analysis used the total soil moisture value in 5 – 10cm depth layer from 1987 to 1991.

Five year mean of weekly NDVI was calculated by averaging the weekly NDVIs in the same week from 1987 to 1991. The first and last weeks of the year were not calculated because 3-week moving maximizing process was done for the NDVI time series. In addition to NDVI, 5 (or 3)-year mean temperature, precipitation, and snow depth from 2nd week (8 – 14 January) to 51st week (17 – 23 December) were calculated. The soil moisture values were utilized as the original 3 time/month value i.e. they were not converted into weekly.

3. Results

3.1 Mean NDVI seasonal cycle in Kazakh and Mongolia steppes

To examine the seasonal characteristic of the NDVI annual trend, the mean weekly NDVI variation was calculated in Kazakh and Mongolia areas (*see* Fig. 1) by averaging all the pixel value within each area (Fig. 2). The seasonal cycle of the NDVI shows obvious unimodal variation, that is, the NDVI in winter indicates small value, and then it shows a dramatic increase (green-up) in spring to summer followed by the occurrence of the maximum NDVI. In autumn, the NDVI gradually decreases to the level of winter. This seasonal cycle of the NDVI would directly reflect the phenological cycle of the vegetation; dormancy, foliation, mature, and senescence phases of the vegetation in these areas.

There is a considerable difference in the NDVI seasonal cycles between Kazakh and Mongolia areas, even though both areas are located in a semi-arid latitudinal zone. The Kazakh-early/Mongolia-late feature is apparent. The maximum peak (0.15) in Kazakh area emerges in the 20th week (14 – 20 May), while that (0.28) in Mongolia area is in the 30th week (23 – 29 July). There is 10 weeks difference of their timings.

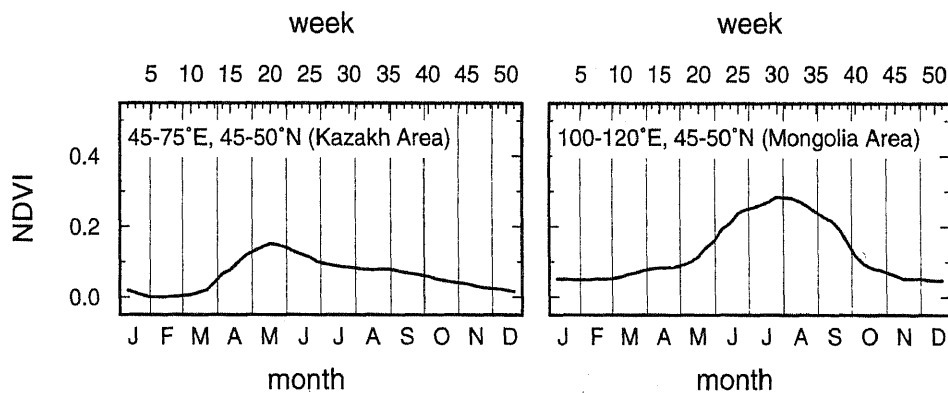


Figure 2 Seasonal cycle of the NDVI averaged in the Kazakh and Mongolia areas.

3.2 West-east phenological contrast in a zonal transect (45N – 50N)

In this section, three specific weeks are picked as the timing parameter of phenological events of the vegetation; (1) green-up time defined by the week when the NDVI exceeds 0.2 first time in the year (W-a), (2) the maximum time defined by the week at the annual maximum NDVI occurrence (W-b), and (3) the senescence time defined by the week when the NDVI drops below 0.2 first time after the occurrence of the maximum (W-c). In the zonal transect of 45 – 50N, W-a, W-b, and W-c were examined in relation to climatological parameters.

Figure 3 shows the mean W-a, W-b, and W-c, averaged over the pixels in individual south-north strips, which were 0.144 degrees longitude wide, in the zone between 45°N and 50°N. There were 800 strips from 30°E to 145°E, and each strip contained 34 NDVI pixels. Pixels for which the annual maximum did not exceed 0.2 were excluded from the calculation of the mean values. The smoothed lines were drawn.

For W-a and W-b, a west-early/east-late gradient was apparent. Near 60°E, W-a and W-b were weeks 20.4 and 21.7, respectively, while near 110°E, they were weeks 23.8 and 30.4. There were 3.4- and 8.7-week time lags in W-a and W-b, respectively. W-c was relatively late in west of 50°E, whereas it was earliest between 55°E and 70°E (i.e.,

near the Kazakh steppe). W-c was 13.4 weeks earlier near 60°E than near 110°E. Moreover, the time between W-a to W-c was noticeably short (3.8 weeks) in the Kazakh region, illustrating the short growing season there.

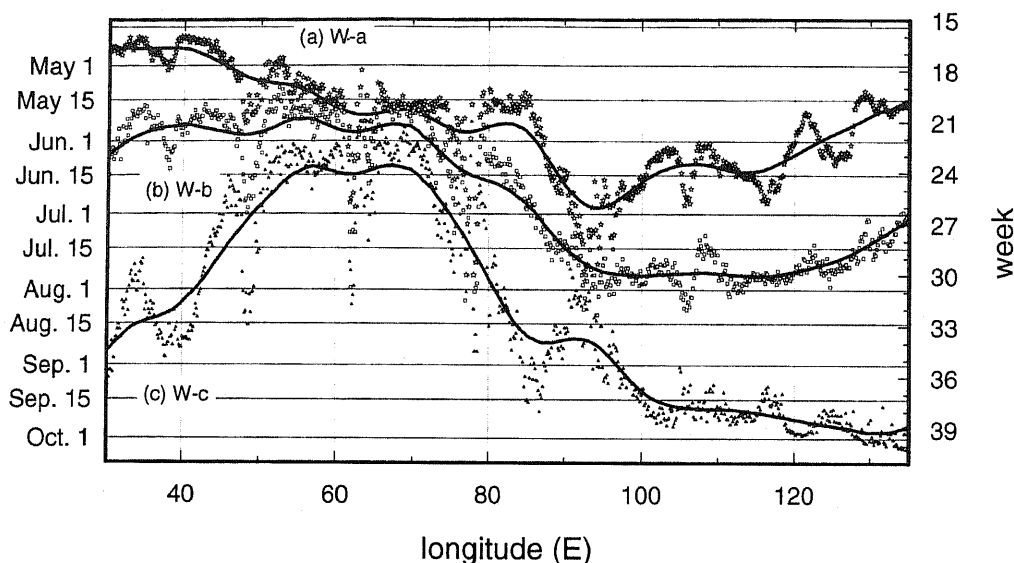


Figure 3 The west-east profile of the weeks in the 45–50°N zonal transect when the NDVI exceeded 0.2 (a), the NDVI annual maximum occurred (b), and the NDVI dropped below 0.2 (c). The solid line is the smoothed line produced using a low-pass filter.

3.3 Phenological contrast and climatological background

In the 45°N to 50°N transect, the Kazakh and Mongolia areas were selected (Fig. 1), and Fig. 4 compares seasonal cycles in weekly temperature, precipitation, snow depth, and soil moisture for the two areas. The soil moisture in the Kazakh area is mean from 1985 to 1987. The snow depth in the Mongolia area is mean from 1994 to 1996. The other statistics are means from 1987 to 1991, the actual time span of this study. Conspicuous differences between these two areas are seen in their precipitation, snow depth, and soil moisture. In the Kazakh area, the snow was deep (about 26 cm) in late February, and it disappeared in mid April. Although soil moisture data before March were unavailable, and the statistical period was from 1985 to 1987, the soil moisture in the Kazakh area was highest (10.3 mm in surface 10 cm layer) in early April, when the snow had almost finished melting. Subsequently, the soil moisture decreased to a minimum in August. The small amount of precipitation in the Kazakh area was insufficient to stop the decrease in soil moisture. Other statistics are mean from 1987 to 1991.

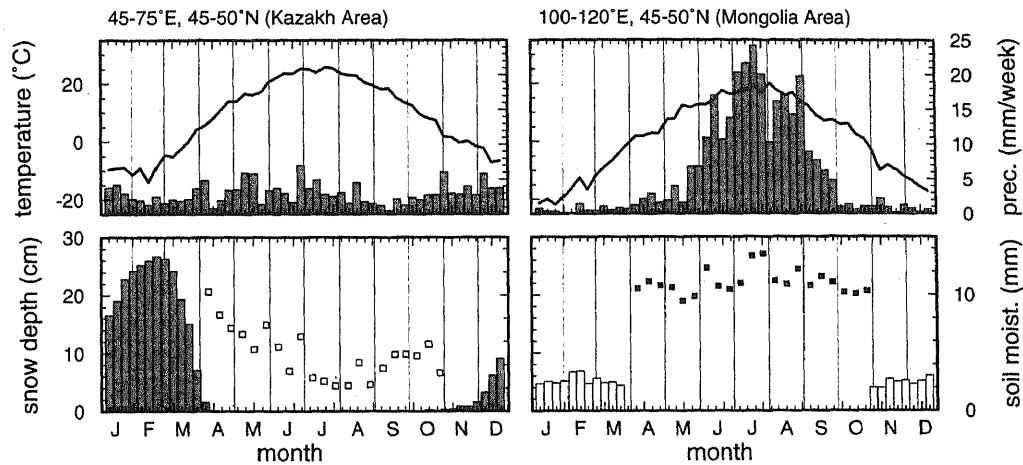


Figure 4. The seasonal change of the weekly temperature, precipitation, snow depth, and 10-daily soil moisture in two semi-arid areas: Kazakh (left row) and Mongolia (right row) areas in 45 – 50N zone. The statistical period of the soil moisture in Kazakh area and the snow depth in Mongolia area are 1985 – 1987 and 1994 – 1996, respectively.

In the Mongolia area, the precipitation showed an obvious unimodal seasonal cycle, with a maximum (22 mm/week) in mid July. Although the snow was not as deep in winter as in the Kazakh area, the soil moisture remained relatively high (around 10 mm in the 5 – 10 cm layer) from April to October. These facts suggest that water is available for vegetation in the Kazakh area only for a very short period after snowmelt, and that this season is the only time that vegetation flourishes. Consequently, the vegetation matures in late May when water from melting snow is still abundant in the soil. In addition, the span from W-a to W-c (growing season) in the Kazakh area is considerably shorter than that in the Mongolia area. In the Mongolia area, large amounts of precipitation in summer support the occurrence of the mature stage of vegetation in mid summer, 8.7 weeks after it occurs in the Kazakh area. It is also possible that the winter soil temperature in the Kazakh area is kept higher by the thick snow cover compared with the Mongolia area, possibly inducing the earlier green-up in the Kazakh area.

4. Conclusion

The phenological regionality of the vegetation in steppe areas (Kazakh and Mongolia) in mid-latitude Asia was investigated using remotely sensed data NDVI. The 5-year (1987 – 1991) mean weekly NDVI time series was calculated from the second-generation weekly GVI dataset, which covers the earth with a 0.144 degree spatial resolution. Temperature, precipitation, snow depth, and soil moisture seasonal cycles were examined to interpret the seasonal NDVI cycle.

Three phenological events were defined and calculated for each pixel: green-up (W-a), maximum (W-b), and senescence (W-c) weeks. Generally, there was a Kazakh-early/Mongolia-late contrast in all three events. In the zone between 45N and 50N, green-up, maximum, and senescence occurred near 60E (Kazakh) about 3.4, 8.7, and 13.4 weeks earlier than near 110E (Mongolia), respectively. The vegetation in Kazakh flourishes during a short period when snowmelt is available from late spring to early summer, while in Mongolia, abundant water is available for the vegetation, even in mid summer, due to the large amount of precipitation.

References

Armstrong R (2001) Historical Soviet Daily Snow Depth Version 2 (HSDSD). Boulder, CO, USA: National Snow and Ice Data Center. CD-ROM.

Kidwell KB (1990) Global Vegetation Index User's Guide. U.S. Department of Commerce, NOAA, NESDIS, NCDC, SDS. National Climatic Data Center (1994) Global Daily Summary (CD-ROM).

Robock A, Vinnikov KY, Srinivasan G, Entin JK, Hollinger SE, Speranskaya NA, Liu S, Namkhai, A (2000) The global soil moisture data bank. *Bull Amer Meteor Soc* **81**: 1281 – 1299.

Suzuki R, Nomaki T, Yasunari T (2003) West-east contrast of phenology and climate in northern Asia revealed using a remotely sensed vegetation index. *Int J Biometeor* **47**: 126 – 138.

DROUGHT MONITORING

M. Bayasgalan

Researcher, The National Remote Sensing Center of Mongolia

Phone: 976-11-327982 Fax: 976-11-315387

E-mail: osm_infor@mongol.net

Abstract

One of the natural disasters occurring in Mongolia is drought. Drought causes losses of livestock, influences human food security, also very seriously affects environment; land degradation and desertification, wildfire and water deterioration. This study presents results of using of Remote Sensing data for drought monitoring, comparison of drought indexes originated from Remote sensing and ground observation data and changes of both indexes past years. Results show drought frequency, severity and affected area have increased significantly for past years, especially since 1995.

2. Introduction

Drought is an insidious hazard of nature. Although it has scores of definitions, it originates from a deficiency of precipitation over an extended period of time. This deficiency results in vegetation grow and water shortages.

68% of Mongolia is drought prone, most affected by droughts are central and southern regions. In these regions every year over drought 40-50 days occur once 2-3 years. In past years drought frequency and intensity have increased as a result of global climate changes.

Nomadic livestock directly depending on natural conditions is the most important economic branch of Mongolia, producing 35.7% of the GDP. In Mongolia, there is a specific relation between drought and livestock. If animals do not have enough weight, fat and nutrients during the short summer and autumn season due to drought, they are unable to cope with harsh cold winter and spring wind storm, and easily can die. Therefore in Mongolia drought monitoring is urgently needed.

Drought has been studied by many researchers (R.Mijiddorj and A. Namkhai 1986, L Natsagdorj 2003) as meteorological phenomenon using ground observation data. To study drought using only sparse ground data and meteorological indicators are insufficient.

The purpose of this study is to monitor drought using Remote sensing and ground data.

3. Data used and methodology

NOAA NDVI 10-day composite 8 km resolution data from 1982 to 2001 monthly average temperature and sum of precipitation at 25 ground stations from 1940 to 2003, at 68 stations from 1982 to 2002 at 68 ground stations.

In order to distinguish drought-affected area from desert area and other none and less vegetated area, drought is considered relative to some long-term average condition of meteorological and vegetation, a condition often perceived as “normal” and “capacity”.

Remote sensing data allows defining drought distribution, affected area, frequency, severity and end/start time more accurately.

Drought index (DI) based on NDVI using Remote Sensed data expressed as follows:

$$DI = (\text{NDVI}_{\max} - \text{NDVI}_i) / (\text{NDVI}_{\max} - \text{NDVI}_{\min}) \quad (1)$$

$$\text{NDVI} = \frac{ch2 - ch1}{ch2 + ch1}$$

Where, NDVI_{\max} – Long term maximum value of NDVI at point, NDVI_{\min} - Long term minimum value of NDVI at point, NDVI_i - Current value of NDVI at point. $ch2$ - reflectance at 0.58-0.68 μm , $ch1$ - reflectance at 0.72-1.1 μm . Long term values of NDVI are different depending decade and place.

Value of DI vary between 0 (non drought, vegetation condition is extreme good) to +1 (very severe drought). Drought start/time is defined by date when DI crosses $DI=0.5$.

Palmer index (PDSI) based on ground meteorological parameters is defined as:

$$PDSI = \sum_{i=1}^t \frac{(P - \hat{P}) \cdot K}{(0.309t + 2.69)}$$

where, PDSI- Palmer Drought Severity Index, t -monthly average temperature, K -coefficient on climatic factor, $P - \hat{P}$ -precipitation deficiency. PDSI ranges from -5 (very severe drought) to +5 (very wet).

4. Results

The PDSI trend for the last 62 years from 1940 to 2002 is shown in figure 1. PDSI is averaged value over the whole territory of Mongolia for growing season, from June to August. Periods of PDSI increasing approximately are 1944-1959, 1980-1994, of decreasing 1959-1980, 1994-2002. According to the Palmer's drought severity classification severe droughts occurred 7 times in 1944, 1978, 1980 and consecutively 1999-2002, moderate 10 times in 1942, 1946, 1947, 1951, 1972, 1981, 1982, 1989, 1998 and slight 8 times in 1941, 1948, 1949, 1952, 1957, 1968, 1979, 1997. Since 1994 drought intensity has been increased significantly.

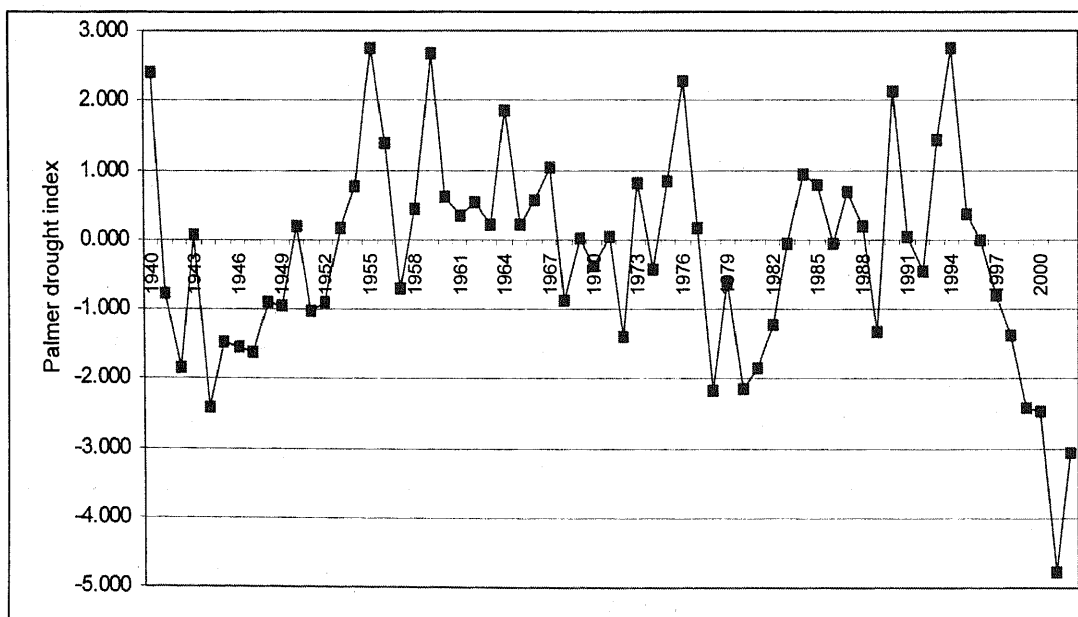


Figure 1. PDSI changes for 1940-2003.

One of the advantages of remote sensing data is continuity in spatial and temporal scale. Therefore Remote sensing allows to define drought affected area and duration more accurately. Figure 2 shows drought index averaged over the vegetation maturity period, continued from 1st July to 20th August, and drought affected area slightly and severely for 1982-2003, obtained using remote sensing data. Tendency of drought index (DI) changes are similar to PDSI changes. Since 1998 drought severity and affected area have been increased significantly.

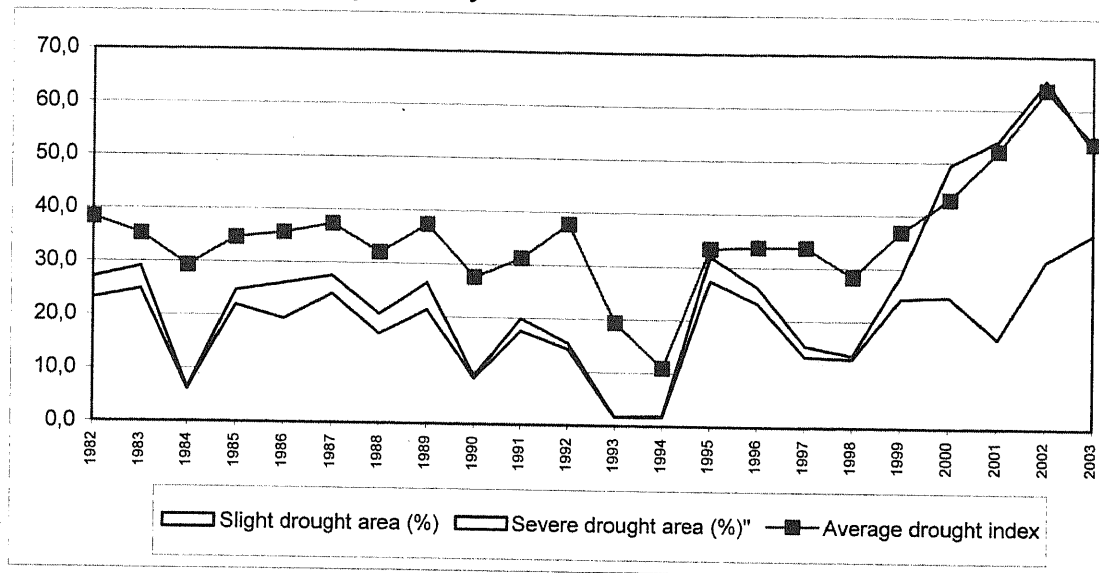


Figure 2. Drought index changes for 1982-2003, obtained from Remote Sensing data

Averaged value of DI over 1982-2003 is presented in fig.3. In the south part of Mongolia value of DI more than 0.5 means drought, especially drought occurs more frequently and more severely in transition zone from steppe to desert steppe zone.

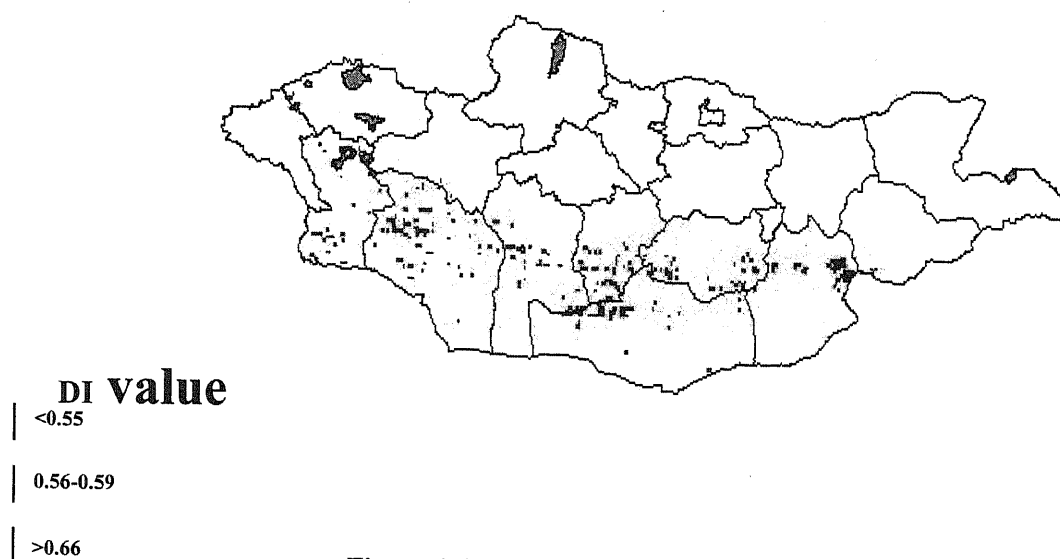


Figure 3. Mean value of DI for 1982-2003

Comparison of PDSI and DI showed good correspondence. Figure 4 shows correlation coefficient between both indexes. Correlation in steppe area is highest, in forest area is weak. It can be explained by that forest are less sensitive to atmospheric drought than grasses with short root growing in the most of area.

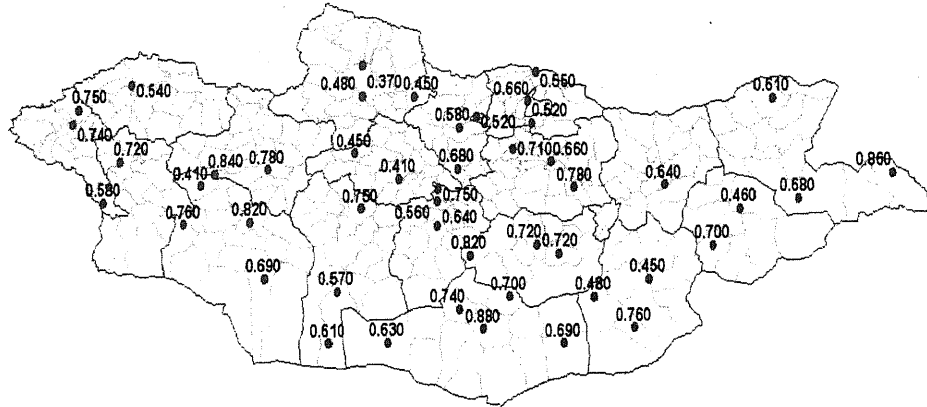


Figure 4. Correlation coefficient between PDSI and DI

5. Conclusion and discussion

Mongolia has large territory, harsh climate, specific agricultural system with adequate numbers of livestock (28 million heads) and low population (2.3 million). Most areas of Mongolia are vulnerable to climate abnormalities, such as drought. The drought monitoring cannot be efficiently done using only conventional ground data with sparse stations, especially in high mountain areas, deserts and remote area without any infrastructure.

For countries, like Mongolia Remote sensing for drought monitoring is important tool. Palmer index is limited due to using monthly and point data. Results of this study show drought can be monitored effectively, continuously and operationally using Remote Sensing data. It doesn't mean ground based drought monitoring is useless. Palmer index is used for atmospheric drought, drought index based on NDVI using Remote sensing data for agricultural drought. Combined use of both indexes can close some gaps and give us more completeness in temporal and spatial context.

In the future, we should improve remote sensing techniques, extend research activities on drought study and establish early warning system on drought. Especially studies on drought modeling, selection of appropriate and adequate drought indexes based on Remote Sensing, drought impact assessment should be highlighted. .

References:

1. M. Bayasgalan. Drought monitoring Proceedings of Institute of Hydrology and Meteorology, No 2000 page 35-42
2. Mijiddorj R, Namkhai A. Drought atlas. Ulaanbaatar 1986
3. Palmer C. W Meteorological drought. Washington 1968
4. Prince S.D, Justice C.O. Coarse Resolution Remote Sensing of the Sahelian Environment. International Journal of Remote Sensing, Vol.12,1135-1421

ESTIMATION OF ATMOSPHERIC OPTICAL THICKNESSES IN ULAANBAATAR CITY

G.Batsukh¹, Ts.Baatarchuluun¹, D.Ochirvaani¹, S.Lantuu¹, D.Ganbaatar², N.Tugjsuren²,
B.Ganbat¹ and J.Osorjamaa³

¹Research Center for Geophysics, National University of Mongolia

²Mongolian University Science and Technology

³State Specialized Inspection Agency

Abstract

Atmospheric optical thickness (AOT), which is calculated in certain spectral region, is one of the main parameters for atmospheric correction of satellite imagery. In this paper we have summarized the results of monthly mean values of atmospheric optical thicknesses, which are calculated by direct solar radiation measurements of infra red, photosynthetically active, biologically active (UV) and solar spectrum maximum (510-650nm) spectral regions, in Ulaanbaatar city of Mongolia. We have shown the relations between the sun's altitude and the atmospheric optical thickness, by using monthly mean values of direct solar radiation, which were measured in 5⁰ gradation of the sun's altitude angle.

1. Introduction

Solar radiation reaching the ground is attenuated by absorption and scattering by atmospheric molecules as well as particles. Atmospheric optical thickness is variable in space and time and an accurate estimate is made by measuring the direct solar radiance at the ground by using a sunphotometer or an actinometer. In this paper we have used hourly measurements of direct solar irradiance, which were obtained by AT-50 actinometer during 1991-2001, in Ulaanbaatar city ($\varphi=47^{\circ} 56'$, $\lambda=106^{\circ} 50'$), Mongolia. In order to measure spectral composition of solar radiation we have used the WG-8, YG-18, RG-15, RG-19 glass filters, which are transparent for the wavelengths greater than 380 nm, 510 nm, 650 nm, 710 nm, respectively. Using these filters we measured direct solar irradiance and calculated atmospheric optical thicknesses for the following 4 spectral region.

- photosynthetically active radiation ($380 \leq \lambda \leq 710$ nm) - PAR
- biologically active or ultra-violet ($\lambda \leq 510$ nm) - UV
- infra-red ($\lambda \geq 710$ nm) - IR
- solar spectrum maximum region ($510 \leq \lambda \leq 650$ nm)

For calculation of atmospheric optical thickness we have used the following formula.

$$\tau_{\Delta\lambda} = -\frac{1}{m} \ln \frac{S_{\Delta\lambda}}{S_{0,\Delta\lambda}} \quad (1)$$

Where, $\tau_{\Delta\lambda}$ - atmospheric optical thickness of the considered spectral region, m - atmospheric optical mass, $S_{\Delta\lambda}$ - measured direct solar irradiance of the considered spectral region, $S_{0,\Delta\lambda}$ - solar constant of the considered spectral region (Table 1.)

Table 1. Solar constant of the spectral regions, W/m²

spectral region	$S_{0,\Delta\lambda}$
$\lambda \leq 510$ nm	344.2
$380 \leq \lambda \leq 710$ nm	587.5
$510 \leq \lambda \leq 650$ nm	254.3
$\lambda \geq 710$ nm	693.4

2. Results

By using the data from the considered spectral region and Equation (1) we have calculated AOT's values. The table-2 shows the monthly mean values and standard deviations of AOT in Ulaanbaatar, in 1991-2001. In addition, in order to compare the results with other researches we have shown the monthly mean values of AOT (525-630 nm spectral region), which were calculated by G.M.Abakumova, Moscow State University, in Russia.

Table 2. Monthly mean values and standard deviations of AOT

	I	II	III	IV	V	VI	VII	VIII	IX	X	XI	XII	site name	Year
PAR	0,383	0,412	0,478	0,501	0,493	0,519	0,530	0,504	0,453	0,417	0,413	0,407	Ulaanbaatar, Mongolia	1991-2001
Stdev	0,047	0,069	0,069	0,078	0,106	0,092	0,111	0,135	0,100	0,085	0,070	0,067		
UV	0,585	0,601	0,672	0,693	0,722	0,744	0,716	0,681	0,641	0,599	0,658	0,514		
Stdev	0,059	0,098	0,081	0,106	0,137	0,128	0,119	0,120	0,115	0,100	0,138	0,080		
510-650nm	0,220	0,220	0,239	0,210	0,231	0,229	0,256	0,256	0,233	0,199	0,221	0,215		
Stdev	0,018	0,023	0,055	0,015	0,041	0,020	0,051	0,059	0,045	0,036	0,020	0,010		
IR	0,137	0,160	0,198	0,232	0,266	0,277	0,284	0,276	0,226	0,193	0,224	0,161		
Stdev	0,015	0,012	0,022	0,029	0,057	0,056	0,060	0,068	0,061	0,043	0,056	0,028		
525-630nm	0,188	0,328	0,35	0,386	0,399	0,329	0,377	0,396	0,31	0,243	0,223	0,234	Moscow, Russia	
Stdev	0,082	0,139	0,106	0,128	0,111	0,121	0,140	0,122	0,103	0,060	0,056			

Figure 1. shows the yearly changes of monthly mean values of AOT, which corresponded to the above mentioned 4 spectral regions. The values of AOT of UV region were greater than other spectral regions' values through the year, maybe it depends on the molecular scattering and ozone layer absorption. For the UV, PAR and IR spectral regions, AOT increases in summer season and reaches the maximum values in June or July and decreases in winter season and reaches the minimum values in the December or January. For the solar spectrum maximum region ($510 \leq \lambda \leq 650 \text{nm}$), there is a peculiarity, that AOT has a stable character through a year.

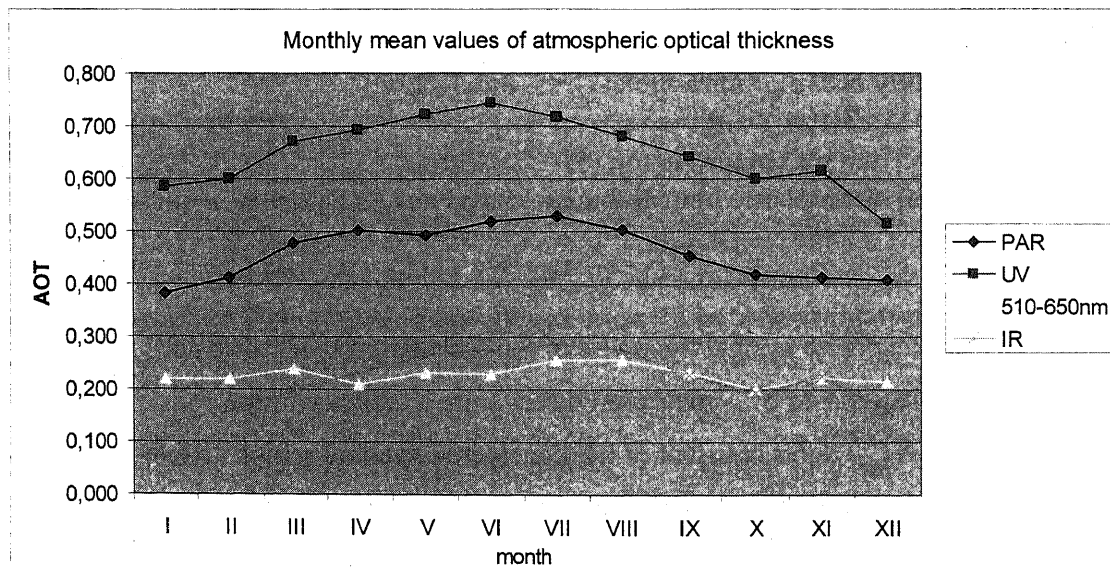


Figure 1. Yearly changes of monthly mean values of AOT

From the Table 3. one can see the minimum and maximum values of AOT of the spectral regions.

Table 3. The minimum and maximum values of AOT

spectral region	minimum	Maximum
UV ($\lambda \leq 510_{\text{HM}}$)	0.514	0.744
PAR ($380 \leq \lambda \leq 710 \text{ nm}$)	0.383	0.530
IR ($\lambda \geq 710_{\text{HM}}$)	0.137	0.284
Solar spectrum maximum ($510 \leq \lambda \leq 650_{\text{HM}}$)	0.199	0.256

In Table 4-7 we have shown the monthly mean values of atmospheric optical thickness in spectral regions. These values were calculated by measurements, which were measured in 5° gradation of the sun's altitude angle. From the Table 4-7, we tried to reveal the relations between the sun altitude angle and the atmospheric optical thickness. For the UV, PAR and IR regions, there was a dependence between the sun altitude angle and AOT through a year, e.g. when the sun's altitude angle raises the value of AOT is increased (Figure 2,3,4). For the solar spectrum maximum region there wasn't a certain relation between the sun's altitude angle and AOT (Figure 5).

Table 4. Monthly mean values of atmospheric optical thickness in PAR, which were measured in 5° gradation of the sun's altitude angle

	I	II	III	IV	V	VI	VII	VIII	IX	X	XI	XII
10-	0,330	0,307	0,399	0,362	0,271	0,371	0,305	0,332	0,315	0,303	0,353	0,332
15-	0,398	0,393	0,418	0,394	0,340	0,433	0,433	0,356	0,346	0,336	0,393	0,432
20-	0,420	0,420	0,426	0,435	0,403	0,390	0,423	0,394	0,405	0,395	0,417	0,458
25-		0,455	0,441	0,533	0,521	0,510	0,485	0,424	0,422	0,488	0,372	
30-		0,487	0,472	0,493	0,529	0,465	0,509	0,506	0,474	0,485	0,532	
35-			0,497	0,527	0,520	0,593	0,591	0,515	0,506	0,497		
40-			0,528	0,579	0,534	0,541	0,587	0,495	0,560			
45-			0,624	0,580	0,562	0,630	0,591	0,598	0,599			
50-			0,493	0,563	0,586	0,579	0,593	0,679				
55-				0,548	0,577	0,596	0,619	0,737				
60-					0,580	0,605	0,696					

Table 5. Monthly mean values of atmospheric optical thickness in UV region,

	I	II	III	IV	V	VI	VII	VIII	IX	X	XI	XII
10-15	0,520	0,479	0,556	0,487	0,410	0,496	0,437	0,488	0,467	0,450	0,542	0,422
15-20	0,599	0,555	0,567	0,589	0,555	0,640	0,654	0,514	0,477	0,511	0,589	0,566
20-25	0,635	0,583	0,647	0,622	0,669	0,600	0,608	0,603	0,617	0,599	0,643	0,555
25-30		0,648	0,667	0,636	0,703	0,720	0,682	0,613	0,641	0,668	0,622	
30-35		0,738	0,690	0,713	0,733	0,698	0,727	0,752	0,710	0,703	0,678	
35-40			0,774	0,761	0,810	0,810	0,714	0,675	0,700	0,663		
40-45			0,700	0,787	0,750	0,751	0,807	0,777	0,748			
45-50			0,771	0,812	0,846	0,899	0,784	0,777	0,766			
50-55			0,000	0,798	0,889	0,824	0,823	0,798				
55-60				0,725	0,792	0,857	0,814	0,813				
60-65					0,782	0,886	0,827					

Table 6. Monthly mean values of atmospheric optical thickness in IR region,

	I	II	III	IV	V	VI	VII	VIII	IX	X	XI	XII
10-	0,122	0,145	0,174	0,223	0,140	0,194	0,151	0,188	0,140	0,135	0,169	0,14
15-	0,137	0,151	0,170	0,200	0,235	0,237	0,247	0,200	0,168	0,162	0,195	0,14
20-	0,151	0,161	0,187	0,190	0,187	0,202	0,244	0,203	0,192	0,176	0,236	0,19
25-		0,168	0,192	0,209	0,290	0,264	0,239	0,240	0,208	0,212	0,205	
30-		0,173	0,200	0,210	0,299	0,242	0,279	0,268	0,230	0,222	0,314	
35-			0,225	0,244	0,279	0,343	0,299	0,284	0,260	0,251		
40-			0,232	0,266	0,267	0,272	0,329	0,309	0,305			
45-			0,201	0,254	0,296	0,361	0,324	0,343	0,306			
50-			0,000	0,248	0,302	0,275	0,340	0,352				
55-				0,272	0,298	0,330	0,340	0,374				
60-					0,329	0,322	0,337					

Table 7. Monthly mean values of atmospheric optical thickness in solar spectrum maximum region,

	I	II	III	IV	V	VI	VII	VIII	IX	X	XI	XII
10-15	0,237	0,179	0,222	0,194	0,165	0,188	0,153	0,219	0,171	0,174	0,220	0,204
15-20	0,201	0,225	0,247	0,201	0,169	0,240	0,257	0,200	0,223	0,158	0,226	0,222
20-25	0,221	0,236	0,221	0,207	0,187	0,224	0,273	0,214	0,263	0,186	0,237	0,220
25-30		0,232	0,225	0,204	0,264	0,245	0,315	0,240	0,197	0,197	0,187	
30-35		0,227	0,215	0,204	0,214	0,228	0,266	0,226	0,217	0,222	0,236	
35-40			0,205	0,217	0,245	0,252	0,304	0,259	0,214	0,257		
40-45			0,371	0,237	0,273	0,222	0,276	0,221	0,263			
45-50			0,207	0,229	0,236	0,249	0,193	0,263	0,312			
50-55			0,000	0,191	0,261	0,218	0,213	0,332				
55-60				0,218	0,245	0,203	0,249	0,386				
60-65					0,281	0,245	0,312					

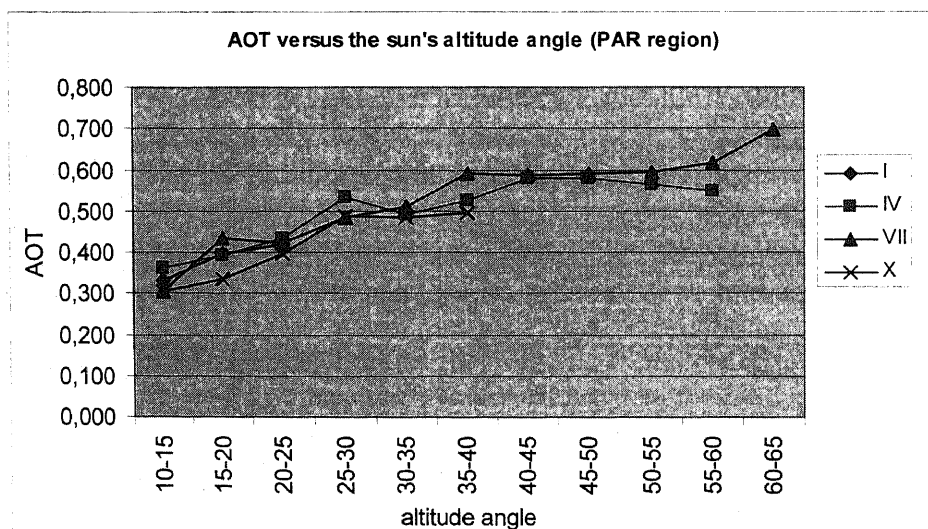


Figure 2. AOT versus the sun's altitude angle (PAR region)

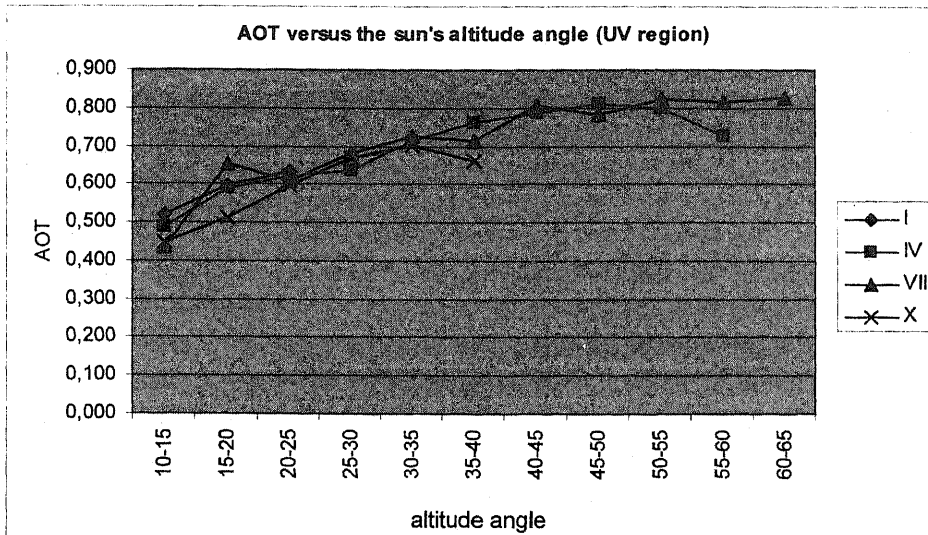


Figure 3. AOT versus the sun's altitude angle (UV region)

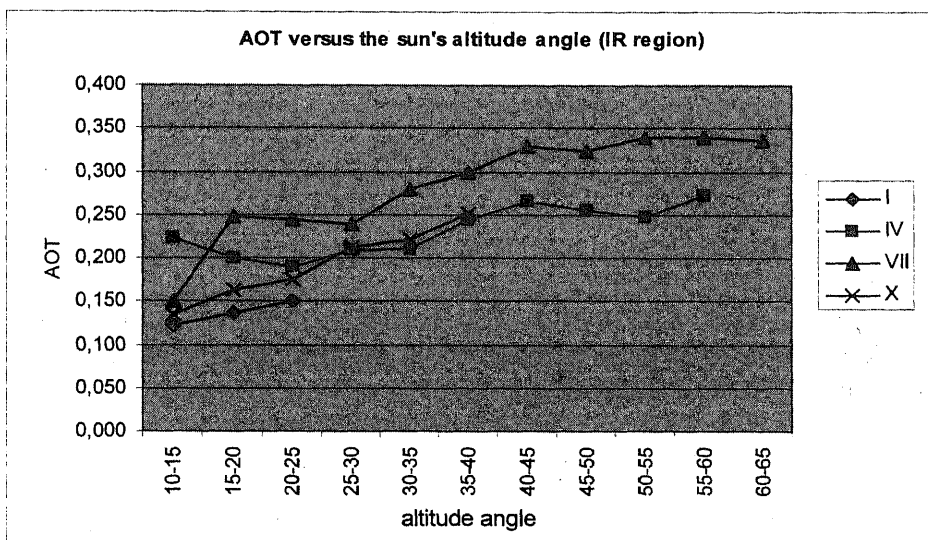


Figure 4. AOT versus the sun's altitude angle (IR region)

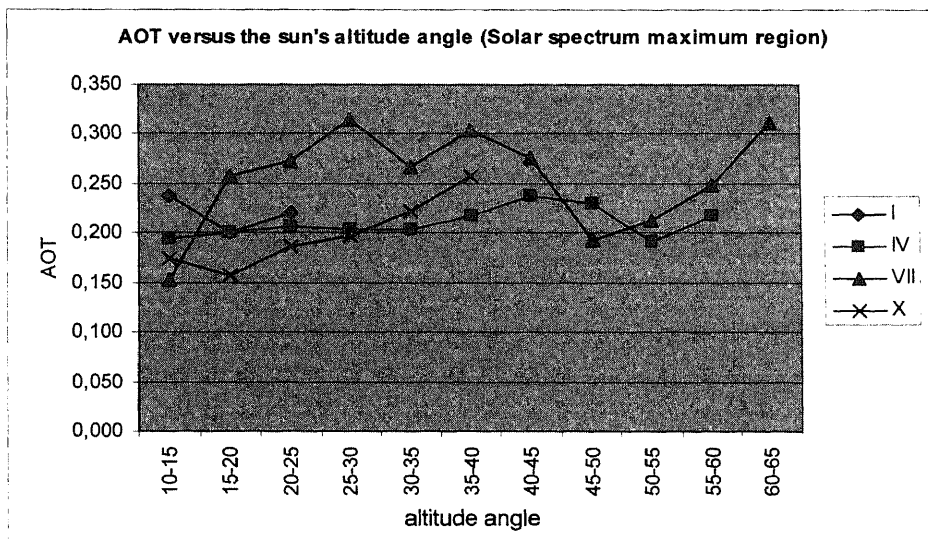


Figure 5. AOT versus the sun's altitude angle (Solar spectrum maximum region)

3. Conclusion

1. In this paper, we have summarized the monthly mean values of AOT, based on direct solar irradiation measurements during 1991-2001 in Ulaanbaatar. The values of AOT in UV region were greater than other spectral regions' values through the year, maybe it depends on the molecular scattering and ozone layer absorption. For the UV, PAR and IR spectral regions, AOT increases in summer season and reaches the maximum values in June or July and decreases in winter season and reaches the minimum values in the December or January. For the solar spectrum maximum region ($510 \leq \lambda \leq 650 \text{ nm}$), there is a peculiarity, that AOT has a stabile character through a year.
2. By using monthly mean values of direct solar radiation, which were measured in 5° gradation of the sun's altitude angle, we have tried to reveal relationship between the sun's altitude angle and atmospheric optical thickness. For the UV, PAR and IR regions, there was a relation between the sun's altitude angle and AOT through a year, e.g. when the sun's altitude angle raises the value of AOT is increased. For the solar spectrum maximum region there wasn't a certain relation between the sun's altitude angle and AOT.

Reference

1. Report of scientific project "Light scattering in the Earth's atmosphere", Ulaanbaatar, 1998, p. 118
2. Report of scientific project "Physics processes in the Earth's atmosphere", Ulaanbaatar, 2002, p. 102
3. Abakumova G.M., Plakhina I.N., Tarasova T.A. "Estimation of aerosol optical thickness using ground based actinometer measurements", Meteorology and Hydrology, 1989, №10, Moscow

LAND COVER CHANGE MONITORING IN MONGOLIA

M. Erdenetuya * and Sh. Munkhtuya*

* National Remote Sensing Center, MNE

Email: m_erdenetuya@yahoo.com, mtuya@yahoo.com

Abstract

Climatic influences can affect sustainable use of land resources as pasture. Vegetation condition and/or Land cover types of the country are sensitively changing upon climate changes and human impacts. Within the last 60 years, air temperature has increased by 1.66 degrees and the total precipitation has almost not changed.

The main goals of this work are to monitor pasture within the last 20 years using long term NOAA/NDVI data set and, to determine the present status of land cover types and to detect their changes in Mongolia.

Key words: pasture, climate change, vegetation cover dynamics, land cover changes.

1. Introduction

Mongolia is the most arid country in the heart of Central Asia, with 70 percent of the population depending on nomadic livestock husbandry. Today the number of livestock has reached 26 million heads and the pastureland occupies more than 80 percent of the territory. Lifestyles of the Mongolians still reflect the dependence on nomadic systems developed in harmony with the largest expanse of intact grasslands in the world. Historically low population densities of nomadic pastoralists have utilized the rich grassland region to graze their mixed herds.

Most of the country experience arid to semi-arid conditions characterized by high annual rainfall variability and low rainfall with the occurrence of drought and heavy winter (dzud) as natural phenomena. Those ecosystems are controlled more by climatic events and sequences, particularly rainfall, than by equilibrating interactions among the biotic components of the system.

Pastoral and wildlife ecosystems of Mongolia pose challenging management problems associated with increasing livestock populations, long or short term variation in precipitation, rangeland degradation, alteration of pastoral migration patterns and climate change (Sneath 1998, Ojima 2001). During the last 60 years, the annual air temperature has increased by 1.66 degrees in average and the total precipitation amount has almost not changed. However, many aspects of the traditional nomadic culture have changed affecting sustainable land use and vegetation cover for pastoral livestock production. In addition, there are a number of observations indicating that vegetation cover is decreasing and that it has a negative influence on the livelihoods of pastoral people depending on the nature.

To monitor land cover types and to detect their changes over Selenge river basin done using Landsat TM data of 1989 and 2000.

2. Study area

Mongolia

Mongolia is situated in the central part of the Asia (41°35'N - 52°09'N and 87°44'E - 119°56'E). Mongolia is bounded in the north by Russia and in the east, south, and west by China, and has a total area of 1,565,000 sq. km (604,250 sq.mi). Mongolia has a

population of more than 2.4 million people. Basic of Mongolian economy is livestock farming. The livestock population is more than 26 million and agricultural area is more than 790,000 hectares.

The topography of Mongolia consists mainly of a plateau between about 914 and 1524 m (about 3000 and 5000 ft) in elevation broken by mountain ranges in the north and west. The greater part of the highlands consist of mountainous areas with gentle to steep slopes, which are placed western, northern and southwest parts of Mongolia. The Altai Mountains in the southwest rise to heights above 4267 m (14,000 ft).

Over Mongolian 200 types of pastureland counted more than 2200 species of plants and its 600 provides the curtain amount of forage and natural hay for the livestock yearly.

Within the last several years the pasture condition degraded intensive due to harsh weather and increasing livestock population and concentration of people, especially around urban areas due to the free market.

Selenge and Orkhon River Basin

The study area for land cover mapping is located in the north part of Mongolia between latitude 40°N – 50°N, and between 104°E – 108°E, Landsat scenes 132-25 and 132-26. The area is characterized by a great diversity of landscapes. Mountain ranges and ridges are covered with forests and grassland. The central parts of the embedded valleys and plains are mainly arable, intersected and surrounded by pasture (wide grassland). Most of the areas are mainly covered by pasture. Traversing rivers and interspersed lakes are accompanied by rich meadows. The altitude at level of the river valleys falls from average 1000m in the south to 600m in the north, surrounding mountain ranges are up to 2000m high.

Crop monitoring is part of this study and there are 7 soums selected for this study (three soums from Selenge aimag: Eroo, Orkhon and Tsagaannuur; three soums from Tuv aimag: Jargalant, Tseel and Ugtaaltsaidam; and one from Darkhan: Khongor).

3. Data and methods

Green leaves have characteristic reflectance properties relating to their function in photosynthesis. Photosynthetically active radiation (PAR; 0.4-0.7 μ m) is largely absorbed while near infrared (0.7-0.5 μ m) is scattered and reflected. These reflectance characteristics have enabled the development of a number of vegetation indices. One of the most common vegetation indices is the normalized vegetation difference index (NDVI) which is the quotient of the difference and sum of the near infrared (NIR) and red reflectance,

$$\text{NDVI} = (\text{RED} - \text{NIR}) / (\text{RED} + \text{NIR}) \quad (1)$$

where, RED – channel 2 of NOAA/AVHRR data (visible red band - 0.58-0.68 μ m)

NIR – channel 1 of NOAA/AVHRR data (near infrared band - 0.725-1.10 μ m)

Near –infra-red (NIR) is strongly reflected due to the structural properties of leaves and resulting high degree of scattering in the plant canopy (Tucker 1979). As leaf cover increases, chlorophyll absorbs an increasing fraction of red light. Calculation of the NDVI results in pixels with a theoretical index value between -1.0 and + 1.0. Vegetated areas will generally yield high index values, water will yield negative values, and bare soil will result in values near zero. Temporal summation of NDVI through the growing season can be used to estimate gross primary production.

Data from advanced very high resolution radiometer (AVHRR) carried on the National Oceanic and Atmospheric Administration (NOAA) satellite series can be used for vegetation monitoring. The relatively coarse spatial resolution (maximum 8 km) means that large areas can be covered, while the high frequency of image collection increases the chances of obtaining cloud free images and ensures that rapid and ephemeral developments in the vegetation are recorded.

Although many studies were conducted on the region, little work has been done so far on the land cover monitoring in particular at large scale and based on remote sensing. The main goal of this research is to assess vegetation cover change within the last 20 years in Mongolia, where advanced very high resolution radiometer (AVHRR) satellite imagery NOAA/NDVI 10 days composite 8 km resolution data from January 1982 to September 2001 and climate data have been used.

For land cover classification and land cover change detection purposes we have used Landsat TM data over Selenge river basin of 1989 and 2000.

4. Classification approach

The main working steps are as follows:

- Geocoding of satellite data
- Preparation of material for ground survey and execution (carried out for Selenge)
- Develop land cover classification and interpretation keys
- Supervised classification using existing information and ground survey results
- Post-processing and filtering of systematic errors
- Interpretation and refinement of classification results
- Generalize land cover classes into big classes
- Generate land cover change map

5. Change detection

NOAA/AVHRR data was selected because of its high frequency, wide coverage for one pass and long duration of data. In this study, we have used 10 days composite NOAA/NDVI 8 km resolution data from 1982 to 2001, provided from NOAA/NASA Pathfinder data set.

Using 20 years NDVI data we have applied the new method of “Two Years Difference”, which is subtraction of the current years’ NDVI value from the previous years’ value of corresponding ground points.

$$cNDVI = \Sigma\{NDVI[i,j,(k-1)]-NDVI(i,j,k)\} \quad (2)$$

where, i, j, k – NDVI value of i row and j column in certain k year

The difference values of consequent 2 years were separated into 2 groups as, negative values indicating increase or no change (coded as 0) from previous year and positive values are decrease (coded as 1), and the summarized values could show the number of years with NDVI decreasing.

6. Results

Vegetation cover change monitoring

Over whole territory of Mongolia

Using long term 10 days NDVI composite images we can determine the temporal and spatial vegetation changes. According to the long term values of NDVI we have estimated monthly, seasonal and 10 days dynamics over Mongolia.

As Mongolia has short summer season and In general, the peak of vegetation growth fits in August within short duration of growing period, from June to early September. The monthly long term average NDVI within 1982 – 2001 and 10 days dynamics of 1992 are showing in Fig. 1. In general, 1994 was quite wet year and 2001 was more drought year within the above 20 years of study.

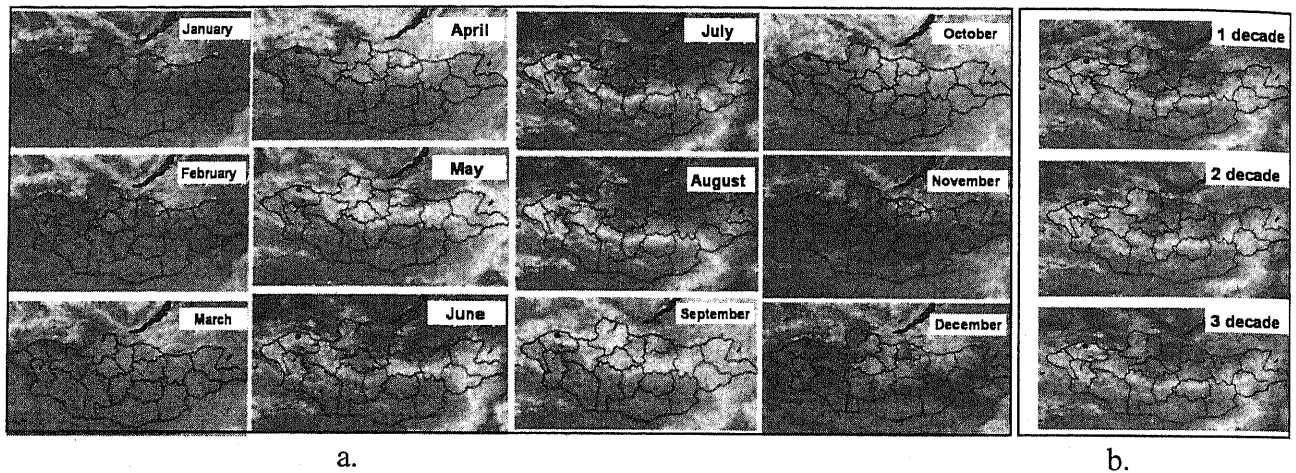


Fig. 1. NDVI dynamics, a. monthly mean NDVI dynamics, 1982-2001
b. 10 days of NDVI dynamic, August, 1992

From NDVI dynamics we could estimate only vegetation condition of certain period. Also we could determine the vegetation condition by comparison with long term mean, maximum and minimum of NDVI values. From the standardized deviation of NDVI within 20 years we could distinguish drought, normal and good summering years.

In order to estimate NDVI changes, we have used Two Years Difference method of corresponding 10 days within 1982-2001.

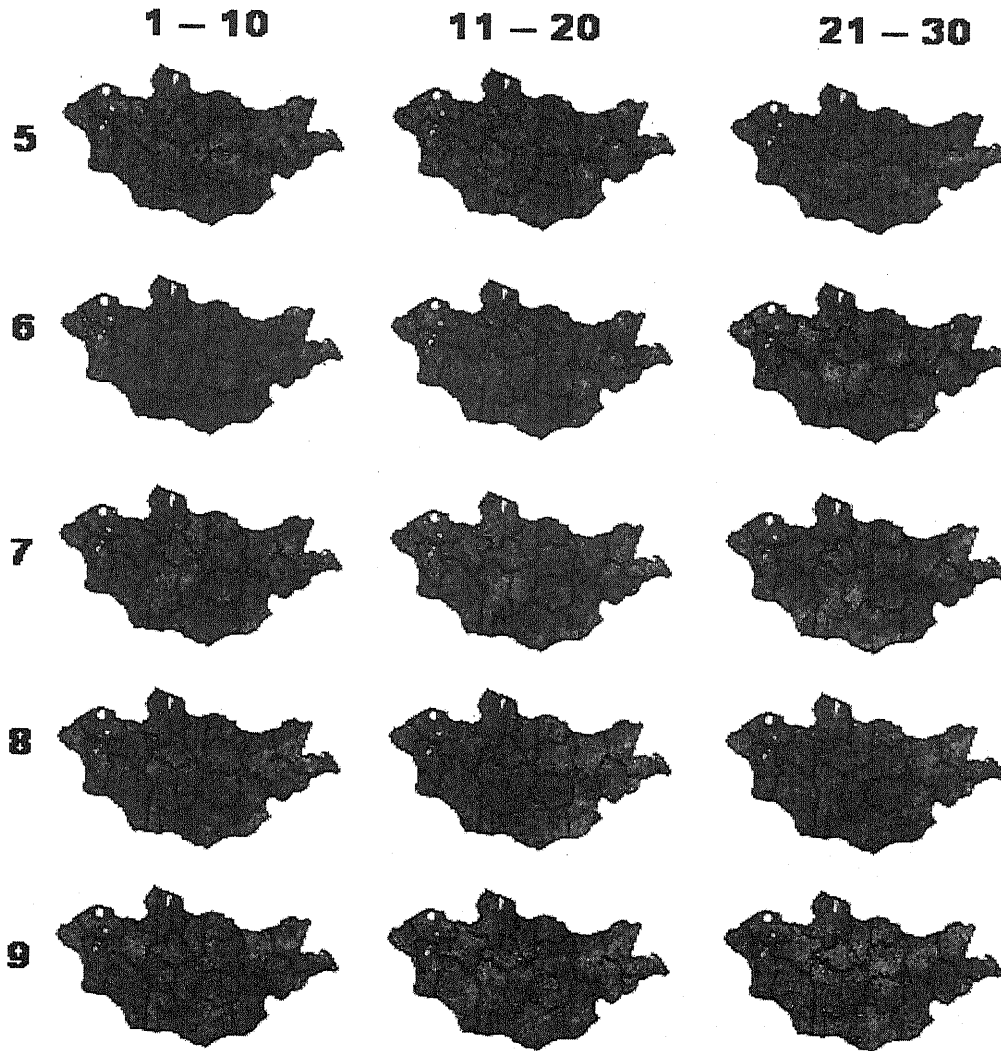
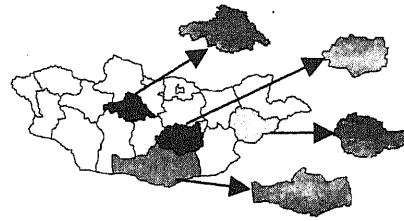


Fig. 2. NDVI changes between May – Sep, 1982 – 2001 (10 days)

The results showed which place had decrease or increase of NDVI compared to previous year, this comparison has repeated within these 20 years, and its output could illustrate that how many years NDVI has decreased at the same place. In Fig. 2 we have showed the spatial distribution of NDVI changes and the green color corresponds to no change or increase of NDVI, colors from yellow to bright red color show the frequency of NDVI decrease. Yellow shows lower and red shows higher frequency of NDVI decreases.

During the 20 years in each month from May to September occurred maximum 9 years had NDVI decreases over Mongolia. Especially, in May in southern and eastern regions, in June, July and in September partly in all regions, and in August central and eastern regions had the negative influence on vegetation growth. In 24.4 – 32.7% of all territory occurred one year decrease of NDVI and in 18% occurred more than 3 years frequent decrease of NDVI.

NDVI changes over different aimags



According to the long term NDVI data we could estimate its dynamics over some part of Mongolia as, from aimag level upto soum and bag level.

We have selected 4 aimags from different natural zones to compare their NDVI dynamics and their NDVI dynamics were completely varying from each other. But all these aimags territories had common characteristics that year of 1994 was occurred as best summering for all aimags.

During the study period, the Umnugobi aimag, which is example of desert zone, had always lower NDVI values and less changes and Bulgan aimag (mountain zone) had highest NDVI values. The Dundgobi aimag's territory covered steppe and desert steppe zones, but its NDVI dynamics shows that most part of this aimag's territory is desert steppe. NDVI values of Sukhbaatar aimag had more frequent changes, which means the steppe zone is much sensitive to the weather variability than other aimags (Fig. 3).

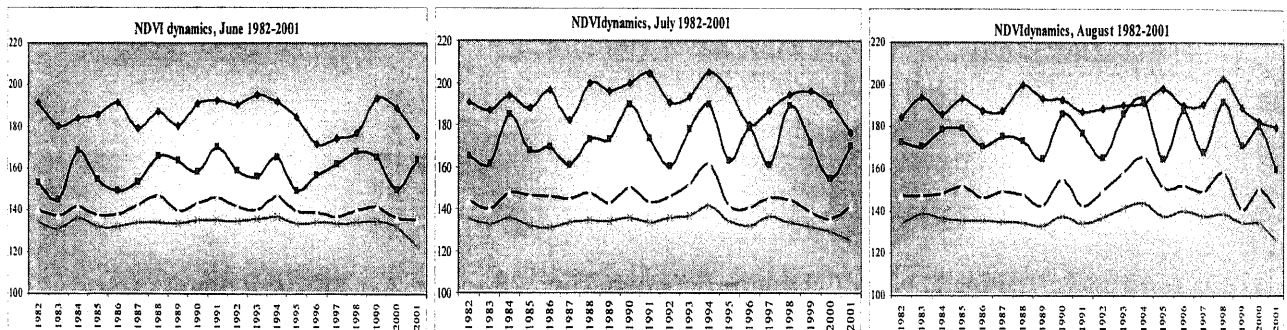


Fig. 3. NDVI dynamics of 4 aimags, June – August, 1982-2001

In Fig. 3 the red graph belongs to the Arkhangai aimag and blue, green, orange colors corresponding to the Sukhbaatar, Dundgobi and Umnugobi aimags, respectively. All these aimags NDVI dynamics had different trends. For example, Sukhbaatar aimags territory had NDVI changes in each 3-4 years, but in total in had increasing trends, like 0.060-0.352 units a year, which could be related with precipitation amount. In Arkhangai aimag occurred decreasing trend of NDVI values in 0.053-0.247.

Land cover classes

The interpretation key helps to organize the information available in the image data for a specific topic, like land cover classification and to correct/identify unknown feature classes during further work. It recommended to describe the appearance of each class by the standard characteristics of image interpretation and to give examples. As any image analysis, regardless interpretation or automatic technique is in the end an individual process, it is important to ensure as much as possible a systematic and consistent identification.

Based on official land cover class system we made the following land cover classes from satellite imagery.



Table 1. Land Cover classes over Selenge river basin

No.	Class
1.	Pasture and Grassland
2.	Arable land
2.1	Cropped/vegetation cover
2.1.1	High density crop land
2.1.2	Medium/low density crop land
2.2	Fallow, abandoned
3.	Forest
3.1	Coniferous forest
3.2	Deciduous forest
4.	Riverine
5.	Burnt areas
5.1	Burnt forest
5.2	Burnt pasture/grassland
6.	Bare soil/eroded area
7.	Wetland
8.	Water bodies
9.	Infrastructure

While supervised classification was very useful for distinguishing land cover features, specially forest types and pasture. For land cover classification study we created GIS database, which consists of the following dataset:

1. Main geographic features like administrative boundaries, lakes, roads, rivers, and relief (scale 1:500,000)
2. Land use map of Selenge aimag (scale 1:500,000)
3. Ecosystem map of Selenge region (scale 1:500,000)
4. Fire map, which produced from NOAA AVHRR data of 2000

Classification accuracy was more than 90%. Fig. 4 shows land cover maps of 1989 and 2000.

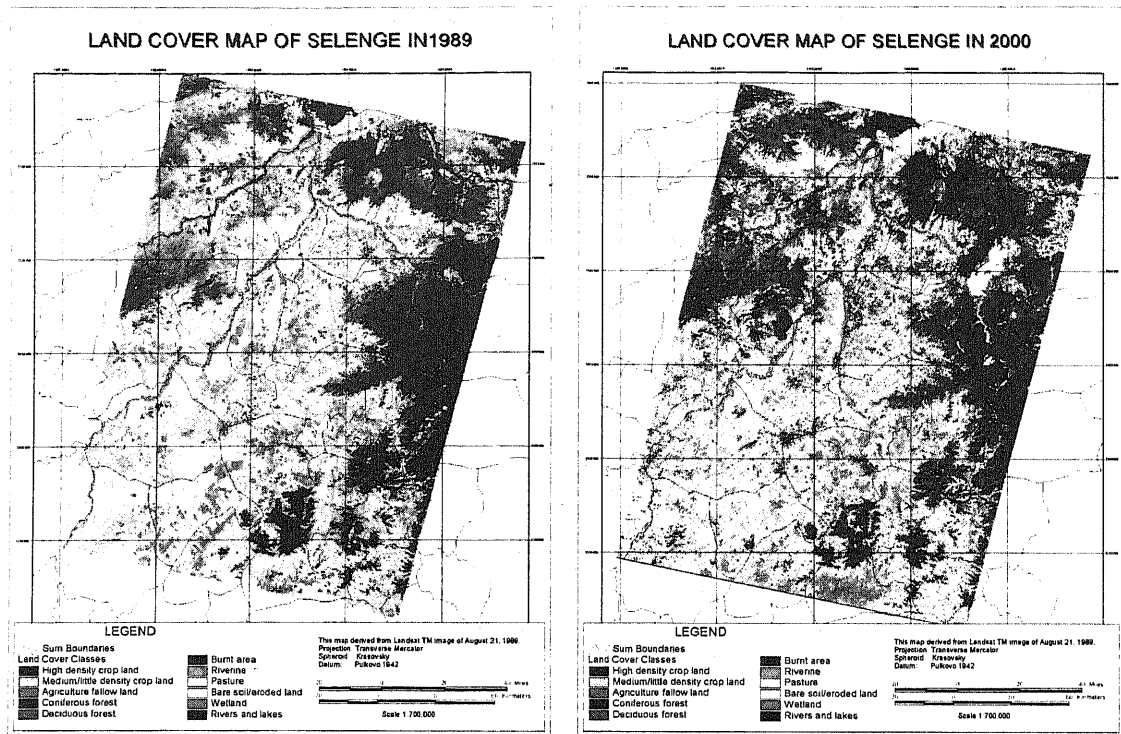


Fig. 4. Land cover classification results

To generate land cover change map we needed to generalize land cover classes into 6 big classes, Crop land, Forest, Bare soil/eroded land, Pasture, Wetland and Water bodies.

After generalizing land cover classes were generated land cover maps of 1989 and 2000 (Fig. 5) in order to detect land cover changes (Fig. 6).

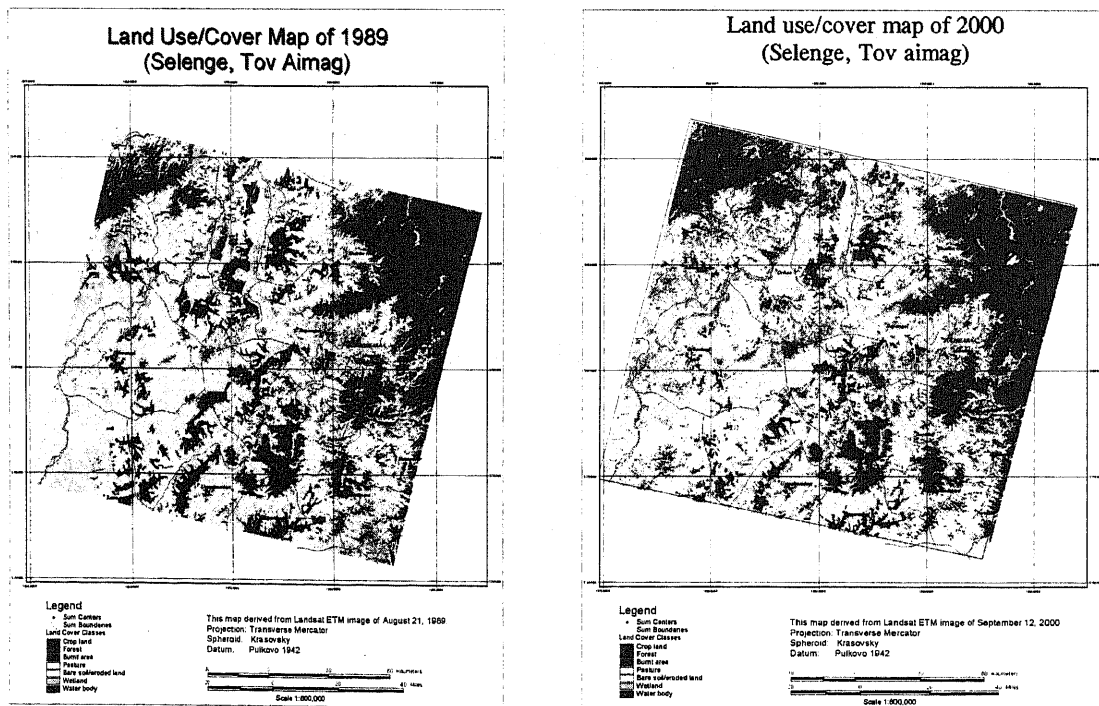


Fig. 5. Generalized land cover maps

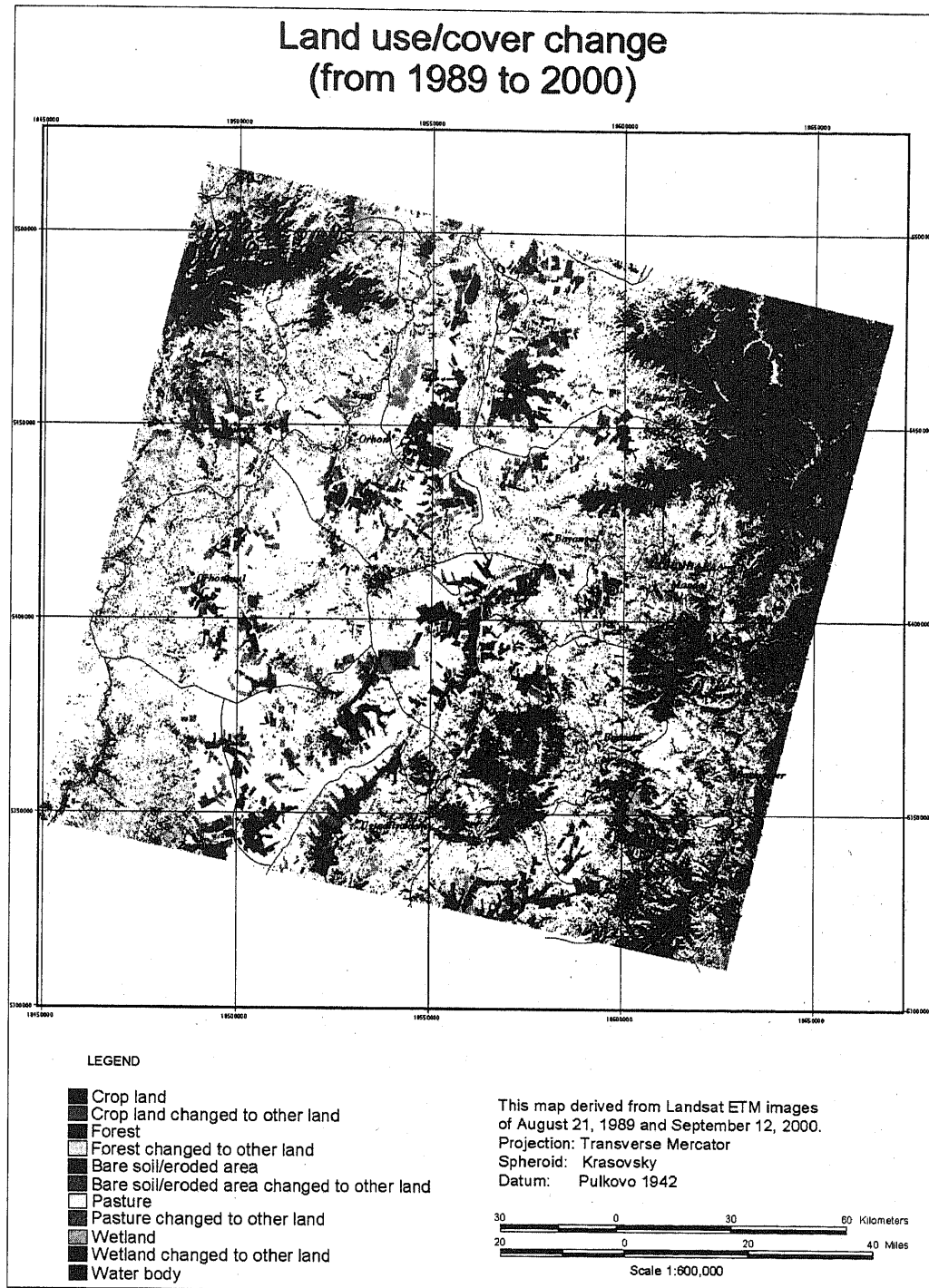


Fig. 6. Land cover change map of Selenge – Tuv aimags

Numerical values of land cover changes in 1989 and 2000 show, there are noticeable changes in some classes, such as cropland, forest and eroded area. In other words, the land cover change analysis determined that from 14 to 53 percentage of land cover classes have changed to any other classes. For example, the area of arable land reduced by 152,000 hectares, bare soil or eroded area increased by 7,300 hectares and forest area decreased by 120,000 hectares from 1989 to 2000.

7. Conclusion

NDVI is used as an indicator of relative biomass and greenness under global warming. If sufficient ground data is available, the NDVI can be used to calculate and predict primary production, dominant species, and grazing impact and stocking rates. Indeed, plant cover changes through time with short term rainfall variability; it also varies in space, both as function of grazing and as a result of natural variability.

By NDVI data of NOAA satellite data, we could estimate the spatial and temporal changes of pasture vegetation condition over Mongolia and in certain regions. The time series analysis showed that, the vegetation condition changed differently in various regions over the territory. The highest frequency of NDVI decrease reached 9 years within the last 20 years and over 18% of whole territory of Mongolia suffered more than 3 years frequent decrease of NDVI.

The land cover change analysis showed that 44 per cent of the crop area changed to pasture and wetland.

References

1. Adyasuren Ts, Erdenetuya M, "Vegetation Cover Monitoring in Mongolian Plateau using Remote Sensing Technology", Yokohama, Japan, 2003.
2. "Asian – Pacific Remote Sensing and GIS Journal" Volume 10, ESCAP, 1998
3. Batima P, Dagvadorj D, "Climate Change and its Impacts in Mongolia", Ulaanbaatar (UB), 2000.
4. Ellis J. 1992. Recent advances in Arid Land Ecology. In: Sustainable Crop-Livestock Systems for the Bolivian Highlands. C.Valdivial, Ed. Univ. of Missouri Press. pp. 1-14.
5. Erdenetuya M, "Pasture monitoring methodology and technology", PhD Dissertation, Ulaanbaatar, Mongolia, 2004.
6. Erdenetuya M, "Pasture monitoring from space", Annual reports, UB, 2001, 2002, 2003.
7. "Land Cover Assessment and Monitoring" UNEP, Bangkok, 1995
8. "Multispectral Imagery reference guide" Spectral Imagery Training Center, LOGICON Geodynamics, Inc. Fairfax, Virginia, USA, 1997
9. Munkhtuya Sh. "Land cover classification methodology using satellite imagery", PhD Dissertation, Ulaanbaatar, Mongolia, 2004.
10. Natsagdorj L, Batima P, "Climate Change of Mongolia", UB, 2002.
11. "National Atlas of Mongolia" Academy of Science Mongolia, Ulaanbaatar, 1990
12. "Observing and analyzing natural resources" Spot Image, Journal, CNES, France, 1998

SNOW RETREAT AS A KEY INDICATOR OF GLOBAL WARMING

Tarzad Ulaanbaatar¹ and Lkhamjav Ochirkhuyag²

¹Research Center for Geophysics, National University of Mongolia,

²Information and Computer Center of NAMHEM, National Remote Sensing Center,
Mongolia,

tarzad@yahoo.com lochir@yahoo.com

Abstract

One of the key indicators of global change and global warming is the change of vertical and horizontal distributions of glacier and snowline in high mountain regions. The 0°C isotherm line of heliogeothermosphere at warmest month defines the lower boundary of “permanent” snow. The increase of global temperature can impact powerfully on the retreat of snowline. Using model results of subsurface temperature regime in comparison with snow reflectance from satellite data, the retreat of snowline and rate of global warming in Khangai Mountain Range/Mongolia are assessed.

1. The scope of problem and background

Our objectives of this study are to assess the retreat of summer snowline and rate of global warming, and to use remote sensing data in investigations of climate change.

Mountain influences on climate and related environmental features are a result of four basic factors: altitude, continentality, latitude and topography, each of which affects several important meteorological variables. These are very important to deeply study environment background of the selected region in estimating global warming.

Today, glaciers and ice caps, particularly the Himalayan, European, Latin-American, Antarctic and African are well studied. However, Mongolian Altai, Khangai and Khentei Mountain Ranges stayed away from scientific eyes.

There are some important methods to study global climate or global warming in high mountains: the mathematical modeling of the thermal regime on and near the earth surface, meteorological monitoring of the selected region (particularly, snowline), borehole logging of geothermics and remote sensing data.

According to my studies the climate and snowline are more sensitive in high mountains of high latitudes. In all these methods meteorological data are very useful to determine the long term climate change in different spatiotemporal scopes. Short term meteorological extreme changes can not impact on:

- The altitude of summer snowline limited by the 0°C isotherm of heliogeothermosphere,
- The depth of the ground where the amplitude of air temperature is eliminated during its diffusing into the deeper layer of shallow lithosphere.

For instance, in order to study deeply the climate system we must begin with these very stable factors.

Based on the above considerations, we choose the glacier of Otgontenger Peak which is located in Khangaj Mountain Range, Western Mongolia. Through studying dynamical changes of snowline under the support of modern remote sensing technique and GIS, we understand the region’s environment background, and global warming.

Problems encountered:

- ✓ Meteorological stations do not cover the selected regions, and the distance between them reaches hundreds of kilometers.
- ✓ Borehole temperature logging is not carried out all over territory Mongolia.
- ✓ High-resolution remote sensing data is limited

For this reason, among above methods we use most methods in this study: the modeling and remote sensing.

3. The theoretical base

Mathematical Modeling of Air Temperature Regime

Both short and long term climate changes in aspect of thermal regime are described by mathematical models. (Berger, A., 1977a, 1977b, 1997; Ulaanbaatar, T., 1992, 1994, 1998)

The consequence of solar irradiance on the earth surface is the subsurface air temperature regime. In other words, insulation is equivalent to air temperature except of their vertical distributions. Some differences between the insulation and temperature are:

- The temperature gradient decreases with altitude, but insulation is inverse.

The air temperature gradient as a whole equals 0.005-0.006 [degree m⁻¹] in planetary-scale. In high altitude this value is very stable, evidence of which is shown by stability of snowline for a long time, so-called permanent snow. For this reason, short term climate change has no great effect on glacial tongue body's advance and recession, but has an impact on ice-snow coverage rate. Long term climate change has a significant influence on global advance and recession.

$$\text{grad}A = 0.005 - 0.006 \text{ deg ree C m}^{-1}$$

- For calculation of air temperature regime we do not use the solar constant.

So, we need another etalon of temperature which must be very stable and measured on the earth surface. It is the air temperature where the solar rays fall perpendicularly on the Earth described by Ulaanbaatar, T., (1994).

$$A_0 = +30^0\text{C} \quad (1)$$

Using above considerations in order to explain and analyze the global change the noon sun air temperature regime on and near the earth surface is written as:

$$A_\phi^n = A_0 \cos(\varepsilon \cdot (0.98 \cdot n) + \varphi) - H \cdot \text{grad}A - A_\phi^n(\alpha(\text{snow})) \quad (2)$$

Where $A_\phi^n(\alpha(\text{snow}))$ is the air temperature influencing by albedo of the snow cover, ε denotes the angle between the ecliptic plane and equator. Its long-term variation by Berger, A., 1977a, 1977b, 1997)

$$\varepsilon = \varepsilon^* + \sum A_i \cdot \cos(f_i \cdot t + \delta_i) \quad (3)$$

Results are shown in Figure 1 and Figure 2. The 0 degree C isotherms around the globe build a thermal sphere as heliogeothermosphere, its shape determines the climate fluctuation so-called World Climate Supercirculation.

In this paper we attempt to describe the snowline changes in high mountain using satellite data because long-term changes of snowlines and glaciers in West Mongolia are induced by global warming.

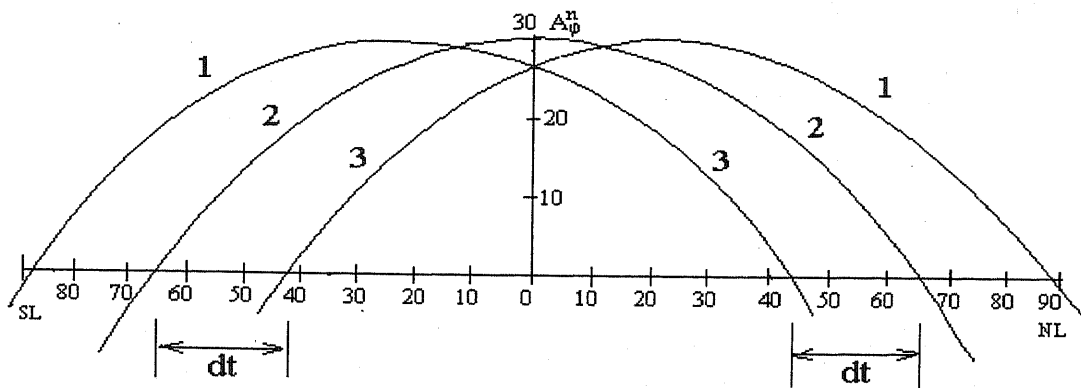


Figure 1. Air temperature curve transfer along meridian, 1- Winter at Northern hemisphere, 2- Equinox, 3- Summer solstice

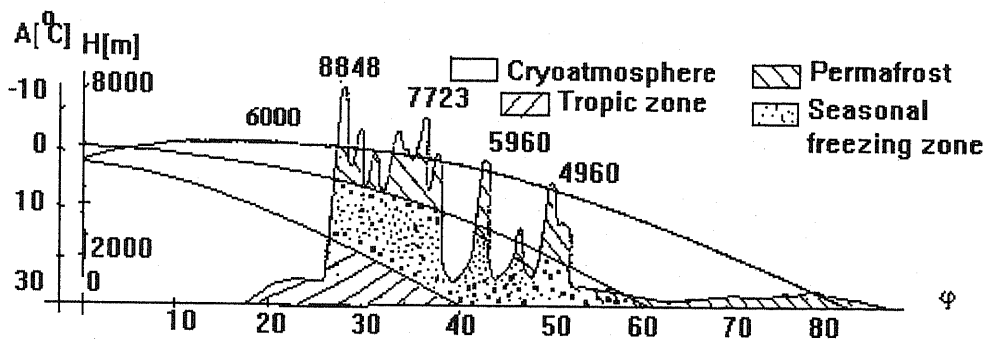


Figure 2. Air temperature regime in altitude-latitude cross section along the 104° degree of meridian in Northern Hemisphere

The long term variations of Figure 1, 2 may be drawn in next Figure 3:

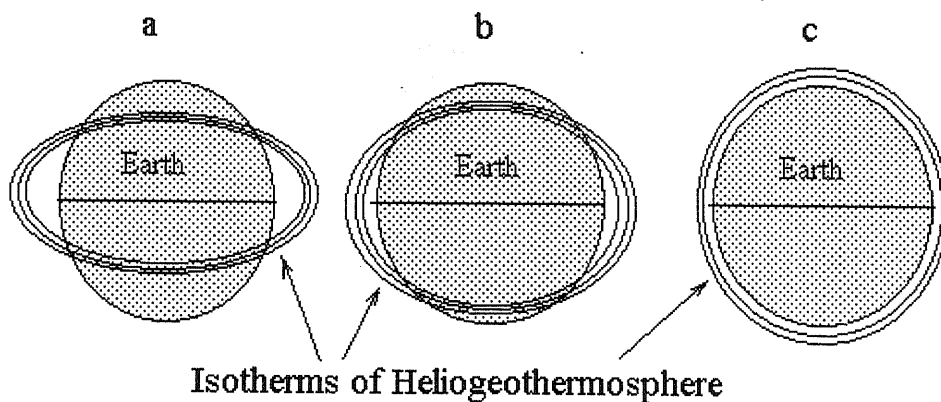


Figure 3. The heliogeothermosphere and changes of its shape during a World Climate SuperCirculation
a- glacial stage, b- present situation, c- interglacial stage

The fluctuations of 0 degree Celsius isotherm of heliogeothermosphere at July and August define the snowline and glacial tongue body.

The elevation of summer snowline or 0 degree Celsius isotherm of heliogeothermosphere in July is 4200 m at the sea level (Equation 2), by which we can calculate the retreat of snowline due to global warming.

Data and Study area

Reflective channels 1 (yellow-red (620.0 – 670.0 nm)) and 2 (NIR (841.0 – 876.0 nm)) of the Moderate Resolution Imaging Spectroradiometer (MODIS/TERRA) satellite data on 19 January 2004, WGS 84 system. This data was processed at level 1b (HDF format data) by the EOS Data Gateway, Land Process Distributed Active Archive Center (LP DAAC) of NASA. The spatial resolution of the MODIS instrument varies with spectral band, and ranges from 250 m to 1 km at nadir. The study area is most area of the Mongolian territory, within 40° - 53° N and 90° - 117° E.



Figure 4. Forest-Mountain snow percentage map in Mongolia.
The arrow shows the Otgontenger Peak.

For detailed interpretation, we select high-resolution map. (Figure 5)

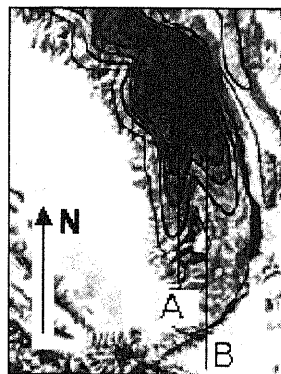


Figure 5. The Otgontenger Peak

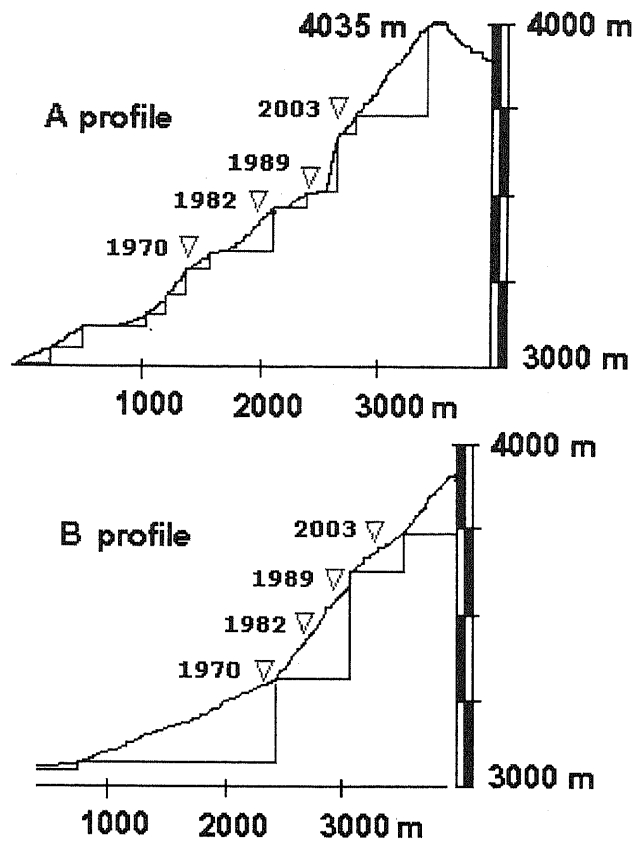


Figure 6 and Figure 7 show the cross sections along the A and B profiles

Table 1. The calculation results by A profile

Year	Elevation of snowline (m)	Duration (yr)	Retreat of snowline (m)	Annual average retreat (m/yr)
1970	3284.6			
1982	3415.4	12	131.0	10.9
1989	3507.7	7	92.3	13.2
2003	3680.7	14	173.0	12.36
Average				12.15

The Table 1 indicates that the yearly mean retreat equals 12.15.

Table 2. The calculation results along B profile

Year	Elevation of snowline (m)	Duration (yr)	Retreat of snowline (m)	Annual average retreat (m/yr)
1970	3292.3			
1982	3423.1	12	130.8	10.9
1989	3538.5	7	115.4	16.48
2003	3692.3	14	153.8	10.98
Average				12.78

The results in Table 1 and 2 are the same. From two tables, the annual average retreat is 12.46 m/yr.

Since 1970, the temperature has risen by 1.98 degree C causing glaciers and snowline to melt rapidly.

The snow cover has decreased by 30 % in area between 1970 and 2003 and diminished by more than 50 % between 1970 and 1989, and today is only 40 % of what it was in 1970.

As a result of recent global warming, permanent snow of Otgontenger may disappear completely by 2034.

4. Conclusion

Our study confirms that snowline indicates the 0 degree C isotherm of heliogeothermosphere. Consequently, global warming pushes the Central Asia into the desertification. The increase of temperature is approximately 2 degree C.

5. Discussion

This study of retreat of snowline would be the precursor of our further scientific cooperation. So, I have attempted to show the challenge of our further cooperations. The consequences of global warming on the social, economic life of Mongolia are very critical. There are many unstudied and unsolved fields and targets, for example, desertification, deforestation, drought, flood and snowstorm. For detailed investigations of the global warming, global change and environmental background, we need high resolution satellite images.

Acknowledgements

The authors are grateful to Dr. R. Tsolmon, President of Mongolian Geoscience and Remote Sensing Society for providing data, technical assistance, valuable discussions and great insight.

Reference

- Berger, A., Long-term variations of the Earth's orbital elements. Celestial Mech., 15, 53-74, 1977a,
- Berger, A., Support for the astronomical theory of climatic changes, Nature, 268, 44-45, 1977b,
- Berger, A., Long-term variations of caloric insolation resulting from the earth's orbital elements. Quat. Res., 9, 139-167, 1978,
- Berger, A., Orbital variations, Encyclopedia of climate and weather, S. Schneider (ed.), pp.557-564, Robert Ubell Associates, Inc., Oxford University Press, 1996,
- Ulaanbaatar, T., Influences of the global average temperature of planet on the degradation of geographical and permafrost zones, Proc. Nat. Sci. Prac. Con. on Actual Problems on Hydrogeology, Geophysics, Hydrology and Geocryology, pp.12-14, Ins. Water Policy, Ministry of Environmental Conservation of Mongolia, Ulaanbaatar, 1992,
- Ulaanbaatar, T., Mathematical modeling for the thermal regime of the Earth's surface and cryosphere, Ph.D Thesis, Mong. Univ. of Technology, Ministry of Science and Education, Ulaanbaatar, 1994,
- Ulaanbaatar, T., Climate Supercirculation of the Earth, Scientific Translation, 3(132), 246-264, Nat. Univ. Mong., Ulaanbaatar, 1998

Ulaanbaatar, T., High latitude thermal variability in relation to lower latitude, Inter-Association

Symposium: Atmospheric and oceanic connections between the polar regions and lower latitudes, IAMAS, IASPO, , XXII General Assambly, IUGG, Birmingham, UK, Vol. A, 96, 18 July-2 August, 1999e.

FOREST MAPPING WITH THE AID OF ERS SAR AND OPTICAL LANDSAT DATA IN THE UVS LAKE BASIN, WESTERN MONGOLIA

Davaasuren Narangerel, RS & GIS specialist, Forest & Water Resources Center,
Mongolian Ministry for Nature and Environment
Gankhuyag Bulgan, Scientific Researcher, Informatics & RS Institute,
Mongolian Academy of Sciences
Damdinsuren Dejiidmaa, "Geomaster Co. Ltd"

1. Introduction

The Synthetic Aperture Radar (SAR) interferometry technique is a promising method for land use classification, forest type discrimination, vegetation density assessment, DEM generation, deformation mapping and environmental change detection studies.

The identified forest and grassland groups on classified optical Remote Sensing images were classified and mapped in terms of forest age group areas. Additional information from ERS SAR data incorporated into the classified images served as a main component for discrimination between forest types, determination of vegetation density and changes in vegetation boundaries.

2. Research background

Experience of GAMMA Remote Sensing group has shown that SAR interferometry could be used successfully in many applications for land use classification, forest type discrimination and determination of vegetation density. Classification methods can distinguish between different types of surfaces and their characteristics can be assessed from in-situ observations of interferometric correlation and the level in back scattering intensity. Coherence information from ERS images obtained from SAR interferometry processing could be used as additional input in optical RS image classification. In this way, reliability of land cover (forest and grassland) classification may be improved, ambiguity reduced, and increased confidence in the results provided.

In our case, image fusion of ERS SAR-2 with optical Landsat TM data enhanced features not visible in any single data alone and provided additional thematic and textural information.

Obtained results were verified and compared with other information in order to determine and explain environmental changes.

3. Research methodology

1. Discrimination of forest type and vegetation density based on visual interpretation of radar images.
2. Classification of optical Landsat TM data into forest and grassland.
3. Image fusion of interpreted radar images and classified optical data.

The lifestyle and economical activities are widely located in the forested areas, and therefore Mongolian forests are severely affected by the on-going process of degradation. Changes in forest and grassland ecosystems affected by degradation and human activities can be shown by simplified forest groups. Traditionally in optical Remote Sensing, vegetation health is monitored by the amount of reflectance in the near

infrared part of the spectrum (Normalized Vegetation Index - NDVI). The hybrid algorithm of multi-spectral, multi-source and multi-seasonal classifications of Remote Sensing images has a strong ability to produce comprehensive and reliable forest and grassland information.

In our case, active fusion of multi-source and multi-spectral data required:

1. ***Spatial co-registration***, in order to compare multi-source images at the pixel level.
2. ***Selection of classification methodology***. For ERS SAR data, a contextual classification approach has been found useful in determining forest volume classes in Siberian boreal forest, in Russia, which is similar to forests in the Mongolian test site. Satisfactory and statistically significant accuracy in multi-source classification of Landsat images could be achieved when texture and ancillary data are introduced.
3. ***Dealing with uncertainty***. Different kinds of uncertainty have to be considered and treated. For example, questions of data quality from different sensors and issue of vegetation communities' boundaries, which are zones of gradual transition- ecotones, can be termed as "soft" or fuzzy boundaries and handled accordingly.
4. ***Issue of multi-scale analysis***. Information fusion on different spatial resolution often aims at either displaying the fused multi-scale data or using them as input to further analysis. The main aim is to merge high-resolution panchromatic image (ERS SAR) with a low-resolution multi-spectral image for better visual interpretation. This very high resolution and image enhancement will enhance target recognition.
5. ***Accuracy assessment*** of the derived forest and grassland information.

4. Results

4.1 Study Area.

The forests of the Uvs Lake Basin, in western Mongolia, belong to the Altai and Sayan mountain systems and cover the whole range of the environment. They represent a mix of forested areas, mountain tundra, steppes and desert regions.

The Altai-Sayan eco-region contains the world's largest unbroken stretches of Siberian Pine forest. The pine forests in the western part of the Altai region is of unique ecological importance. The health of the largest Siberian river basins of Ob and Yenisei depends on future preservation of ecological processes in this region, because two extreme upper watersheds are located here. The study area under consideration is located in the forests of Harhira Mountain.

4.2 Classification process

Mongolian forests can be classified according to age and corresponding landscape groups within high mountain meadow-steppes; taiga forest; mountain taiga forest; actual forested area (mature forest); forest-steppes (areas with low forest density) and steppes with open forest (areas with low distributed forest areas with low forest density inside).

NDVI was calculated and visual interpretation done for selection of training classes from Landsat images and their verification with topographic and thematic map information. Areas with forested regions were separated into separate layers after supervised classification by maximum likelihood classifier. Classified images of different seasons, such as October, August and June, were compared at the pixel level.

The overall accuracy of classified images was calculated by dividing the number of pixels correctly classified by the total number of pixels included in the evaluation process. Forested areas were categorized in terms of dense, middle and low-density areas. The separation between steppe-forest and areas with very low forest density has been done based on visual interpretation of radar images.

In our case, it was not possible to perform SAR interferometry due to the absence of special image processing module. In order to significantly improve visual interpretation of radar images, different filtering was applied. Enhancement of radar images significantly contributed to the interpretation process and the selection of training classes in the optical image (Fig.2).

However, separation between steppe-forest and areas with very low forest density were possible in the cases of coniferous forest. This was because deciduous forests had already shed off in the October images. Also, forests are mostly located on northern slopes; those on southern slopes are very rare due to the contents of moisture and solar radiation. The probability of forests growing in open space areas, such as steppes, is also very low, due to the specific climatic conditions of this area. Steep forested slopes were very difficult to identify on radar images due to image processing, including satellite image foreshortening, layover, and shadow effects. In order to improve the interpretation process of radar images, areas with low mountains were selected and high mountain regions were neglected (Fig.1).

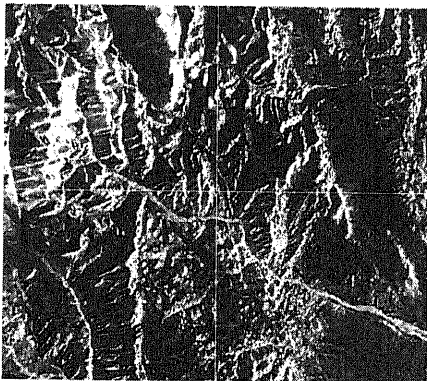


Fig. 1 Excluded areas

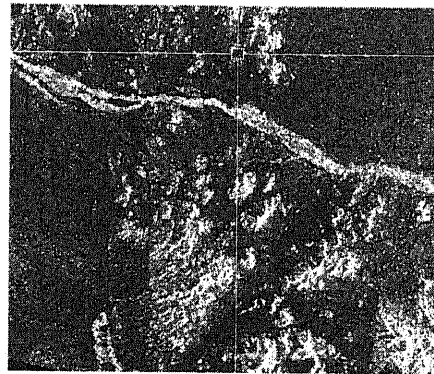


Fig.2 Area with identified forested areas (with topographic map aid)

A Landsat image from the October season had almost no cloud coverage, but an extensive spread of glaciers at high mountain region.



Fig. 3 Forest groups on Landsat image



Fig. 4 Fused subset of radar image & Landsat data

Transitional zones between steppe-forest and open-forest were almost impossible to distinguish in Landsat images due to their “soft” or fuzzy boundaries. Therefore, gradual transition zones were identified by overlaying of digitized forest contours from topographic maps. However, the issue of positional accuracy and even acceptable RMS error of less than 30 m (1 pixel) during geo-referencing, leads us to assume that such areas could be identified as areas with no forest or open areas with low forest density, which is almost identical. Overlaying forest contours from topographic maps onto radar images showed areas with low forest density, which can be further classified as open areas with no forest. The application of principal component analysis (PCA) allowed us to determine 10 vegetation classes, including forests of high and middle densities.

We applied radar image interpretation to the area excluding high mountains. High mountain regions covered by glaciers were classified as areas with no information.

5. Conclusion

Visual interpretation of radar images could significantly improve classification processes of optical information. However, this assumption is very true in steppe and, low land areas, not affected by foreshortening, layover and shadow effects of the satellite imaging system. However, previously it was impossible to determine the phase and gain altitude information in the Uvs Lake forested region (R. Karsner, 2000). But this research considered altitude information for the image processing in the study area. Because the Uvs Lake Basin and Harhira Mountain region was included into SPA, closing such gaps with old topographic information from the 1940s and 1960s can be done due to the remoteness of this region, the rarity of forest fires and its lack of pastoral land use activities.

References

1. M.Burkart, S.Itzerott, M.Zebish, 2000, Classification of vegetation by chronosequences of NDVI from remote sensing and field data: The example of Uvs Nuur Basin, *Extended Abstracts of the International Symposium, State and Dynamics of Geosciences and Human Geography of Mongolia*; Reihe A, Band 205, Berliner Geowissenschaftliche Abhandlungen, FU Berlin, Germany.
2. R.Karstner, 2000, Patterns of forest distribution in Western Mongolia, *Extended Abstracts of the International Symposium, State and Dynamics of Geosciences and Human Geography of Mongolia*; Reihe A, Band 205, Berliner Geowissenschaftliche Abhandlungen, FU Berlin, Germany.
3. J.M. Paruelo, C.Di Bella, M.C. Giallorenzi, F.Pacin, 2003, Land cover classification in the Argentine Pampas using multi-temporal Landsat TM data, *International Journal of Remote Sensing*.
4. J.D. Shepherd, J.R.Dymond, 2003. Correcting satellite imagery for the variance of reflectance and illumination with topography, *International Journal of Remote Sensing*.

REFLECTOMETERS

D. Enkhbat and S. Damdinsuren

Department of Biophysics, Faculty of Biology, National University of Mongolia

Email: sdamdinsuren@yahoo.com, damdinsuren@num.edu.mn

The reflection and scattering of light, fluorescence and luminescence of chlorophyll is widely used as a nondestructive, remote and quick method in plant research (1). The objective of this article is to introduce simple reflectometers and their application.

We assembled a simple apparatus for measurements of light intensity at 19 wavelengths of reflected light. The apparatus consists of an interference filter wheel, photomultiplier and its power supplier (voltage converter), photocurrent amplifier and an analog device to read light intensity (Fig. 1). The photomultiplier is sensitive in the range of wavelength from 380-830 nm with a maximum around the yellow range of spectra. Therefore, the spectra of reflected light looks like it has a maximum reflection in this region of spectra (Fig. 2).

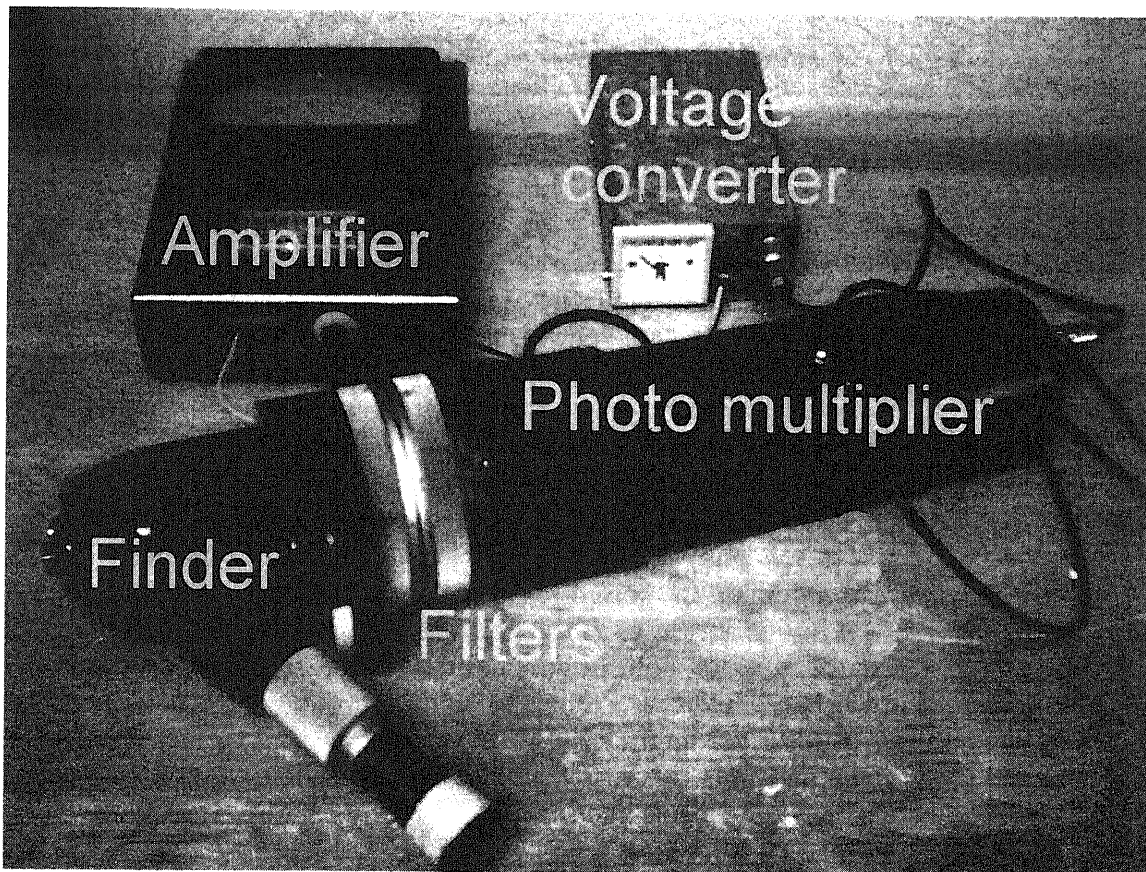


Fig. 1. Reflection spectrometer for registration of reflected light intensity at 19 wavelengths. The intensity of reflected light is proportional to the output reading of analog device.

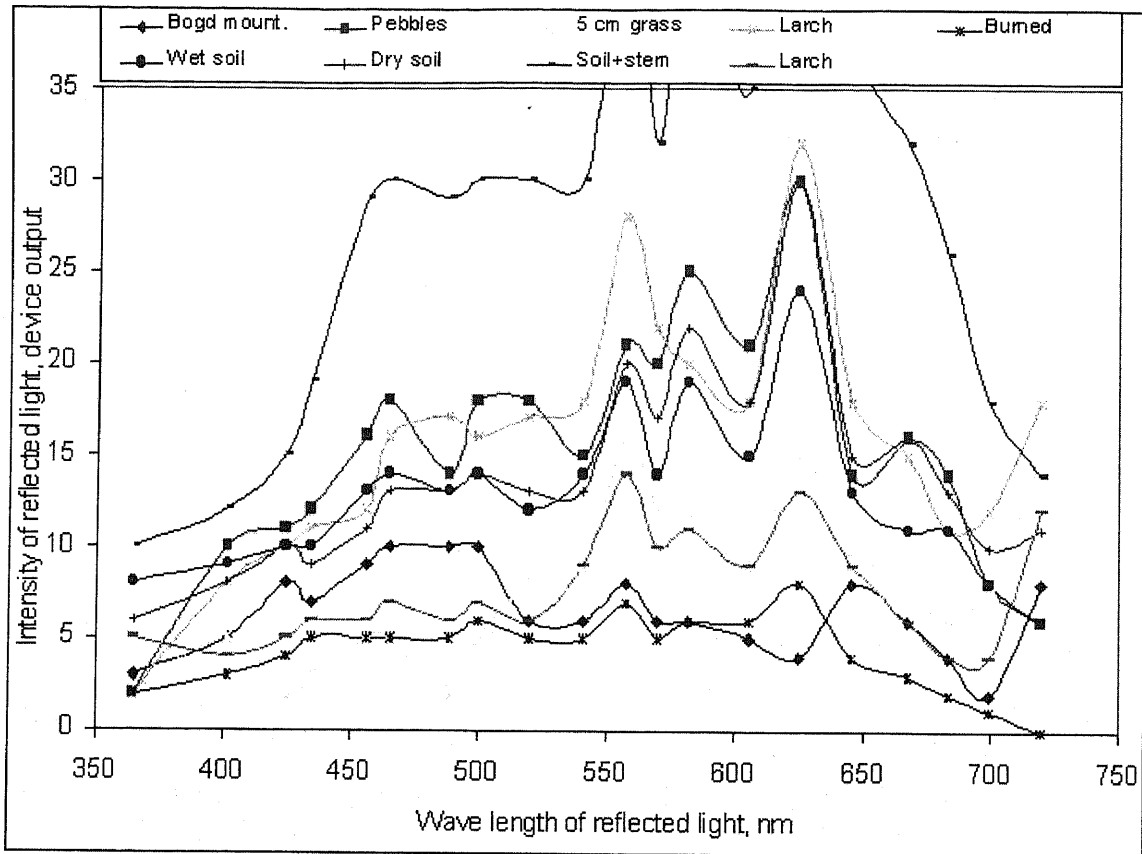


Fig. 2. Spectra of reflected light from Bogd Mountain, including pebbles soil, young grass, larch, burned field, field with yellow stem, other larch, and wet and dry soil, measured with a reflection spectrometer (Fig. 1).

Spectra of light reflection from different objects are shown in the Fig 2. The intensity of reflected light increases to a maximum with the increase in wavelengths from blue to yellow-red (625 nm) region of the spectra, and then monotonically decreases in the case of soil and yellow stem fields. The intensity of reflected light from green plants shows a minimum in the red region of spectra, where it was absorbed by chlorophyll, and then further increases in the near-red region of spectra. Therefore, the ratio of the intensity of reflected light in the near red (720-830 nm) and red (650-683 nm) region of the spectra should characterize green plants (Table 1). It is interesting to note that the ratio of reflected light (R_{720}/R_{683}) from blue and cloudy skies, green paper and other green materials was less than 1.0. The reflection spectrometer detects the whole reflection, including plants and soil.

Table 1. The ratio of reflected light intensities (R_{720}/R_{683}) in green plants is greater than that in the soil and other objects.

Objects	Bogd Mountain	Grass	Larch A	Larch B	Burned field	Yellow stem	Wet soil	Dry soil
$\frac{R_{720}}{R_{683}}$	2	3	1.7	3	0	0.5	0.5	0.8

Therefore, we constructed a portable reflectometer for quick measurements of the ratio- R_{720}/R_{650} (Fig. 3 left). The reflectometer also detects the whole reflection.

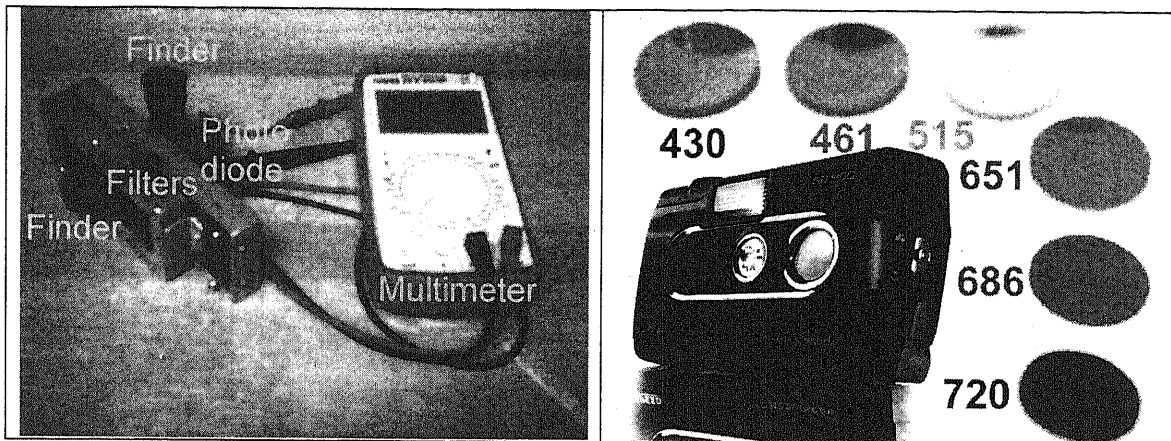


Fig. 3. A portable reflectometer for quick measurements of the ratio R_{720}/R_{650} (left) and a digital camera with interference filters for taking reflection image at different wavelengths (right).

The reflectometer used for estimation of the ratio R_{720}/R_{650} , which is equal to 0.9 ± 0.2 for non-plant materials such as soil, paper, a cloudy sky, a clear sky, and the moon. The ratio, measured along the field expedition route in 1990, was as following:

(1.8±0.3)	(1.8±0.5)	(1.6±0.2)	(2.5±0.2)	(1.4±0.04)
Ulaanbaatar-> Bagahangai->.....->Tsagaandelger-				
(07 July 1990)			(10 July 1990)	
(1.5±0.3)	(2.7±0.2)	(1.8±0.3)	(5.3±0.4)	(3.9±
->Herlen bridge-> Huduu aral> Undurhaan, Herlen, Crof field-> Shuuz				
(13 July 1990) (15 July 90)		(16 July 1990)	(21 July)	
0.4)	(5±1.2)	(4.5±1.2)	4.7	
river-> Berh -> Undurhaan-> Murun, Chandgana -> Avrगतoson-				
		(21 July 1990)	(23 July)	
(3.9±0.1)	(4.1±0.5)			
>Bayanjargalan, Arhyst->Bagahangai-> Ulaanbaatar				
(24-30 August 1990) (06 August 1990)				

The dry weight of grass around Bagahangai was 3.6 times increased per month. If we know the relationship between the ratio and dry weight of the grass, then we can estimate the amount of grass and the rate of grass growth. Therefore, we measured the ratio R_{720}/R_{650} in dependence on the dry weight of grass (Fig. 4), and a linear relation between them was established. According to this relation, the grass growth rate was equal to 4.5 g/(m² day) around the Bagahangai station.

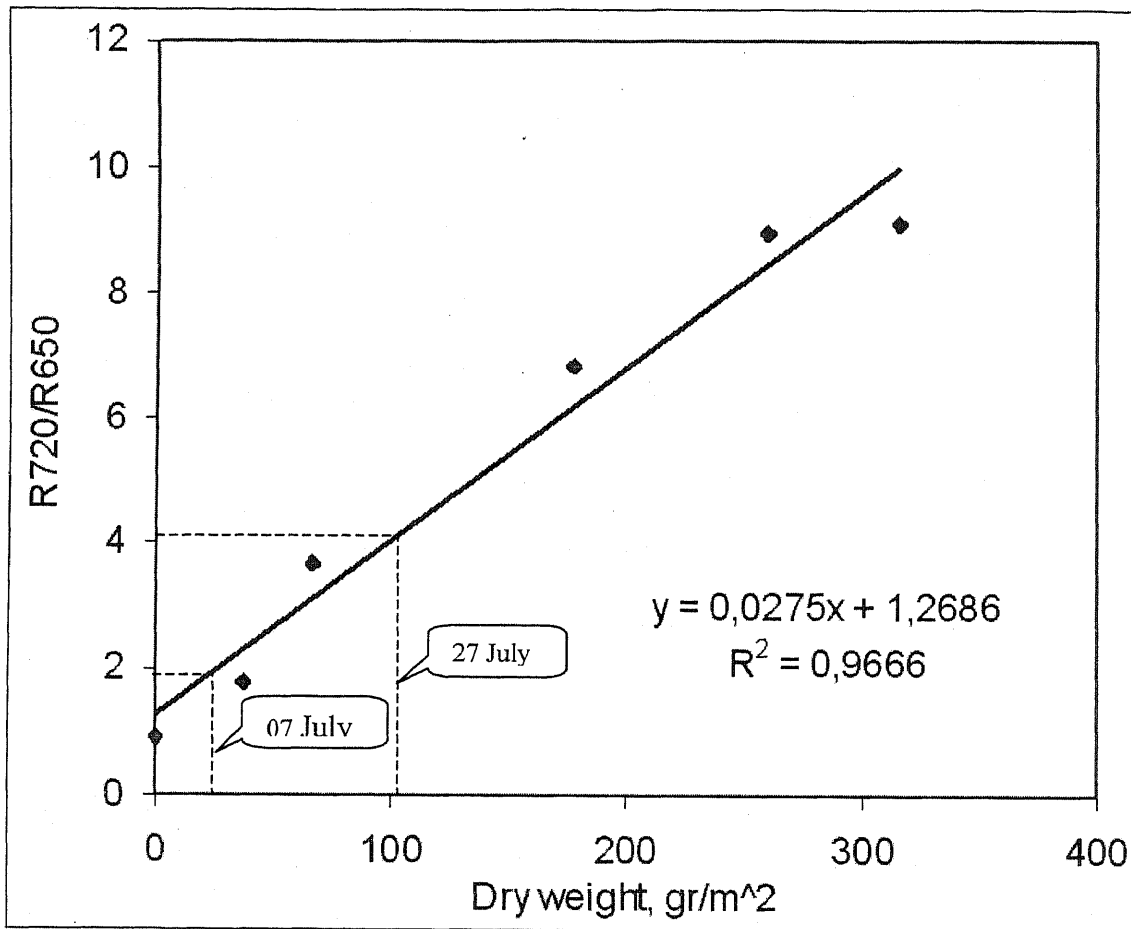


Fig. 4. The relation between the ratio R720/R650 and the dry weight of grass.

The digital camera with interference filters (Fig. 3 right) was used for taking the reflection image from pteridophyta leaves (Fig 5).



Fig. 5. The reflection image or digital photograph of leaves taken with interference filters,
which transmits light of wavelength (from the right to the left)
461, 515, 651, 686, and more than 720 nm.

The maximum reflection from the green plants reached the near-infrared (740-820 nm) region of spectra (3). Naturally, the change of spectral values cannot be seen visually. Therefore, we choose a glass filter combination, which transmits light of wavelengths more than 720 nm instead of a 820 nm interference filter. The color image was converted into a gray image in order to obtain the ratio of images (Table 2), such as R720/R686, R720/R651, R515/R461, and R515/R431.

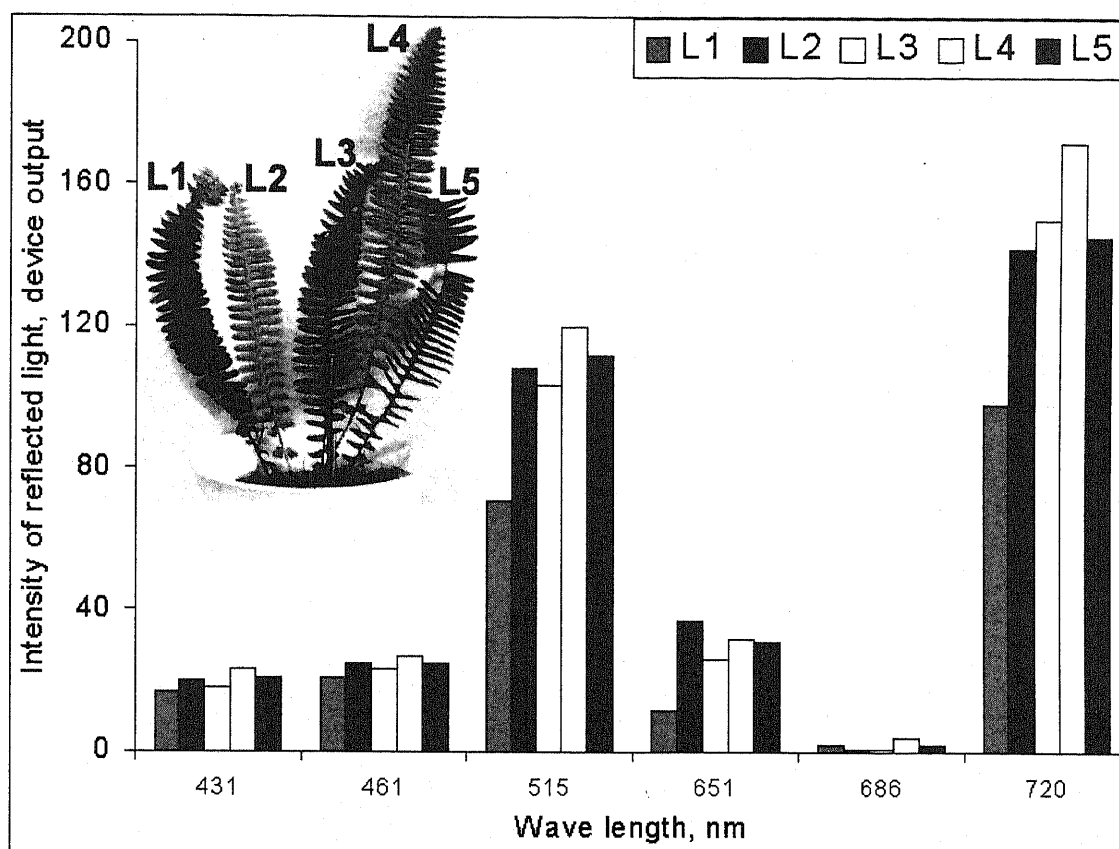


Fig. 6. Average image intensity of reflected light from pteridophyta leaves at the different wavelength. The leaves L2 and L4 are younger than the other leaves.

Light with wavelength of 515 and 720 reflected from the leaves was less than the light of other wavelengths. The light with wavelength of 431 and 686 nm was mainly absorbed in the chlorophyll-a, and that with wavelength of 461 and 651 nm in the chlorophyll-b. The light with the wavelength of 686 nm was strongly absorbed in the chlorophyll-a and it was difficult to read the intensity of the image output. We can calculate many different ratios between the intensity of reflected and absorbed light, some of which are shown in Table 2. Using this method, we can see the image of ratios directly, which we do not show here.

Table 2: The ratio of images of pteridophyta leaves.

Ratio	L1	L2	L3	L4	L5
R720/651	8.2	3.8	5.8	5.4	4.7
R515/461	3.4	4.3	4.5	4.4	4.5
R515/431	4.2	5.4	5.7	5.2	5.3
Average	5.2	4.5	5.3	5.0	4.8
SD	2.6	0.8	0.7	0.5	0.4

There is no significant difference between the leaves in terms of these ratios. But the ratios R720/651 and R720/686 were 1.6, and R515/431 and R515/461 3.2 in the case of non-plant material (green wall), and the ratios in Table 2 correspond only to leaves. The ratio from leaves was 2 times greater than that in the non-plant material, which shows that with these ratios we can estimate the amount of dry weight of plants.

We constructed chlorophyll luminescence and fluorescence image systems with a more expensive and very sensitive digital camera with 2 multi-channel plates (2). With this system it was easy to acquire the reflection image of leaves and we acquired the reflection images of wheat plants at wavelengths of 822, 730 and 660 nm (Fig. 7 and Fig. 8).

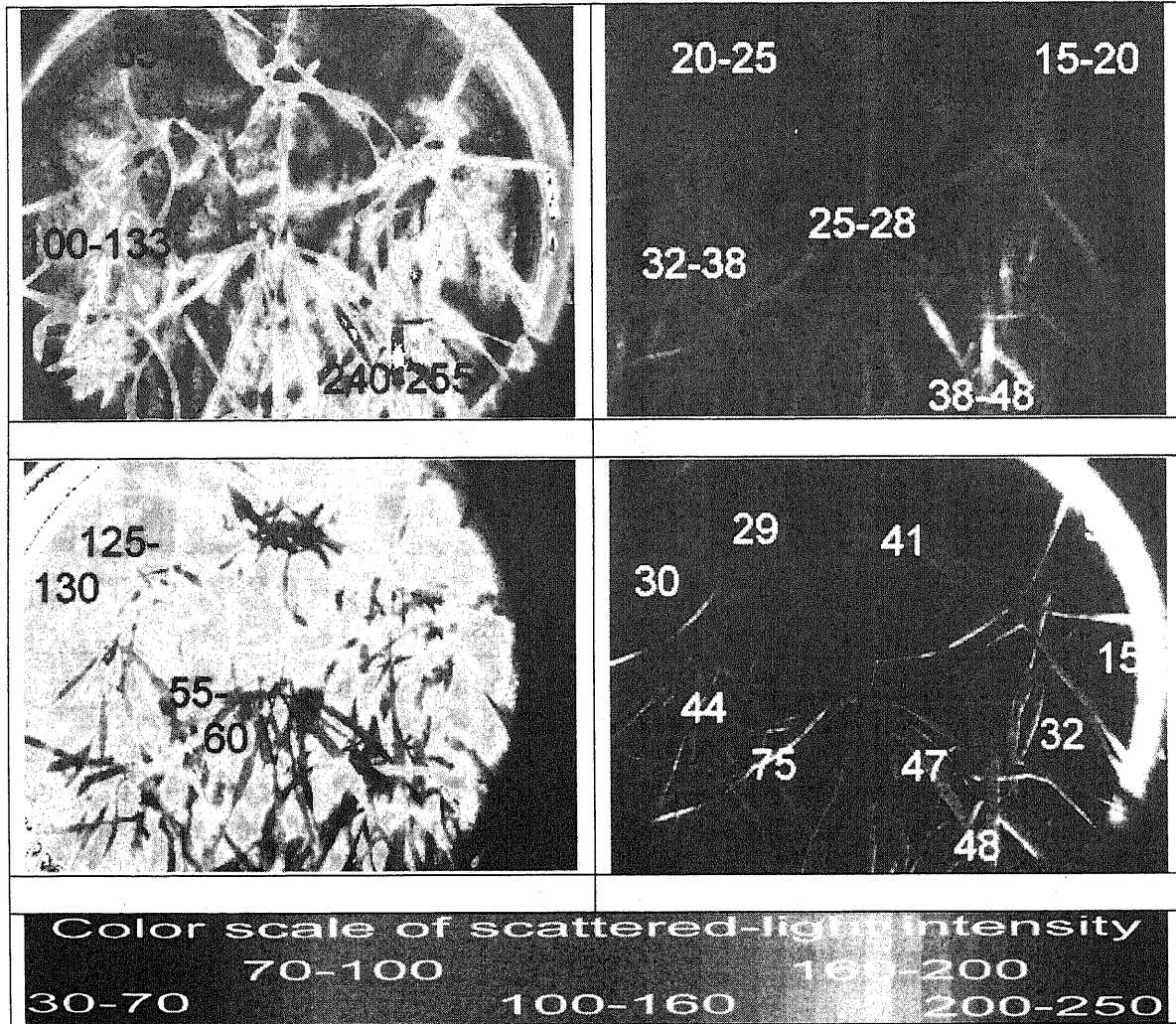


Fig. 7. Image of wheat plants, acquired from the top side of the pot, which was grown in dry soil with 13% water content:

Acquired at the wave length of 820 nm	Acquired at the wave length of 700 nm
Acquired at the wave length of 660 nm	The image of the ratio $10 \cdot R_{820}/R_{700}$

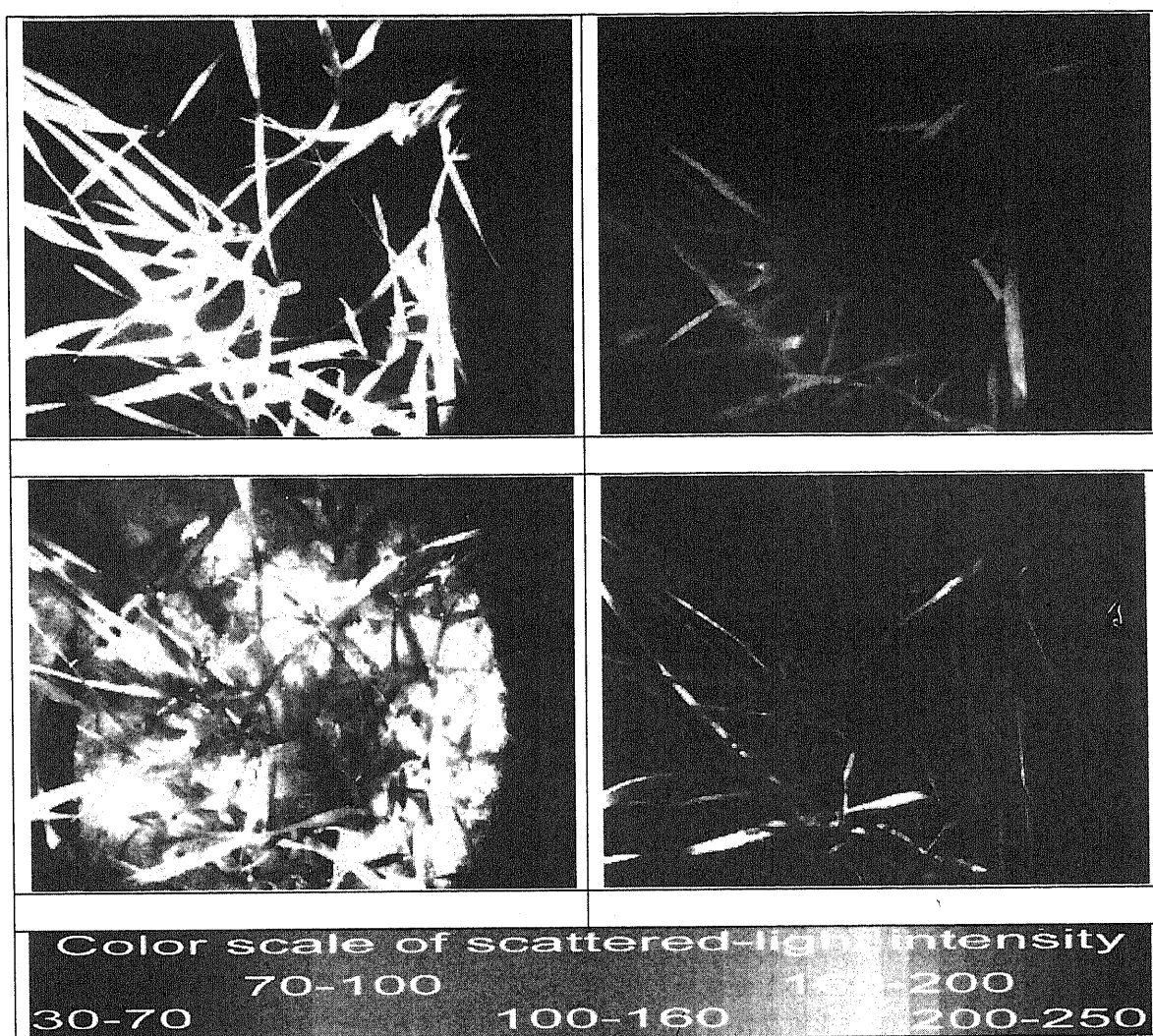


Fig. 8. Image of wheat plants, acquired from the top side of the pot, which was grown in wet soil with 18% water content:

Acquired at the wave length of 820 nm	Acquired at the wave length of 700 nm
Acquired at the wave length of 660 nm	The image of the ratio $10 \cdot R_{820}/R_{700}$

Table 3. Relative light reflection (R_{820}/R_{700} and R_{820}/R_{660}) from leaves of wheat plants grown in wet (18% of water content) and dry (13% of water) soil (n=30 for leaves and 8 for soil).

Wheat at wet soil		Wheat at dry soil		Wet (18%) soil		Dry (13%) soil	
820/700	820/660	820/700	820/660	820/700	820/660	820/700	820/660
4.6±2.0	2.6±0.7	4.5±0.9	2.9±0.9	1.7±0.1	0.7±0.1	2.9±0.2	0.6±0.1

Table 3 shows that there was no significant change between the ratios in the leaves of wheat grown in the wet and dry soil in normal air. The experiments with luminescence images showed that the photosynthesis and dry matter production in the wheat plants, grown in the wet soil, increased in the case of high CO₂ (700 ppm) in air, but not in the normal air (2).

References

1. Damdinsuren S., Enkhbayar P., and Tumurbaatar T, Mathematical modeling of photosynthetic induction and light reflection, NUM, Scientific Journal No 116, pp 49-60
2. Damdinsuren S., Enkhbayar P., and Osaki M: 2001. Leaf luminescence image of wheat grown in conditions, distinguished by CO₂ in air and water in soil. NUM, Scientific Journal of Biology, NUM No 13, pp 27-49
3. Field C. B., Gamon J. A, and Penuelas J. 1995. Remote sensing of terrestrial photosynthesis. In: Ecophysiology of photosynthesis. Springer, pp. 511-528

APPLICATION OF REMOTE SENSING FOR ECONOMIC GROWTH ANALYSIS IN PARTICULAR AREAS OF MONGOLIA

B. Erdene* R. Tsolmon**

*Technology expert of the Secretariat State Great Khural

E-mail: erdene_bz@parl.gov.mn

**Remote Sensing Laboratory, Center for Geophysics, National University of Mongolia

E-mail: tsolmon@num.edu.mn

1. Introduction

From the viewpoint of macro-economical policies, the long-term objective to improve living standards cannot be attained without the achievement of the short-term objective of providing for sustainable economic growth. Sustainable economic growth contributes positively to:

- satisfaction of increasing economic and social needs, and
- provision of investment sources to produce new wealth.

The basis of sustainable development was laid down by the "Declaration on the Environment and Development," a document consisting of 27 chapters, issued by the 1992 Rio De Janeiro Symposium. The three cornerstones of sustainable development are:

1. Social procedures (equality, social relations, social changes, participation, and cultural identity),
2. Economic growth (growth, return, and stability),
3. Protection of the environment (healthy environment, rational use of renewable natural resources, and protection of depletive natural resources)

There is a pressing need for our country, having a wide territory and with a significant part of the population running animal husbandry dispersed over the territory, to define and implement its objectives of sustainable development on the basis of cooperation among its provinces. Studies of the peculiarities of every province are needed for the definition of sustainable development objectives in harmony with the nature and ecological environment.

The application of Remote Sensing to socio-economic analyses is an important asset to Mongolian sustainable development and its ecosystems. Remote sensing offers an efficient and reliable means of collecting the information required to conduct research about linking socio economic and environmental databases.

Remote sensing methods have the following advantages:

1. Saving time for carrying out studies;
2. Possibility of gathering an enormous amount of information inexpensively and analyzing it;
3. Displaying data collected over many years and identifying correlations among them;
4. Covering a wide territory at the same time;
5. Full possibility to carry out all aspects of natural and ecological studies.

2. Objectives

It is regarded as possible to develop the animal husbandry and agricultural sectors as the key sectors of the economy determining the sustainability of development of Mongolia. This can be accomplished in a rational and balanced way with the use of the remote sensing methods. The following goals are set for this purpose:

1. To study the vegetation changes over the last 4 years, selecting one province from each of the Gobi and Khangai regions and analyzing the findings.
2. To identify the interrelation between the changes of the economic indicators from statistical data and the changes in the vegetation cover from satellite data.

3. Scope of the research and issues of sustainable development

- 3.1 For this research, Ovorkhangai province was selected from the Khangai region and Gobi-Altai province was selected from the Gobi region.

Table 1. Comparison of resident population and numbers of livestock

	Aimags	Population, thousands of persons				Number of livestock, thousands of heads			
		1999	2000	2001	2002	1999	2000	2001	2002
1	Govi-Altai	63.7	63.6	64.2	62.7	2113.2	2035.1	1714.7	1010.5
2	Ovorkhangai	111.4	113.0	114.0	113.9	2956.6	2159.0	1869.1	1665.4

3.2 The issues of sustainable social development

For the last 10 years, the yearly increase of Ulaanbaatar's population averaged 3%, while that of the western and Khangai regions were 0.2% and 1.3%, respectively. These trends are attributable to the abnormally disproportionate move of rural residents to Ulaanbaatar. Therefore, the settlement of demographic issues is becoming a priority. There is a big difference of the unemployment rates among the regions.

3.3 The issues of sustainable economic development

The economic growth and structural reform of the regional communities are too slow. It is important to reduce the gap between the levels of economic and social development among the regions relying on their resources for the acceleration of the growth of national economy.

There is a need to accelerate the economic growth of the macro economic regions and, further, to establish a rational economic structure adaptable to the equilibrium of the ecosystem.

3.4 Use and protection of the environment

Disruption of the equilibrium of the ecosystem in Mongolia is taking on a more regional character. It is attributable to the over-concentration of human, animal, and industrial populations in some regions and mismanagement of the exploitation of natural resources, structure of animal herds, and pasture use. In consequence of the intensified exploitation of natural resources in all the regions of Mongolia in recent years, the earth surface and soil are deteriorating. It is vital to improve the rational use of natural resources and environmental protection in all the regions and safeguard the equilibrium of the ecosystem.

4. Study area

The study area, the Gobi-Altai province (figure 1), is located in the western part of Mongolia. It lies between 42° 30' - 47° N and 93°- 99°E .Govi-Altai province is located in the western part of the country. It borders on the south-west the People's Republic of China. The highest peak among them is Sutai Mountain, clad in eternal snow at 4,226 meters above sea level. There are wide semi-deserts such as Sharga, Dukhum, Zakhuu, Zarman, Biger, Alagnuur, Tsengkher, Nomin between these mountains.

There are populus diversifolia, saksaul, tamarisk in some Govi area and hippobopac, peplars, willows are along the humid areas and larch, curgana pygmaya, sympegma and

bramble grow in mountainous parts. Wild animals include wild sheep, ibex, deer, mountain-faunas, snow-leopard, lynx, corsa, wild cat, wolf, fox, ermin and marmot. Birds include eagles, falcons, condors, snow-cocks, bearded vultures and divers. All of these animals live in the Altai Mountains. There are wild camels, wild-horses, saiga, tatarica Mongolica, black tailed antelope, and govi-bears in the semi-desert. The main direction of the aimag's (province's) economy is agriculture and animal husbandry and it has 2112.5 thousand heads.

As for the livestock number, this aimag ranks 4th place in its goat stock and 1st in the number of camels in the country. Vegetation of Govi–Altai province compares with vegetation of Uvurkhangai province (figure 2) visually. The NDVI value in the Govi region is lower than Khangai region. Table 1 describes comparison of resident population and number of livestock in both regions. Figures 3,4 and table 1 shows that there are differences in socio economic growth and environment between these provinces.

5. Data

The Normalized Difference Vegetation Index (NDVI) from SPOT/VEGETATION data from 10-day composite 11-20 September for years 1998-2003 was carried out for this research. NDVI is related to the proportion of photosynthetically absorbed radiation, is calculated from ground reflectance from the visible and near infrared channels as $NDVI = (RED - NIR) / (RED + NIR)$

The SPOT4/VEGETATION satellite data is developed jointly by France, the European Commission, Belgium, Italy and Sweden. The satellite component of the program was launched in October 1997 onboard SPOT4 and it delivered measurements which were specifically tailored to monitor land surface parameters with a frequency of about once a day on a global basis and a medium spatial resolution of one kilometer. It has four spectral bands.

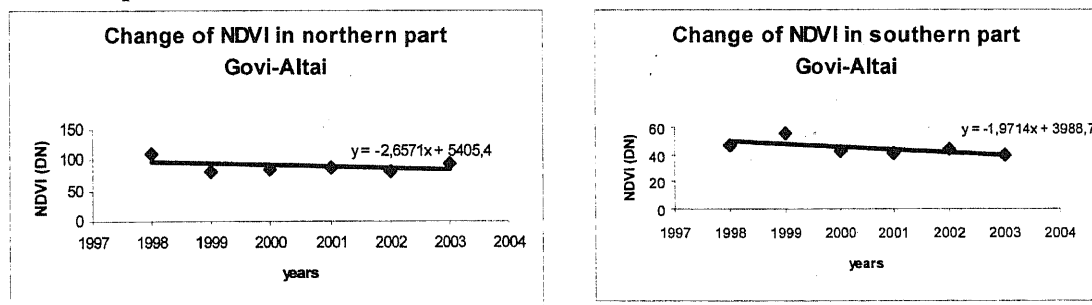


Figure 1 Change of vegetation cover years 1998-2003 in Gobi-Altai province

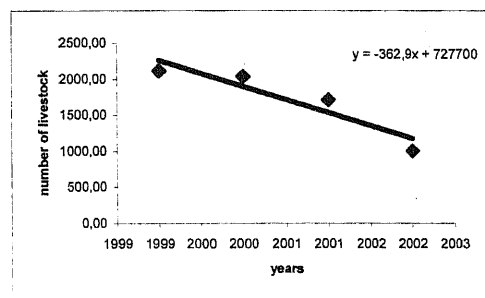


Figure 2 Change of livestock in Gobi-Altai province between

6. Results and Discussion

The objectives of this study are to contribute to policies that promote environmentally sustainable and profitable pastoral livestock husbandry. This study indicates that the development of social economic growth depends on environmental factors such as land cover change and vegetation growth. Figures 3 and 4 describe changes in the NDVI from years 1998 to 2003 in both provinces. This study analyzed two parts of the Govi province, north and south. The NDVI value in the north was higher than in the south. From figure 2 it can be seen that livestock is dramatically decreasing. The analysis of land use condition and change gives us a chance of developing information relating to the regional structure and environment in Gobi-Altai province. The condition of regional vegetation and livestock and its perspectives and the influence on natural environment can be obtained from the analysis. Therefore, the environment should be actually preserved, conserved, improved and restored. Furthermore, not only the environment must be improved and restored, but also regional developmental measures should be taken in the study areas Gobi-Altai and Uvurkhangai provinces respectively, considering their economic and environmental condition.

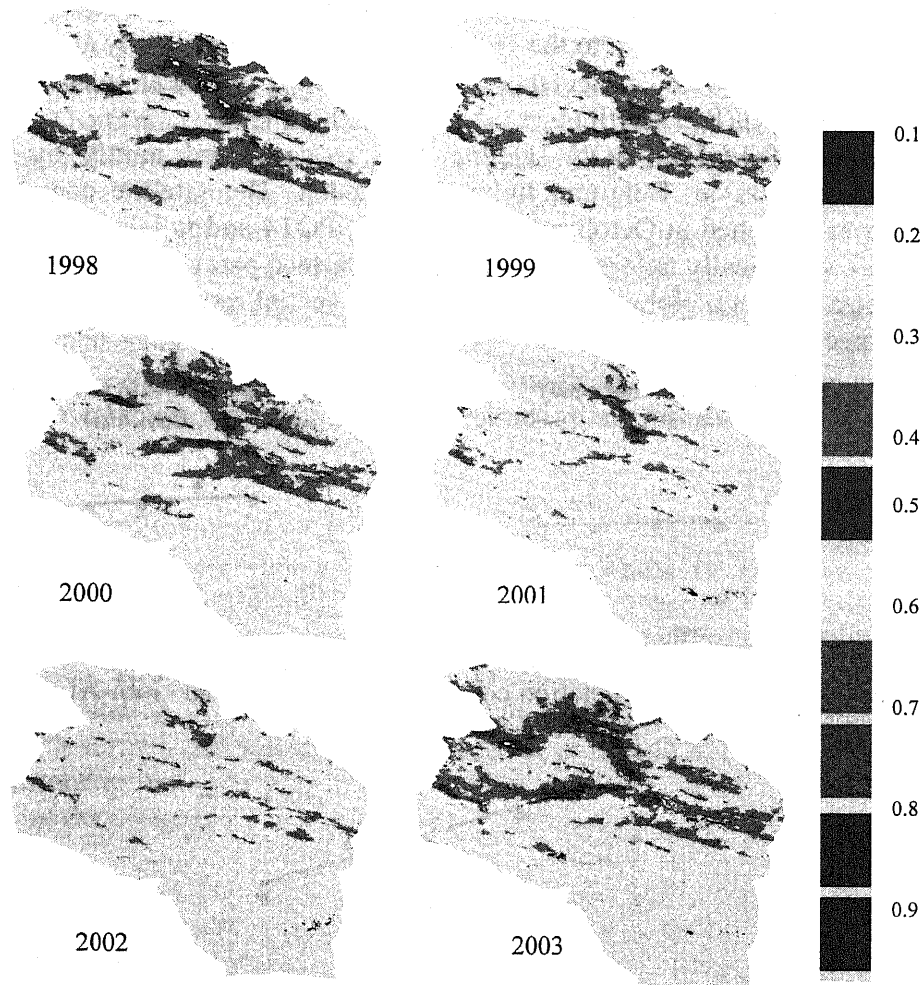


Figure 3 Vegetation coverage in the Gobi –Altai province over years 1998-2003

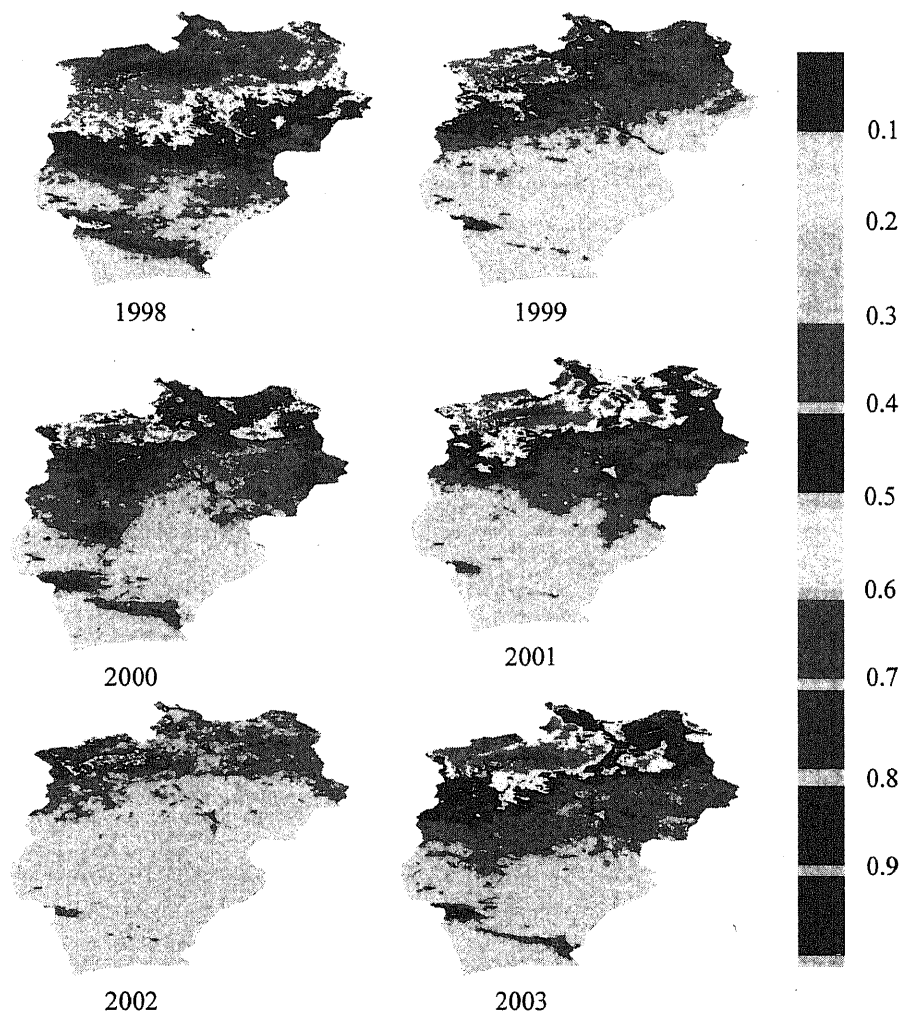


Figure 4 Vegetation coverage in Uvurkhnagai province over years 1998-2003

Acknowledgements

The authors are grateful to VEGETATION/SPOT-4 PROGRAMME from the European Union, France, Belgium, Sweden and Italy for supplying the VEGETATION data.

References

1. Mongolian statistical yearbook, 2002, Ulaanbaatar